②

NCS TIB 88-7

NATIONAL COMMUNICATIONS SYSTEM

AD–A206 107

TECHNICAL INFORMATION BULLETIN
88-7

THE EFFECTS OF HIGH-ALTITUDE
ELECTROMAGNETIC PULSE (HEMP) ON THE
NORTHERN TELECOM INC.
DMS-100™ SWITCH

VOLUME III

DATA ANALYSIS

DTIC
ELECTE
3 1 MAR 1989
S   E
D

SEPTEMBER 1988

OFFICE OF THE MANAGER
NATIONAL COMMUNICATIONS SYSTEM
WASHINGTON, D.C. 20305

► 89 3 30 00?

REPORT DOCUMENTATION PAGE		Form Approved OMB No. 0704-0188

1a. REPORT SECURITY CLASSIFICATION Unclassified	1b. RESTRICTIVE MARKINGS
2a. SECURITY CLASSIFICATION AUTHORITY	3. DISTRIBUTION/AVAILABILITY OF REPORT Approved for public release; distribution unlimited
2b. DECLASSIFICATION/DOWNGRADING SCHEDULE	

4. PERFORMING ORGANIZATION REPORT NUMBER(S) NCS TIB 88-7, Vol. III	5. MONITORING ORGANIZATION REPORT NUMBER(S)

6a. NAME OF PERFORMING ORGANIZATION Booz, Allen & Hamilton	6b. OFFICE SYMBOL (If applicable)	7a. NAME OF MONITORING ORGANIZATION
6c. ADDRESS (City, State, and ZIP Code) 4330 East West Highway Bethesda, MD 20014		7b. ADDRESS (City, State, and ZIP Code)

8a. NAME OF FUNDING/SPONSORING ORGANIZATION National Communications System	8b. OFFICE SYMBOL (If applicable) NCS-TS	9. PROCUREMENT INSTRUMENT IDENTIFICATION NUMBER DCA100-87-C-0063

8c. ADDRESS (City, State, and ZIP Code) Office of Technology & Standards Washington, DC 20305-2010	10. SOURCE OF FUNDING NUMBERS			
	PROGRAM ELEMENT NO. 33127K	PROJECT NO. Q019	TASK NO	WORK UNIT ACCESSION NO

11. TITLE (Include Security Classification)
The Effects of High-Altitude Electromagnetic Pulse (HEMP) on the Northern Telecomm Inc. DMS-100 Switch, VolumeIII, Data Analysis

12. PERSONAL AUTHOR(S)

13a. TYPE OF REPORT Final	13b. TIME COVERED FROM _____ TO _____	14. DATE OF REPORT (Year, Month, Day) September 1988	15. PAGE COUNT 90

16. SUPPLEMENTARY NOTATION

17. COSATI CODES			18. SUBJECT TERMS (Continue on reverse if necessary and identify by block number)
FIELD	GROUP	SUB-GROUP	High-Altitude Electromagnetic Pulse (HEMP)

19 ABSTRACT (Continue on reverse if necessary and identify by block number)
This report is part of a three volume set that presents the results of simulated High-Altitude Electromagnetic Pulse (HEMP) testing of a Northern Telecom Inc. DMS-100 Switching System. This volume describes the post test analysis of the measured electromagnetic fields and induced transients. This volume also includes a comparison of the characteristic attributes of the various simulator environments.

20. DISTRIBUTION/AVAILABILITY OF ABSTRACT ☑ UNCLASSIFIED/UNLIMITED ☐ SAME AS RPT ☐ DTIC USERS	21 ABSTRACT SECURITY CLASSIFICATION Unclassified	
22a NAME OF RESPONSIBLE INDIVIDUAL A. H. Rausch	22b TELEPHONE (Include Area Code) 202-692-2124	22c OFFICE SYMBOL NCS-TS

DD Form 1473, JUN 86 — Previous editions are obsolete

NATIONAL COMMUNICATIONS SYSTEM

TECHNICAL INFORMATION BULLETIN
88-7

THE EFFECTS OF HIGH-ALTITUDE
ELECTROMAGNETIC PULSE (HEMP) ON THE
NORTHERN TELECOM INC.
DMS-100™ SWITCH

VOLUME III

DATA ANALYSIS

SEPTEMBER 1988

**OFFICE OF THE MANAGER
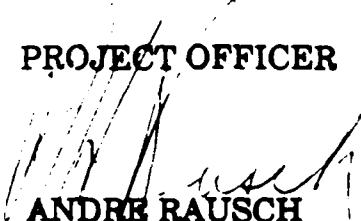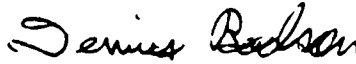NATIONAL COMMUNICATIONS SYSTEM
WASHINGTON, D.C. 20305**

THE EFFECTS OF HIGH-ALTITUDE ELECTROMAGNETIC PULSE (HEMP) ON TELECOMMUNICATIONS ASSETS

SEPTEMBER 1988

PROJECT OFFICER

ANDRE RAUSCH
Electronics Engineer
Office of Technology
and Standards

APPROVED FOR PUBLICATION

DENNIS BODSON
Assistant Manager
Office of Technology
and Standards

FOREWORD

The National Communications System (NCS) is an organization of the Federal Government whose membership is comprised of 23 Government entities. Its mission is to assist the President, National Security Council, Office of Science and Technology Policy, and Office of Management and Budget in:

- The exercise of their wartime and non-wartime emergency functions and their planning and oversight responsibilities.

- The coordination of the planning for and provision of National Security/ Emergency Preparedness communications for the Federal Government under all circumstances including crisis or emergency.

In support of this mission the NCS has initiated and manages the Electromagnetic Pulse (EMP) Mitigation Program. The objective of this program is the removal of EMP as a significant impediment to timely reestablishment of regional and national telecommunications following an attack against the United States that includes high-altitude nuclear detonations. The program approach involves estimating the effects of High-altitude EMP (HEMP) on telecommunication connectivity and traffic handling capabilities, assessing the impact of available HEMP mitigation alternatives, and developing a comprehensive plan for implementing mitigation alternatives. This report summarizes EMP test results on the NTI DMS-100 as they apply to the EMP Mitigation Program.

Comments on this TIB are welcome and should be addressed to:

Office of the Manager
National Communications System
ATTN: NCS-TS
Washington, DC 20305-2010
(202) 692-2124

PREFACE

This report is part of a three volume set that presents the results of simulated High Altitude Electromagnetic pulse (HEMP) testing of a Northern Telecom Inc. DMS-100™ switching system. The efforts described herein were funded by the Office of the Manager, National Communications System (OMNCS) and were performed by US Army Harry Diamond Laboratories (HDL) and by Booz•Allen and Hamilton Inc., Northern Telecom, Inc. (NTI), and Bell Northern Research (BNR) under HDL Contract Number DAAL02-86-D-0042, Delivery Order Numbers 7, 18, 35, and 43.

The technical contributors from HDL include J. Miletta (Program Manager), R. Reyzer (Project Leader), L. Ambrose, W. Coburn, A. Hermann, C. Reiff, and D. Troxel. The technical contributors from Booz•Allen include R. Balestri, A. Bueno, R. Henrickson, D. Palleta, W. Shiley, and T. Styer. Technical contributors from NTI/BNR include A. Childerhose, D. Dowse, J. Edwards, A. Hussein, D. O'Connor, and J. Skinner.

Volume I presents a brief discussion of the test events and the test results, and summarizes the conclusions and recommendations of the test program. Volume II is a detailed description of the test procedures, the test results, and the mitigation alternatives evaluated. Volume II also presents a discussion of the conclusions and recommendations of the program. This volume describes the post test analysis of the measured electromagnetic fields and induced transients. This volume also includes a comparison of the characteristic attributes of the various simulator environments.

Accession For	
NTIS GRA&I	X
DTIC TAB	
Unannounced	☐
Justification	
By	
Distribution/	
Availability Codes	
Dist	Avail and/or Special
A-1	

™DMS-100 is a registered trademark of Northern Telecom, Inc.

TABLE OF CONTENTS

LIST OF FIGURES

LIST OF FIGURES (CONT.)

LIST OF FIGURES (CONT.)

LIST OF FIGURES (CONT.)

LIST OF TABLES

1.0 INTRODUCTION

The DMS-100 is a digital telephone switch used extensively in the commercial communication network. The primary objective of this test was to collect data to support the statistical characterization of the performance of the switch as a function of the incident electromagnetic field strength related to high altitude nuclear electromagnetic pulse (HEMP). The operational performance of the switch in the HEMP environment is presented in Volumes I and II of this report. The operational performance data are limited to observations of the ability of the switch to process calls and to recover from upset in the simulator environment. All of the data were extrapolated to a representation of DoD-STD-2169 early time environment, so that the data could be evaluated at a common point.

In addition to examining the operational performance of the switch, this test presented an unique opportunity to investigate the impact of the simulator environment on the conclusions reached as a result of an HEMP test. That is, since conclusions are based upon threat extrapolated data, the questions arises whether the extrapolation process modify the data such that different conclusions would be reached if the test were conducted in a threat level simulator. For this test, there were three simulators used to excite the DMS-100 switch. As described in Volume II, tests were conducted at Ottawa, Canada, using a low level, fast rise time pulser. This pulser generated an incident field of approximately 2.5 kV/m on the switch with a rise time of approximately 1 ns and a duration of approximately 100 ns. The purpose of this phase of the test program was primarily to survey the expected coupling to support further test and to test the system with NTI engineers on hand to correct any major deficiencies uncovered during the initial test. The second test environment was the REPS simulator at the HDL WRF. This simulator produced an incident field of approximately 12 kV/m at the test object with a rise time of 8 ns. The pulse duration of REPS is on the order of 1 μs and thus could induce more low frequency energy into the DMS-100 system. Finally, the switch was illuminated in the HDL WRF AESOP simulator at incident field strengths of 33, 48, 60 and 69 kV/m with a pulse shape essentially the same as the REPS simulator. System performance data were thus obtained at five different field levels.

None of the simulators generates the DoD-STD-2169 threat waveforms. In this volume, the AESOP 60 kV/m data are compared directly to extrapolated data to determine if the peak field strength is the dominant contributor to system failure or if the spectrum differences between the AESOP and the early time threat waveform altered the data to a point at which the test results would be questioned. As a second analysis, all data are extrapolated to determine the effects of the simulator on the extrapolated waveform attributes. This aids in determining the applicability of waveform attribute specifications in HEMP survivability testing.

There were several important lessons learned from the analysis of the data taken on the DMS-100 switch. The first is that the stresses placed on the switch by AESOP would meet or exceed the stresses placed on the switch by a simulator that radiated the field of the DoD-STD-2169 threat. The second lesson learned was that the

grounding configuration is very important. The switch exhibited signal strengths of up to an order of magnitude higher when a ground loop existed than when the ground loop problem was corrected. As a result, it can be seen that it is extremely important that no grounding problems exist during testing. The addition of filters and panels also had a large effect of the signal strengths measured. The filters provided approximately six to ten dB of attenuation. The final lesson learned was that norm comparisons based upon test data extrapolated to a threat are sensitive to the test environment, frequency spectrum, and the extrapolation method used.

The details of this analysis are presented in subsequent sections. Section 2 presents a brief discussion of the data treatment and the extrapolation functions used to convert all data to an unclassified approximation of the DoD-STD-2169 early time threat. Section 3 presents the norm attributes of the data which are used for comparisons made in Sections 4, 5 and 6. Section 4 presents a direct comparison of the AESOP raw data obtained at 60 kV/m with the same data extrapolated to the early time threat. Section 5 treats the effects of configuration changes in the grounding between REPS and AESOP and also between the shielding configurations at AESOP. Section 6 analyzes the differences between the data obtained at the three AESOP field levels. Summaries are provided for each section. Test point references in this volume may be found in Appendix A, which contains extensive details of the test article and test point locations.

2.0 DATA PROCESSING AND EXTRAPOLATION

The data associated with this test fall into two distinct categories. Ottawa data were obtained using Polaroid photographs of oscilloscope traces and subsequent digitization. Additionally, the pulser used at Ottawa has not been adequately field mapped to determine the total incident field. The primary field sampling performed at Ottawa was performed to relate the pulser charging level to the peak field. As such, the Ottawa data were not intended for detailed analysis and are included only in the summary information provided in **Table 2-1**.

The data obtained at both REPS and AESOP were acquired using the HDL IVAN data acquisition system. This system uses Tektronix 7912AD transient digitizers to obtain high quality recordings of the sensor output. Only two digitizers are employed on any given channel at a time and this results in the need to concatenate or time tie data from several consecutive pulser shots to fully construct the response waveform. Additionally, the probe correction used did not compensate for the bandpass nature of the probe. Nominal values were used, but this should have minimal impact on the analysis.

2.1 DATA PROCESSING PROCEDURE

The IVAN data files corresponding to a given test point and configuration were analyzed to determine the most compatible data based on peak amplitudes, sweep speed and reference sensor output. The time shift to be applied to the recordings was determined using an adaptive cross correlation technique[1,2]. The data sets were then temporally aligned and blended together using a continuous weighting function to maintain continuity through the overlap region. A similar procedure was followed for the Ottawa data with the exception that reference sensor data were not available to aid in the process and only two oscilloscope sweep speeds were available.

The second step in the procedure was to detrend the data[3]. This process removed any dc offset bias and linear trend from the time tied recording. This is done to minimize the effects of instrumentation errors on subsequent processing in the frequency domain.

The third step was to apply a window to the last 10% of the data in order to smoothly transition the data to a zero value at the end of the record. This is done to minimize truncation effects in the fourier transform domain. Truncation produces erroneous dc value and high frequency hash on the high frequency portion of the spectrum.

The final data processing was the application of an adaptive time domain noise cancellation filter to the data to remove uncorrelated noise due to the digitization process[4]. This process uses what is referred to as the Widrow Least Mean Square adaptive filter and is an auto-regressive process with the filter weights updated as the data is processed. The process improves the behavior of the data in the frequency domain.

2.2 DATA EXTRAPOLATION

Once the data are properly conditioned, they are extrapolated to the early time waveform. This procedure is accomplished by computing the transfer function from the threat waveform to the simulator environment in the frequency domain. This transfer function is then used to multiply the frequency domain representation of the measured data with the resulting product inverse Fourier transformed back to the time domain.

The H-field data were used to determine the spectrum content of the simulators for REPS and AESOP and develop the transfer function. The field data and the threat waveform were then normalized to unit amplitude and the unit transfer function was developed. The measured data were scaled linearly to the peak of the early time threat representation.

The unit transfer functions are presented in **Figure 2-1**. Both REPS and AESOP overdrive the low frequencies while the Ottawa pulser under drives the low frequencies. The reverse is true for the high frequencies. The unwrapped phases are also plotted. Extrapolating the Ottawa will introduce very little phase shift while REPS and AESOP will introduce several phase shifts. These phase shifts will contribute to changes in the peak derivative and impulse norms. However, they will not introduce significant wrap around in the extrapolated data. The shortcomings of this approach are that the ground reflection cancellation present in the E-field was not properly compensated for the associated time delay (phase shift) and the H-field reflection was assumed to not distort the magnetic field waveform.

The impact on the results is difficult to quantify, however most of the responses in the REPS and AESOP are dominated by the low frequency content induced by coupling to the exterior trunk lines, which is largely unaffected by this procedure.

For the Ottawa data, the transfer function was determined from the E-field data at a single point with the ground reflection accounted for. However, the time domain data were truncated at about 40 ns for both E and H field measurements, which could cause significant low frequency enhancement in the extrapolated waveforms. At this point in time, the Ottawa pulser has not been field mapped to determine the impact of the extrapolation process. For this reason, and the fact that the DMS-100 was not fully configured during the Ottawa test, Ottawa data are included only in a summary manner.

Independent of the field data, the extrapolation process, which is based on a single field measurement, is inherently incorrect. The true extrapolation process should account for field inhomogeneities over the test article. The trunk cables were the dominant source of coupling and they had a large spatial extent in the simulator environments. Proper extrapolation would require a spatial deconvolution of the incident field from the measured data. The effect of a single point extrapolation function is not known.

AESOP, OTTAWA, and REPS EXTRAPOLATION FUNCTION MAGNITUDE

EXTRAPOLATION FUNCTION PHASE
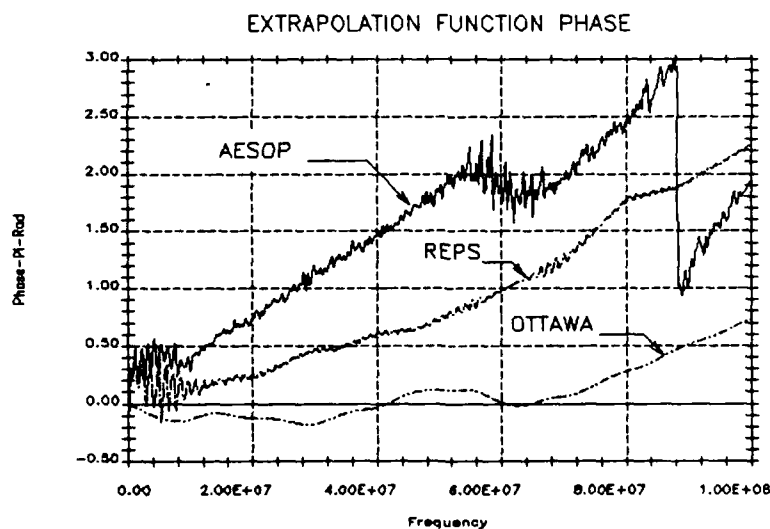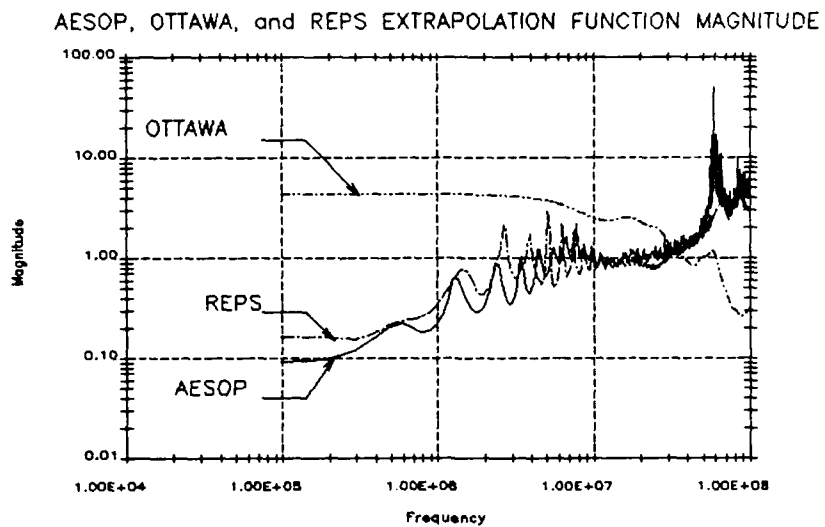
Figure 2-1. Unit Extrapolation Functions for Ottawa, REPS and AESOP Data

3.0 DATA ATTRIBUTES

To compare results, it is necessary to have some attributes of the data. The so-called norm attributes of peak amplitude, peak derivative, maximum impulse, rectified impulse and action integral have been chosen for this analysis[5]. Whether or not norm attributes are useful in the EMP assessment process is not the issue. They do possess the necessary mathematical properties for data comparison. That is, if norm attributes display a relationship in one environment, that relationship should also be true in another environment as long as the operations performed upon the data are linear operations.

The extrapolation process to a common threat waveform is a linear process and therefore, the norm attributes are appropriate descriptors of the impact of the simulators. This does not imply that the extrapolation process as performed is the correct application of the procedure, as a matter of fact, the results of this analysis seem to imply that single point extrapolation is not sufficient when comparing data from different simulators or, for that matter, when comparing data from the same simulator operated at different charging levels.

The norm attributes are mathematically defined as:

1 - $|f(t)|_{max}$ Peak Absolute Amplitude (PAA)

2 - $\left|\dfrac{df(t)}{dt}\right|_{max}$ Peak Absolute Derivative (PAD)

3 - $\left|\displaystyle\int_{0}^{t} f(x)dx\right|_{max}$ Peak Absolute Impulse (PAI)

4 - $\displaystyle\int_{0}^{\infty} |f(x)|\,dx$ Rectified Impulse (RI)

5 - $\sqrt{\displaystyle\int_{0}^{\infty} [f(x)]^2 dx}$ Root Action Integral (RAI)

These attributes have been proposed based upon physical arguments relating them to system survivability. Specifically, the peak amplitude relates to overstress breakdown at device junctions, the peak derivative should relate to upset in logical devices or data communications and the action integral is related to the energy input to a device, which should relate to burnout. The roles of the impulse and rectified impulse norms is less clearly related to failure and sometimes are associated with latch-up phenomenon. The rectified impulse and action integral norms are usually specified as the maximum value of the integral, however, the maximum value is the total integral so that distinction is omitted here. The square root of the action integral is often used in order to compare it to the rectified impulse. That convention is followed in subsequent discussion.

The values of norms computed from measured data are very susceptible to biases, trends, noise content and sampling rate. The data processing removes the biases and trend from the data. The noise filtering process minimizes this effect. Sampling rate is fixed by the instrumentation, however, the integration and differentiation techniques are based on cubic spline fits to the data and subsequent analytical integration and differentiation. This procedure minimizes the effects of sampling rate and residual noise.

Figures 3-1 through **3-5** show the minimum, maximum, average and sigma of all of the test points for the A and D configurations. Some of the configuraions were not tested with all of the simulators for example; there were no tests conducted at REPS on the D configuration. Thus, there is no RD graph. The simulator and configuration codes are given below.

FACILITY KEY

A - AESOP   (30KV/M)
B - AESOP   (45KV/M)
C - AESOP   (60KV/M)
R - REPS   (6KV/M)
O - OTTAWA (2.5KV/M)

CONFIGURATION KEY

A - PANELS OFF, FILTERS OFF
B - PANELS OFF, FILTERS ON
C - PANELS ON, FILTERS OFF
D - PANELS ON, FILTERS ON
E - CCC PANELS ON, TRUNK FILTERS ON, LCM PANELS OFF, LCM FILTERS ON
F - CCC PANELS ON, TRUNK FILTERS OFF, LCM PANELS OFF, LCM FILTERS ON, LCM CABLE LOOPED AROUND
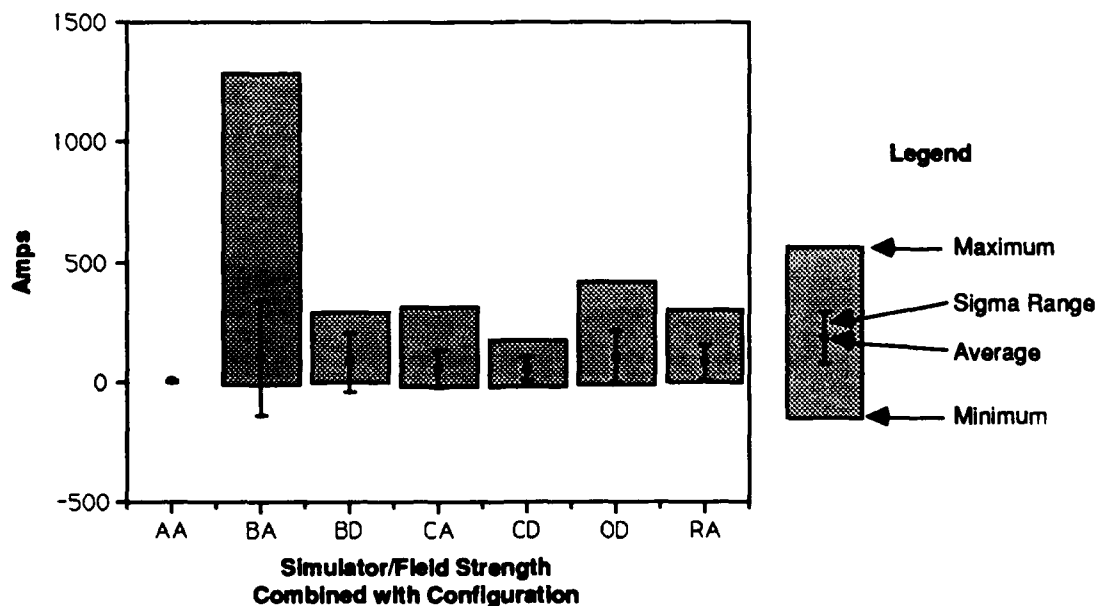
Figure 3-1. Maximum, Sigma, Average, and Minimum of the Peak Amplitude
Norm Versus Simulator and Configuration for All Test Points
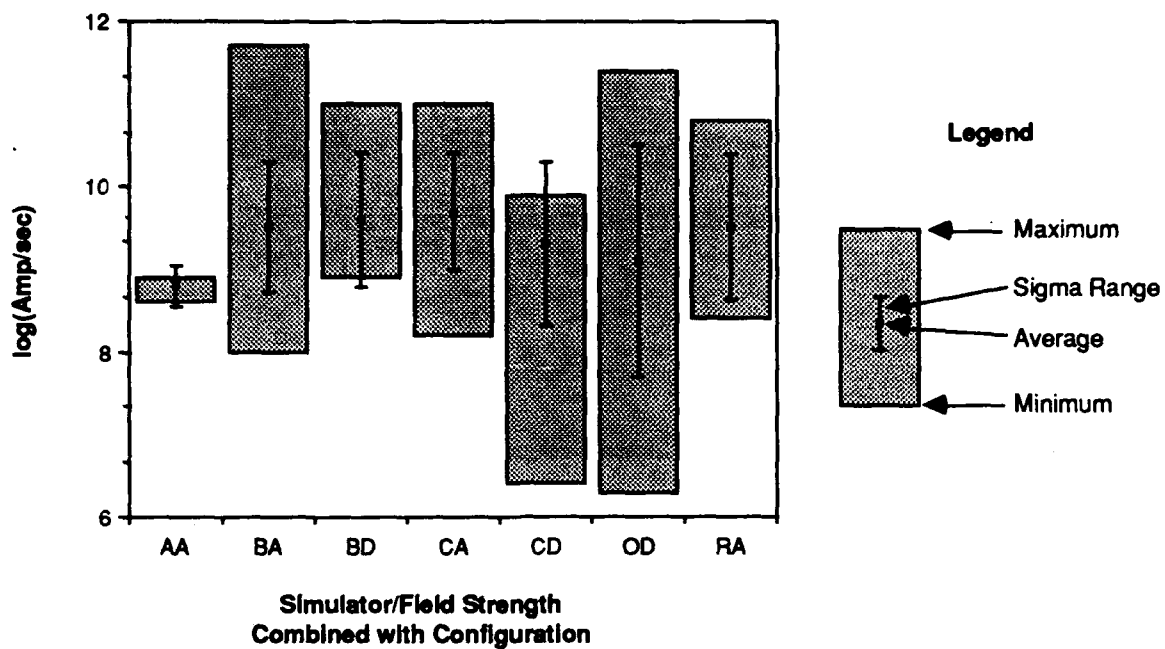
Figure 3-2. Maximum, Sigma, Average, and Minimum of the Log of the Peak Derivative Norm Versus Simulator and Configuration for All Test Points
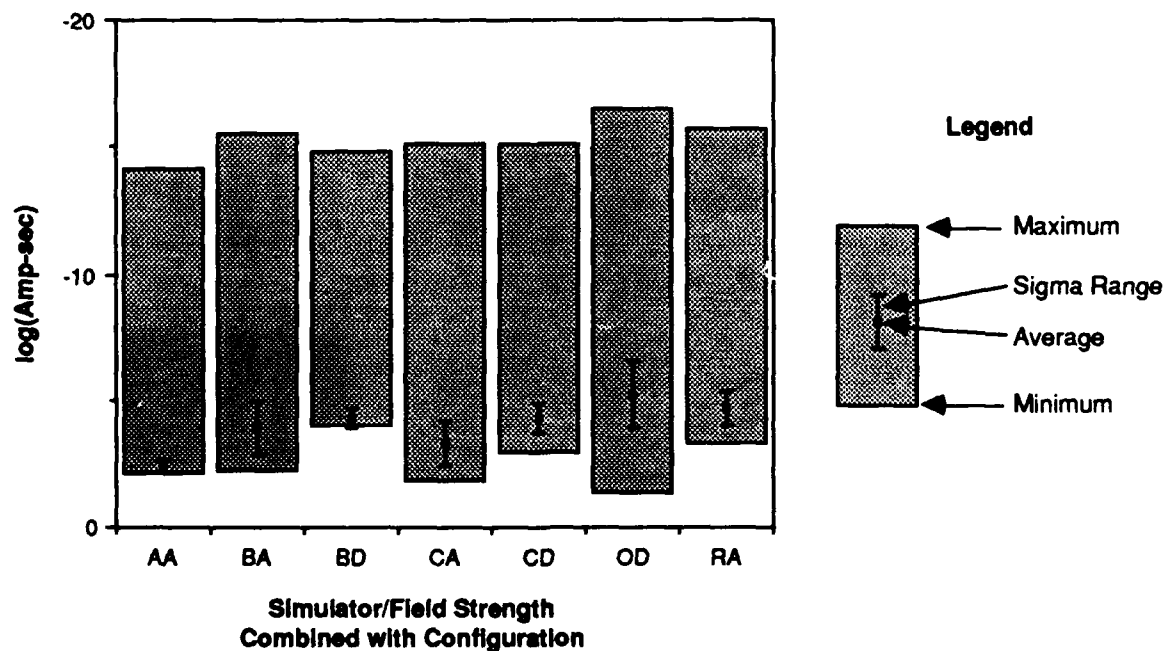
Figure 3-3. Maximum, Sigma, Average, and Minimum of the Log of the Impulse Norm Versus Simulator and Configuration for All Test Points

3-3
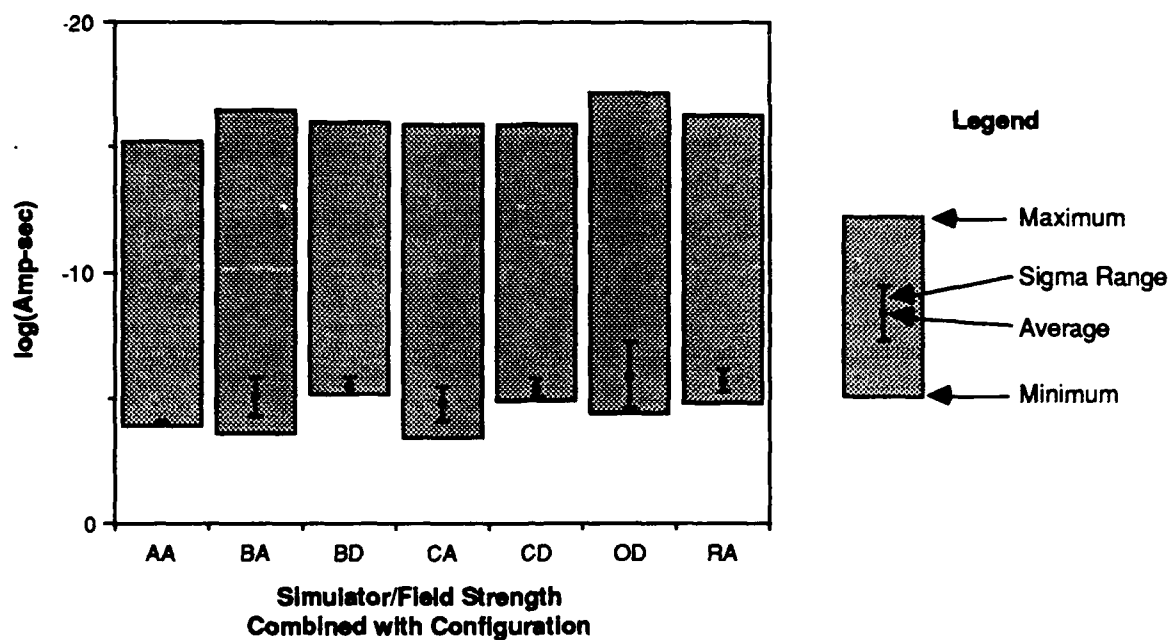
Figure 3-4. Maximum, Sigma, Average, and Minimum of the Log of the Rectified Impulse Norm Versus Simulator and Configuration for All Test Points
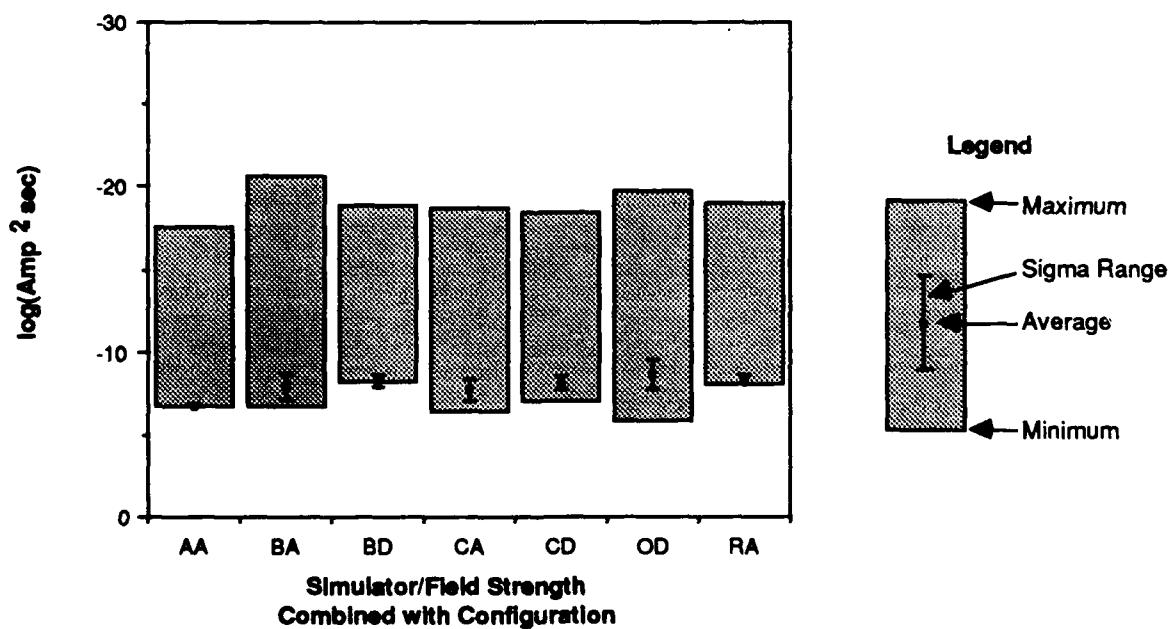
Figure 3-5. Maximum, Sigma, Average, and Minimum of the Log of the Action Integral Norm Versus Simulator and Configuration for All Test Points

4.0 AESOP 60 KV/M DATA ANALYSIS

The purpose of this portion of the analysis is to determine if the switch performance under the early time threat could be expected to differ from that observed at AESOP for a 60 kV/m incident field. The procedure to accomplish this is a direct comparison of the norm attributes for the extrapolated and raw data obtained at this field level.

These data are presented in **Table 4-1** below. The raw or unextrapolated data norms are the first entry for each test point and configuration while the corresponding extrapolated data norms are the second entry. Data for which the extrapolated peak amplitude norm exceeds the raw norm by a factor of 2 are indicated by an * preceding the configuration field. This occurs in 13 out of the 67 data sets. The largest increase in the peak amplitude due to extrapolation is a factor of 3. Based on this analysis, there is no evidence to indicate that the DMS-100 will perform any differently in the DoD-STD-2169 early time environment than it did at the AESOP simulator at the 60 kV/m field level, however, this may not be the case for all systems. As a matter of fact, most of the norms indicate that the switch was overdriven during this phase of the test. A caveat is in order relative to this point. That trunk lines attached to the switch were much shorter than those expected in an operational switch. This may have reduced the induced signal. With the EMI filters installed, this does not appear to be a problem since most of the late time signals internal to the switch resulted from the filter ring down. Also, most of the cable induced signals are dispersed in nature and in a frequency band which the system filters are designed to handle.

4.1 CONFIGURATION EFFECTS

This section investigates the effects of the configuration on the extrapolated data. The grounding configuration was modified greatly when the DMS-100 was moved to AESOP for testing resulting in larger amplitude signals. While at all three simulators, the shielding configuration was varied by removing portions or all of the EMI package. However, due to the grounding changes between REPS and AESOP and the incomplete system at Ottawa, only configuration changes at AESOP are analyzed.

Table 4-1

Comparison Of Raw and Extrapolated Data for Aesop 60 Kv/m Field

(Raw Data Followed By Extrapolated Data Norms)

T P T	C F G	PEAK AMPLITUDE	PEAK DERIVATIVE	IMPULSE	RECTIFIED IMPULSE	ACTION INTEGRAL
100	D	1.07E+02	6.52E+09	3.55E-06	3.59E-05	2.88E-02
100	D	1.41E+02	7.30E+09	7.82E-05	1.18E-04	5.14E-02
104	D	55.	1.42E+10	1.32E-05	8.06E-05	2.29E-02
104	D	62.	8.91E+09	1.40E-06	1.51E-05	1.22E-02
105	C	29.	1.48E+10	1.35E-05	9.40E-05	2.01E-02
105	C	7.1	1.33E+08	1.14E-06	1.18E-05	4.08E-03
105	D	30.	3.97E+09	1.18E-06	1.23E-05	8.27E-03
105	D	31.	6.29E+09	1.03E-05	6.72E-05	1.98E-02
107	A	78.	1.98E+10	4.47E-05	1.10E-04	3.54E-02
107	A	83.	7.29E+09	1.81E-06	3.43E-05	2.41E-02
108	A	26.	3.34E+09	7.17E-07	8.34E-06	6.12E-03
108	A	31.	3.60E+09	5.20E-06	2.27E-05	8.57E-03
109	A	25.	2.68E+09	6.96E-07	1.15E-05	9.11E-03
109	A	29.	3.33E+09	6.33E-06	2.40E-05	1.02E-02
110	D	4.9	1.98E+09	3.59E-05	1.28E-04	1.12E-02
110	D	0.36	2.57E+06	5.59E-07	7.07E-06	9.05E-04
111	D	26.	1.14E+10	7.26E-08	8.64E-06	6.96E-03
111	D	9.9	3.81E+09	3.21E-06	4.74E-06	2.97E-03
115	A	19.	6.34E+09	1.13E-07	3.70E-06	3.38E-03
115	A	6.4	1.67E+09	2.86E-06	4.83E-06	3.01E-03
140	A	84.	2.39E+10	2.76E-06	7.74E-06	1.39E-02
140	*A	2.44E+02	8.02E+10	1.01E-06	4.55E-05	4.54E-02
200	D	62.	7.06E+09	6.82E-06	3.27E-05	2.36E-02
200	D	84.	2.39E+10	1.74E-06	2.75E-05	2.01E-02
201	C	2.12E+02	2.05E+10	7.28E-05	1.38E-04	7.79E-02
201	C	2.16E+02	4.49E+10	4.38E-06	3.81E-05	3.54E-02
201	D	1.55E+02	7.39E+09	1.08E-05	4.00E-05	2.97E-02
201	D	2.00E+02	1.62E+10	9.45E-05	2.53E-04	0.10

Table 4-1 (cont'd)

TPT	CFG	PEAK AMPLITUDE	PEAK DERIVATIVE	IMPULSE	RECTIFIED IMPULSE	ACTION INTEGRAL
203	A	33.	5.56E+09	5.99E-06	1.94E-05	1.55E-02
203	A	49.	1.49E+10	1.04E-06	2.28E-05	1.52E-02
215	D	45.	3.45E+09	1.31E-05	7.84E-05	3.51E-02
215	*D	1.38E+02	3.29E+09	9.49E-05	3.56E-04	0.13
300	D	21.	5.74E+08	1.90E-06	2.32E-05	1.17E-02
300	*D	48.	1.16E+09	7.74E-05	1.19E-04	2.26E-02
300	E	25.	8.55E+08	1.65E-06	3.03E-05	1.29E-02
300	*E	70.	1.54E+10	5.01E-05	1.31E-04	2.65E-02
301	D	31.	9.21E+08	2.03E-06	2.84E-05	1.46E-02
301	*D	65.	2.46E+09	9.78E-06	7.83E-05	2.27E-02
301	E	60.	6.69E+09	2.00E-06	2.15E-05	1.60E-02
301	E	70.	8.20E+09	3.26E-05	6.78E-05	2.49E-02
301	F	58.	5.01E+09	7.04E-06	5.09E-05	2.77E-02
301	*F	1.18E+02	8.75E+09	4.81E-05	1.60E-04	7.57E-02
310	A	66.	3.10E+09	1.33E-05	5.63E-05	2.54E-02
310	A	1.13E+02	5.86E+09	1.20E-04	2.91E-04	0.12
310	D	41.	1.57E+09	1.12E-05	6.10E-05	2.33E-02
310	*D	1.09E+02	1.38E+09	9.79E-05	2.77E-04	0.10
311	A	26.	1.26E+09	5.72E-06	1.99E-05	1.10E-02
311	A	49.	6.51E+09	5.07E-05	1.83E-04	5.45E-02
311	D	23.	6.34E+08	5.35E-06	2.01E-05	1.08E-02
311	D	41.	5.21E+11	4.93E-05	1.62E-04	4.96E-02
316	D	70.	1.76E+10	6.25E-06	5.00E-05	2.70E-02
316	D	1.21E+02	3.08E+09	9.42E-05	1.82E-04	9.99E-02
318	D	34.	4.42E+08	6.11E-06	5.80E-05	2.17E-02
318	*D	87.	2.28E+09	1.06E-04	2.97E-04	7.33E-02
319	D	26.	2.27E+09	1.09E-06	8.41E-06	6.11E-03
319	D	39.	3.85E+09	9.15E-06	3.19E-05	1.30E-02
325	E	1.13E+03	3.41E+11	3.17E-04	9.56E-04	0.38
325	E	1.35E+03	1.34E+11	3.24E-05	2.66E-04	0.30
325	F	1.30E+03	1.44E+11	7.20E-05	4.09E-04	0.30
325	F	1.42E+03	3.66E+11	5.34E-04	1.71E-03	0.67

Table 4-1 (cont'd)

TPT.	CFG	PEAK AMPLITUDE	PEAK DERIVATIVE	IMPULSE	RECTIFIED IMPULSE	ACTION INTEGRAL
401	E	39.	3.53E+11	1.52E-05	1.87E-05	1.45E-02
401	E	62.	2.22E+10	7.59E-07	2.60E-05	1.59E-02
402	E	64.	8.91E+09	3.28E-06	1.24E-05	1.34E-02
402	E	75.	2.28E+10	1.22E-06	2.71E-05	1.83E-02
403	E	62.	6.87E+09	1.01E-05	2.60E-05	2.03E-02
403	E	65.	2.29E+10	1.20E-06	2.97E-05	1.94E-02
404	A	1.88E+02	5.65E+10	1.08E-05	2.80E-05	3.74E-02
404	A	3.07E+02	9.87E+10	2.15E-06	7.13E-05	6.50E-02
404	C	1.52E+02	2.40E+10	1.54E-05	1.97E-05	3.26E-02
404	C	2.07E+02	4.91E+10	2.58E-06	3.19E-05	3.67E-02
407	D	1.61E+02	2.00E+10	1.95E-05	4.78E-05	3.96E-02
407	D	1.83E+02	3.64E+10	3.70E-06	4.18E-05	3.15E-02
407	E	91.	2.09E+10	4.37E-06	4.40E-05	3.33E-02
407	E	1.60E+02	1.00E+10	3.61E-05	6.01E-05	5.22E-02
409	E	92.	2.38E+10	4.33E-06	4.30E-05	3.33E-02
409	E	1.60E+02	8.31E+09	3.56E-05	5.98E-05	5.21E-02
410	A	1.04E+02	3.07E+10	1.05E-06	1.24E-05	2.07E-02
410	A	1.66E+02	6.42E+10	7.70E-07	3.27E-05	3.15E-02
411	A	5.8	1.85E+09	2.77E-07	2.81E-06	2.13E-03
411	A	8.5	2.37E+09	1.05E-07	3.04E-06	2.33E-03
411	E	22.	7.30E+09	1.51E-07	7.73E-06	4.75E-03
411	E	6.7	2.81E+09	5.16E-07	2.78E-06	2.50E-03
414	A	16.	5.87E+09	1.18E-07	5.63E-06	4.16E-03
414	A	7.2	4.25E+09	2.91E-07	2.84E-06	2.31E-03
415	A	20.	7.34E+09	1.98E-07	6.56E-06	5.00E-03
415	A	9.4	4.11E+09	9.81E-07	5.29E-06	3.74E-03
415	E	13.	5.13E+09	1.30E-07	3.94E-06	2.96E-03
415	E	5.4	1.13E+10	6.78E-07	2.43E-06	2.20E-03
416	A	3.3	6.86E+08	5.99E-08	7.64E-07	7.29E-04
416	A	5.1	1.30E+09	4.37E-08	1.33E-06	1.01E-03
418	A	15.	3.10E+09	2.65E-07	3.19E-06	2.95E-03
418	A	16.	2.54E+09	6.51E-07	3.90E-06	3.65E-03

Table 4-1 (cont'd)

T P T	C F G	PEAK AMPLITUDE	PEAK DERIVATIVE	IMPULSE	RECTIFIED IMPULSE	ACTION INTEGRAL
429	C	3.9	1.50E+09	4.97E-07	4.45E-06	8.89E-04
429	C	0.91	2.62E+07	4.91E-08	9.04E-07	3.52E-04
460	A	20.	6.84E+09	9.82E-08	5.09E-06	4.10E-03
460	A	6.9	4.15E+09	5.18E-07	2.35E-06	2.18E-03
471	A	3.5	1.10E+09	7.58E-08	5.10E-07	5.27E-04
471	*A	7.7	3.22E+09	2.68E-08	1.20E-06	1.11E-03
500	D	20.	7.13E+08	6.56E-07	2.47E-05	9.70E-03
500	D	25.	7.78E+09	1.70E-05	5.09E-05	1.33E-02
601	B	1.7	5.12E+08	5.32E-09	1.89E-07	2.50E-04
601	B	0.76	2.74E+08	5.74E-09	4.22E-08	1.02E-04
602	A	1.6	1.19E+09	1.17E-07	5.33E-07	3.21E-04
602	A	1.7	1.72E+08	2.02E-08	2.79E-07	3.31E-04
700	A	11.	4.20E+09	3.62E-08	2.62E-06	1.79E-03
700	A	5.4	1.99E+09	3.21E-08	2.71E-07	4.53E-04
701	A	1.4	5.62E+08	8.61E-09	6.29E-07	3.86E-04
701	A	0.60	3.53E+08	2.34E-08	1.64E-07	1.90E-04
702	A	1.1	5.45E+08	2.90E-08	1.21E-07	1.64E-04
702	*A	2.9	1.15E+09	8.92E-09	1.30E-06	6.96E-04
703	E	2.4	9.42E+08	6.76E-08	3.17E-07	5.56E-04
703	E	3.3	1.51E+09	4.28E-08	7.55E-07	8.43E-04
706	A	1.1	4.44E+08	2.36E-08	3.30E-07	2.95E-04
706	*A	2.2	8.44E+08	1.32E-08	7.27E-07	5.11E-04
707	A	1.4	4.45E+08	8.96E-09	4.80E-07	3.18E-04
707	A	0.63	4.29E+08	3.09E-08	2.33E-07	1.86E-04
707	E	1.8	7.63E+08	6.42E-09	7.98E-07	4.83E-04
707	E	0.72	3.10E+08	1.11E-08	1.67E-07	1.68E-04
707	F	14.	3.88E+09	8.95E-08	3.95E-06	2.69E-03
707	F	6.8	1.26E+09	1.19E-07	1.00E-06	1.29E-03
770	E	1.9	5.86E+08	1.45E-08	5.02E-07	3.96E-04
770	E	0.98	2.69E+08	3.46E-08	3.82E-07	2.86E-04
771	E	0.51	1.25E+07	4.62E-08	7.40E-07	2.46E-04
771	E	0.77	3.52E+08	4.35E-07	4.68E-06	7.93E-04

Table 4-1 (concluded)

T P T	C F G	PEAK AMPLITUDE	PEAK DERIVATIVE	IMPULSE	RECTIFIED IMPULSE	ACTION INTEGRAL
800	A	51.	1.92E+11	1.40E-06	1.66E-05	1.59E-02
800	A	60.	1.31E+10	1.19E-06	1.91E-05	1.66E-02
801	A	19.	3.26E+09	2.19E-07	3.19E-06	4.22E-03
801	A	22.	4.90E+09	2.19E-07	5.73E-06	5.01E-03
802	A	97.	7.87E+11	2.34E-06	2.61E-05	2.59E-02
802	A	1.19E+02	3.21E+10	2.28E-06	3.67E-05	3.04E-02
803	A	68.	3.65E+10	7.13E-07	6.84E-06	1.21E-02
803	*A	1.40E+02	4.39E+10	6.84E-07	1.44E-05	2.02E-02
804	A	48.	1.35E+10	4.32E-07	6.09E-06	9.63E-03
804	*A	95.	2.82E+10	4.37E-07	1.13E-05	1.41E-02

4.2 GROUNDING CONFIGURATION EFFECTS

The grounding configuration of the DMS-100 was modified significantly when the test article was moved to the AESOP simulator. The grounding configurations are illustrated in **Figures 4-1** and **4-2**. The primary difference was that the Ottawa and REPS grounding scheme provided for a large ground loop with an aperture defined by the length and height of the trailer. When the DMS-100 was moved to AESOP, a single point ground was provided and the grounding cable from the trunk line entry point to the power supply at the rear of the trailer was opened. The power supply ground was routed to the front of the trailer and connected to the splice case ground. Based upon the loop area in the REPS configuration (45 m^2) and assuming a wave impedance of 377 Ω, the extrapolated REPS data for common test point would be a factor of 7 higher than the AESOP data. Norm attributes for common test points under common configuration are presented in **Table 4-2**. With the exception of test points 108 and 500, all of the REPS data norms are greater than the corresponding AESOP data by factors of 4 to 10. **Figures 4-3** through **4-8** present the extrapolated responses. The time domain extrapolated data are in the top two graphs for AESOP and REPS respectively. The bottom graph represents the gain of the transfer function in dB from the AESOP to REPS measurements. In all cases, including test point 500, there is significant low frequency gain as would be expected. Typically, 20 to 30 dB gains are seen across broad portions of the spectrum. This is consistent with the loop induced current and substantiates the notion that the grounding configuration is extremely important.
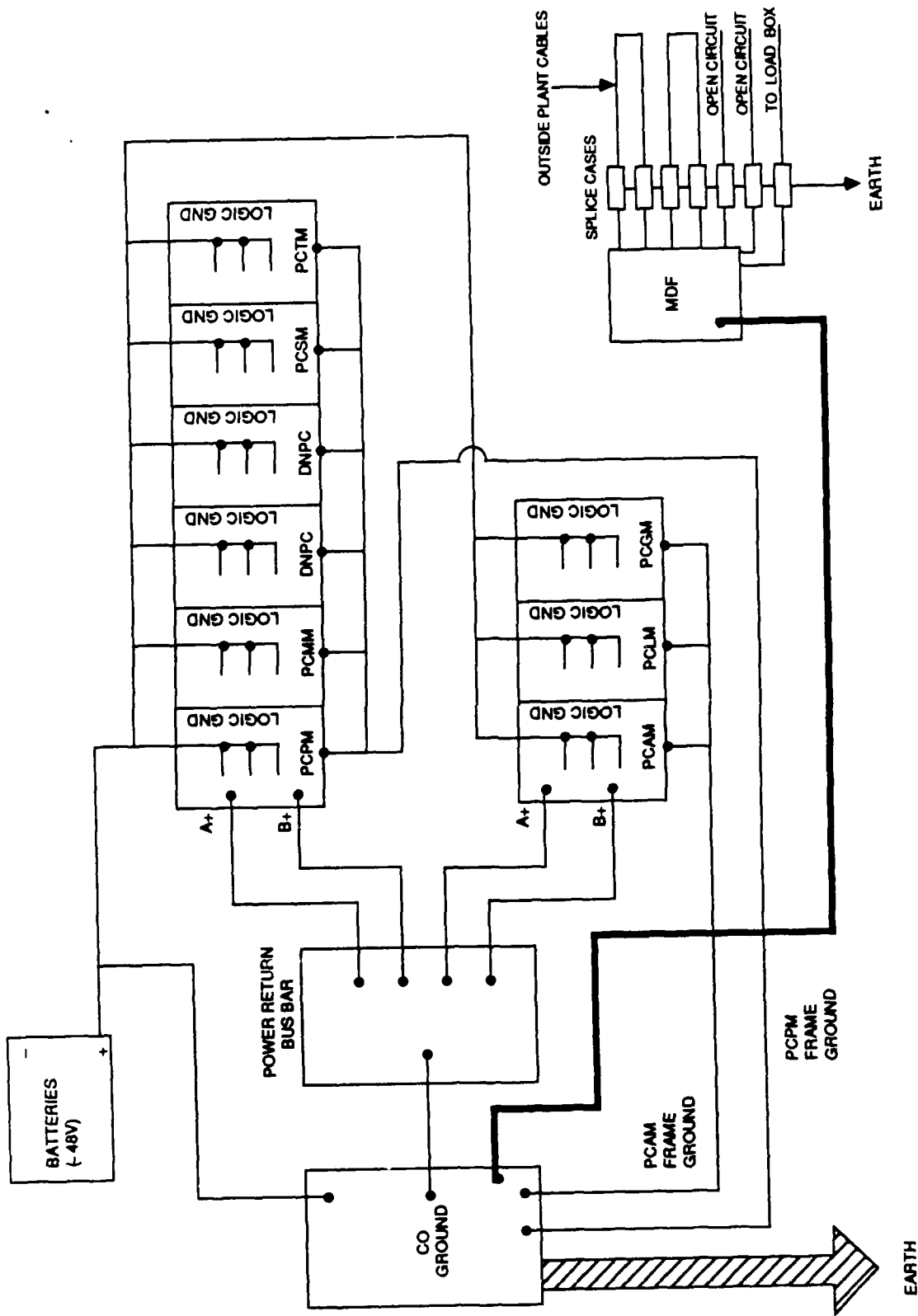
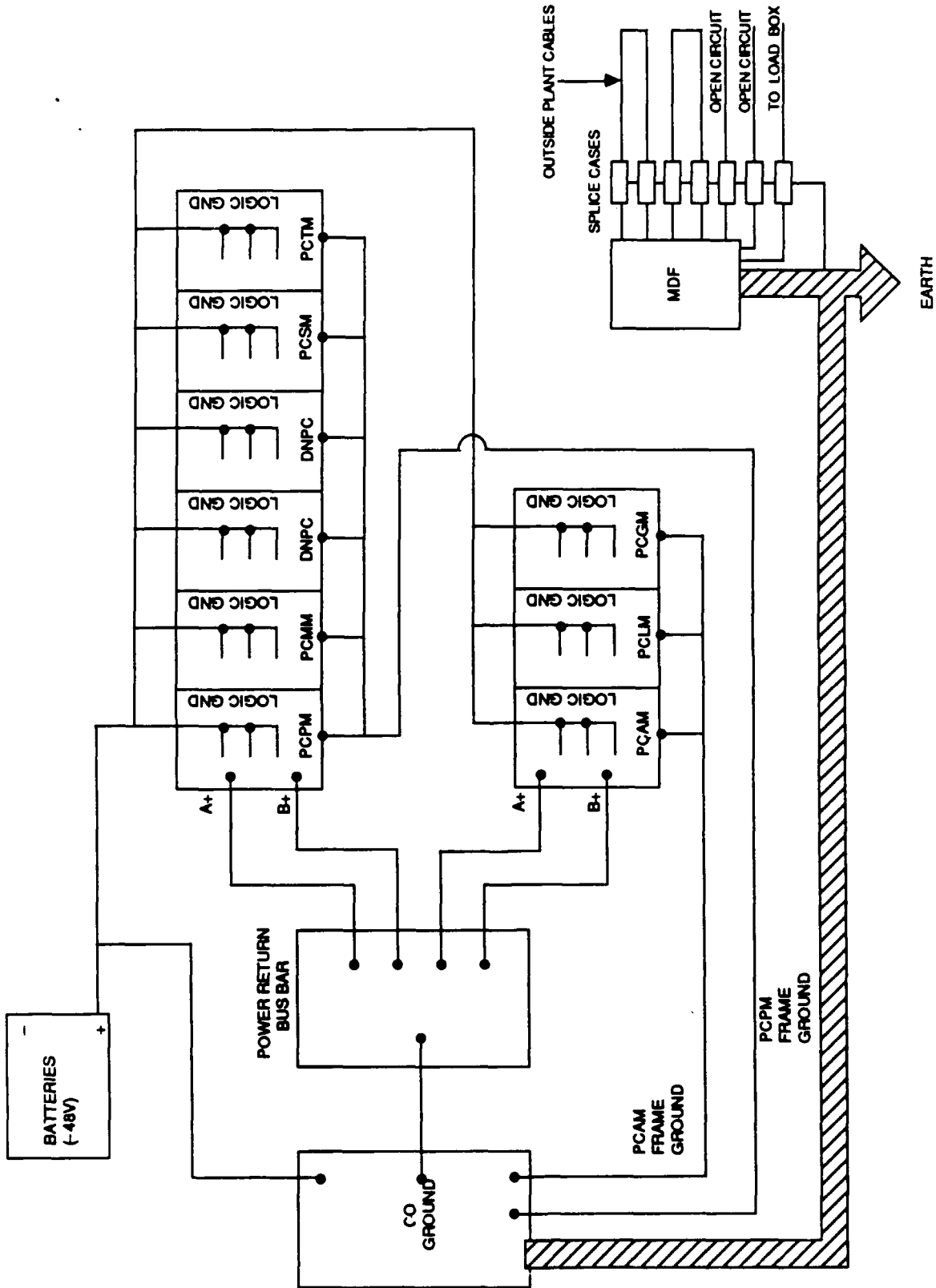**Figure 4-1. Grounding Configuration for Ottawa and REPS Tests**

Figure 4-2. Grounding Configuration for AESOP Test

Table 4-2. AESOP/REPS Common Test Point Norms Comparison

FACILITY	AESOP	REPS	AESOP	REPS
NORM/TESTPOINT	A110AA30	R110AR25	B450AA30	R450AR25
PEAK 6.33	25.3	3.69	7.78	
PEAK DERIV	2.648E+08	1.224E+10	2.940E+08	1.085E+08
IMPULSE	1.206E-06	1.361E-06	1.351E-07	2.711E-06
REC IMPULSE	4.216E-06	7.652E-06	1.299E-06	2.515E-05
RMS ACTION	2.637E-03	6.077E-03	9.808E-04	4.851E-03
C108AA30	R108AR25	C415AA30	R415AR25	
PEAK 25.8	25.2	18.0	88.7	
PEAK DERIV	1.215E+09	8.090E+08	8.423E+09	4.659E+10
IMPULSE	7.401E-07	3.040E-06	2.007E-07	2.195E-07
REC IMPULSE	7.262E-06	3.273E-05	4.426E-06	8.821E-06
RMS ACTION	5.829E-03	8.891E-03	4.639E-03	1.457E-02
B500AA30	R500AR25	C700AA30	R700AR25	
PEAK 576.	18.8	8.35	61.3	
PEAK DERIV	1.689E+10	3.331E+08	2.700E+09	2.286E+10
IMPULSE	2.201E-05	6.147E-06	3.117E-08	1.071E-07
REC IMPULSE	2.802E-04	4.357E-05	2.431E-06	3.973E-06
RMS ACTION	0.257	1.145E-02	1.666E-03	1.081E-02

Figure 4-3. AESOP-REPS Comparison for Test Point 108

AESOP Data for Testpoint 110

REPS Data for Testpoint 110

AESOP to REPS Transfer Function Gain for Testpoint 110

Figure 4-4. AESOP-REPS Comparison for Test Point 110

4-11

Figure 4-5. AESOP-REPS Comparison for Test Point 415

AESOP Data for Testpoint 450

(graph: AMPERES vs TIME, vertical axis from -6.00 to 4.00, horizontal axis from 0.00 to 1.00E-05)

REPS Data for Testpoint 450

(graph: AMPERES vs TIME, vertical axis from -6.00 to 4.00, horizontal axis from 0.00 to 1.00E-04)

AESOP to REPS Transfer Function Gain for Testpoint 450

(graph: dB GAIN vs FREQUENCY, vertical axis from -10.00 to 60.00, horizontal axis from 1000.00 to 1.00E+07)

Figure 4-6. AESOP-REPS Comparison for Test Point 450

4-13

AESOP Data for Testpoint 500

REPS Data for Testpoint 500

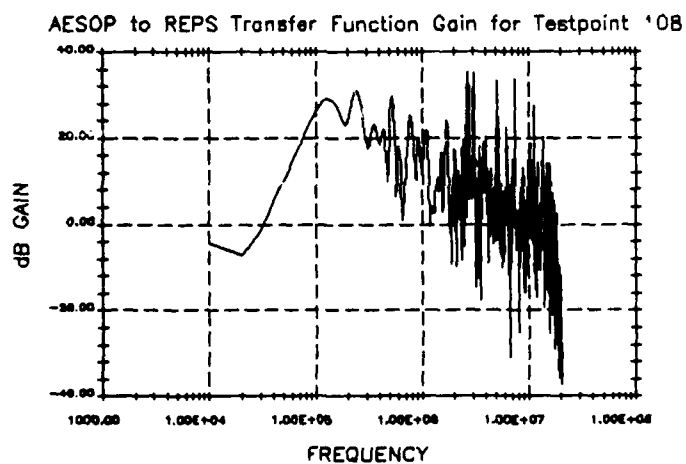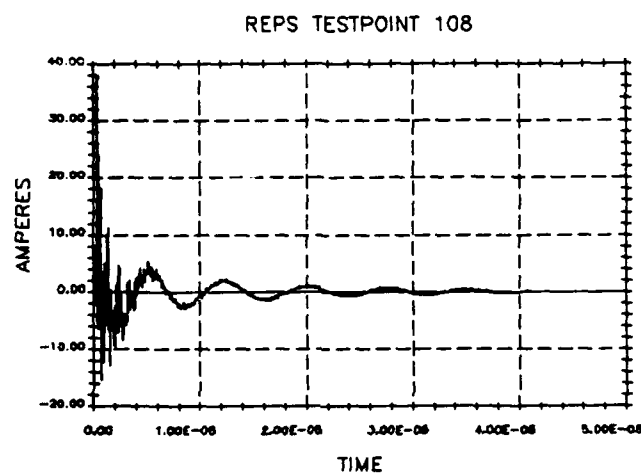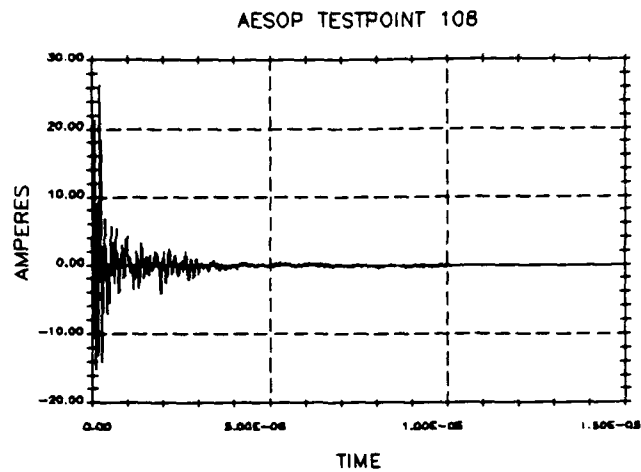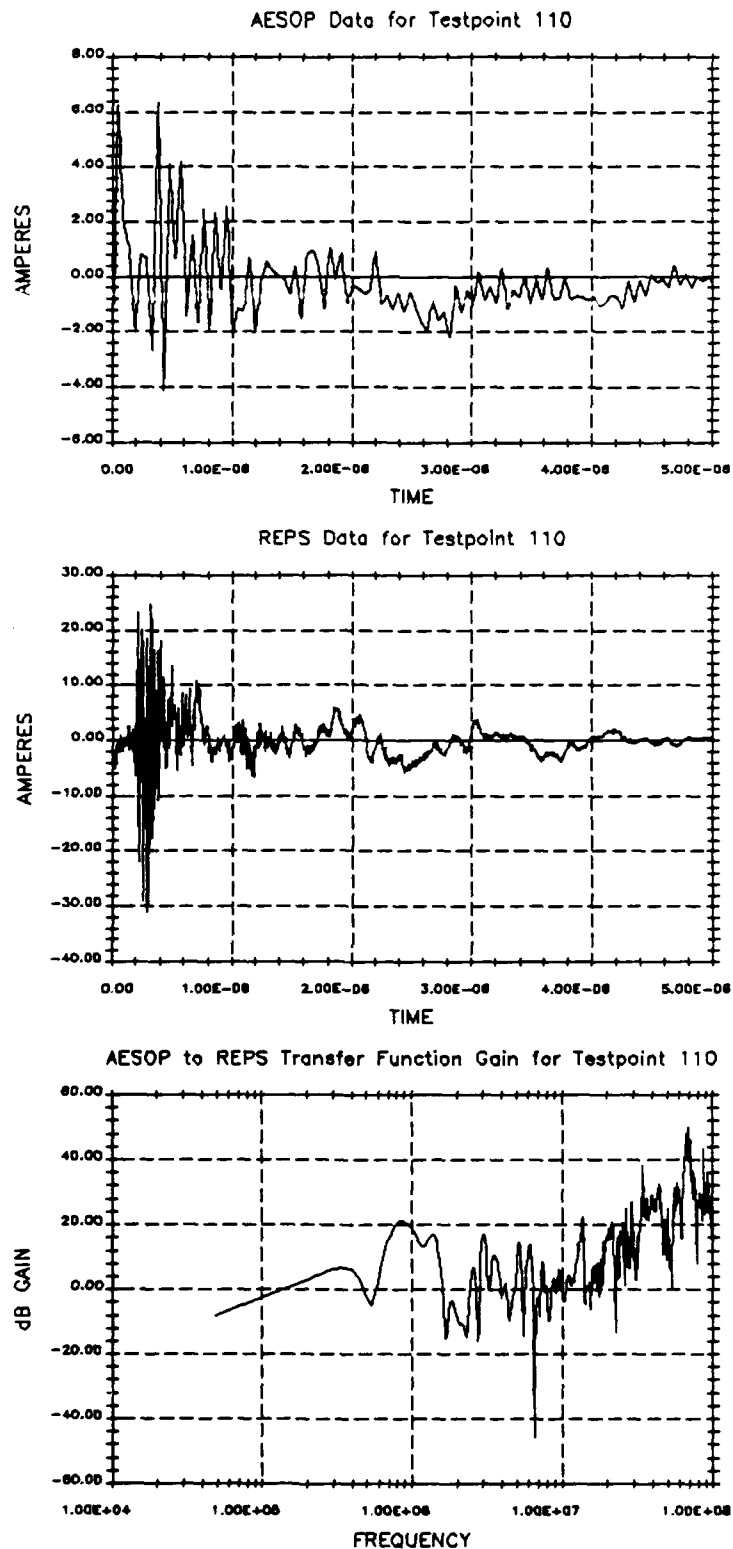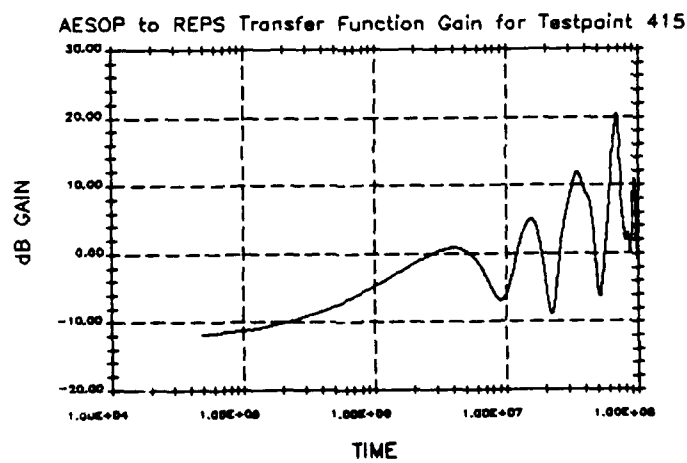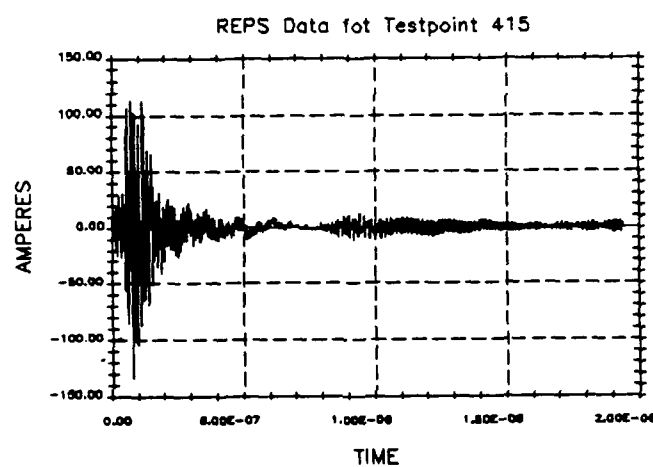AESOPT to REPS Transfer Function Gain for Testpoint 500

Figure 4-7. AESOP-REPS Comparsion for Test Point 500
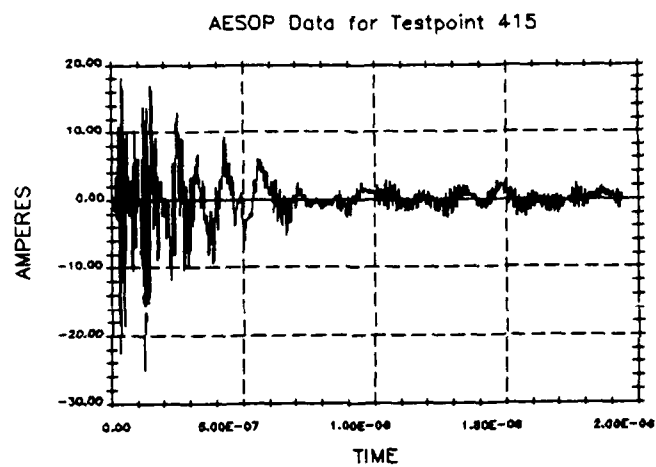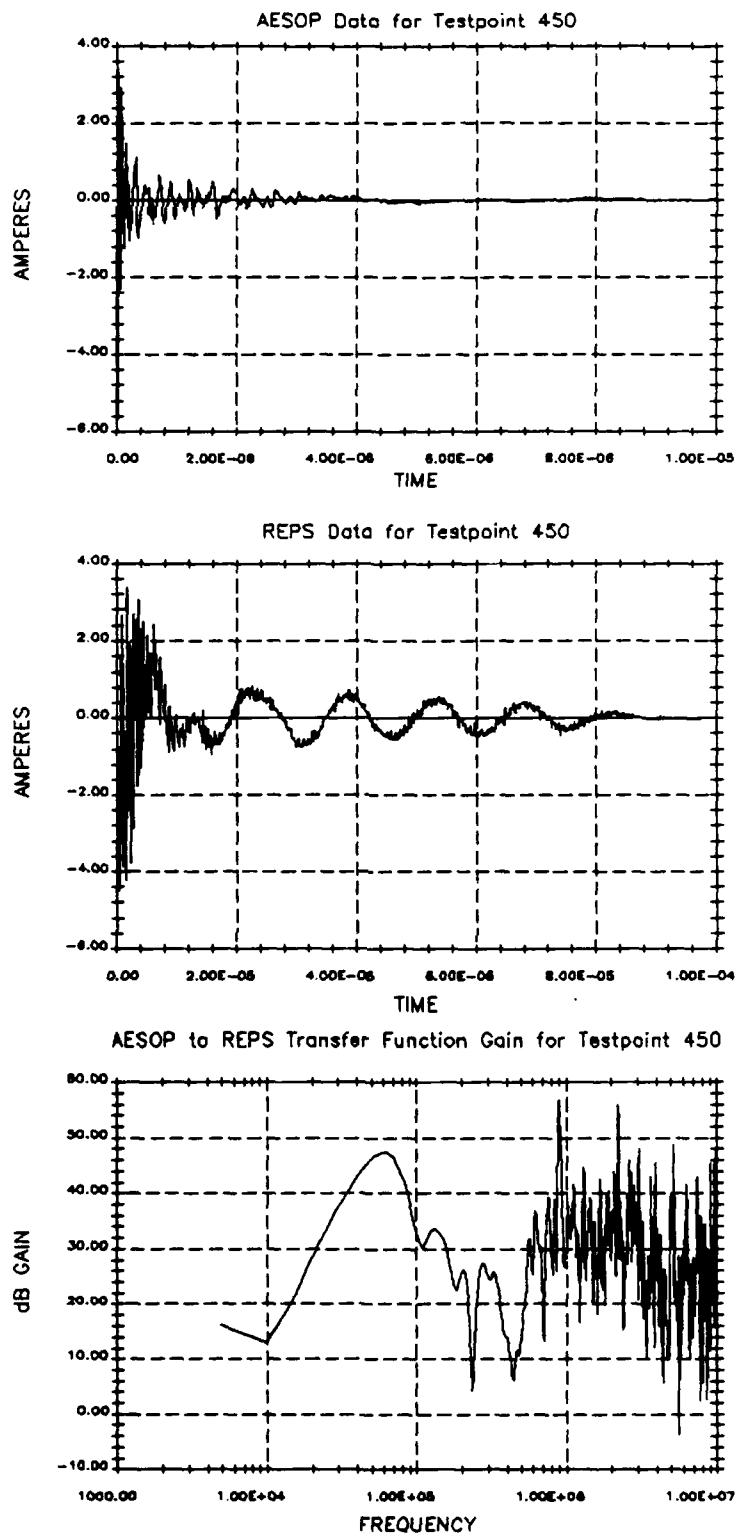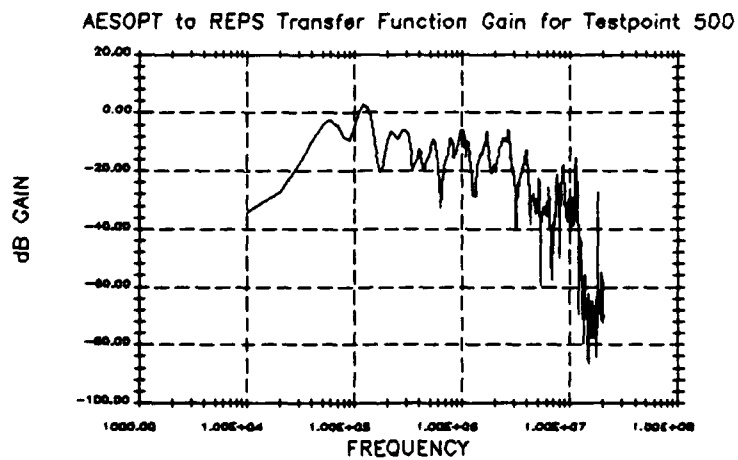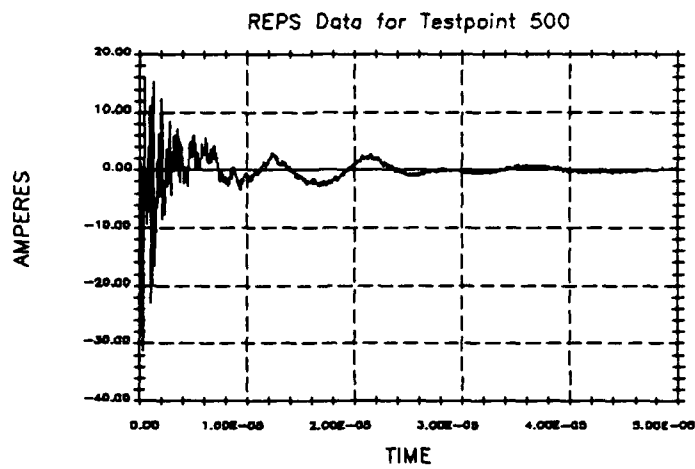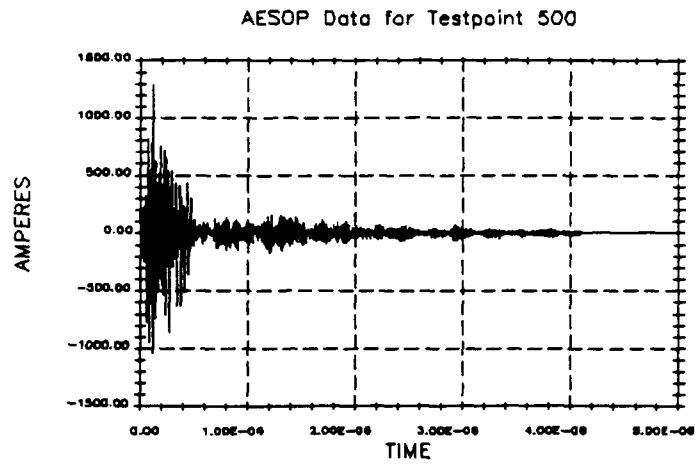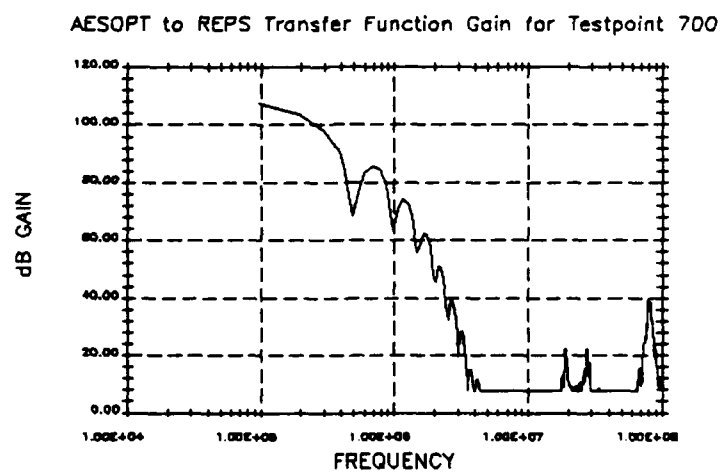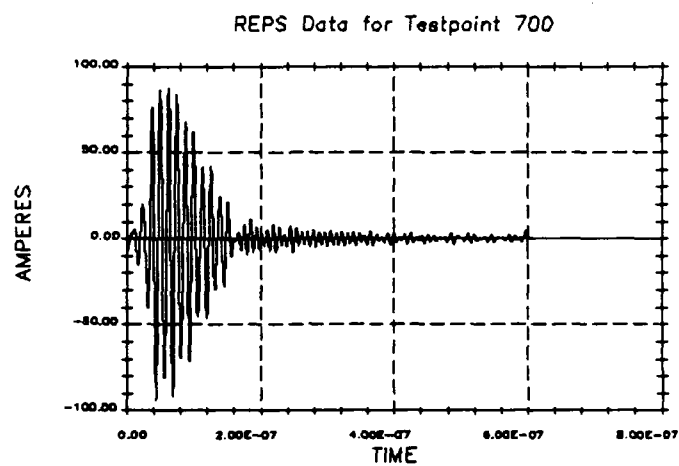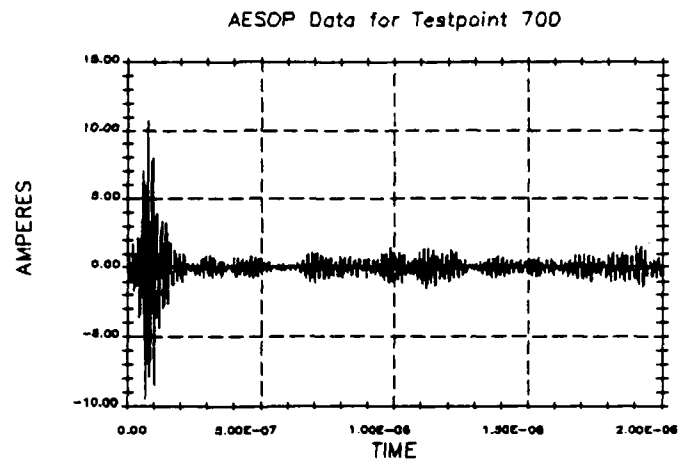
Figure 4-8. AESOP-REPS Comparsion for Test Point 700

4.3 AESOP EMI SHIELDING CONFIGURATION EFFECTS

The effects of the various panel, filter and LCM cable routing have been investigated. The facility and configuration keys are repeated below:

FACILITY KEY	CONFIGURATION KEY
A - AESOP (30KV/M)	A - PANELS OFF, FILTERS OFF
B - AESOP (45KV/M)	B - PANELS OFF, FILTERS ON
C - AESOP (60KV/M)	C - PANELS ON, FILTERS OFF
R - REPS (6KV/M)	D - PANELS ON, FILTERS ON
O - OTTAWA (2.5KV/M)	E - CCC PANELS ON, TRUNK FILTERS ON, LCM PANELS OFF, LCM FILTERS ON
	F - CCC PANELS ON, TRUNK FILTERS OFF, LCM PANELS OFF, LCM FILTERS ON, LCM CABLE LOOPED AROUND

There are 24 data sets that have a common pulser field level and test points but have configurational changes in the DMS-100 limited direct comparisons. The analysis is limited to common field levels since the norm attributes appear to be dependent upon the field levels. This is presented in the following section. The transfer function gains were determined in alphabetical order between each configuration. For example, there are three measurements in configuration A (panels off, filters off) with corresponding measurements in configuration E (CCC panels on, Trunk filters on, LCM panels off and LCM filters off and LCM filters off) and the transfer function of the configuration A measurements to the configuration E measurements were determined. This procedure was used for all common test measurement that have only a configuration change at AESOP. Ottawa and REPS data were excluded due to the impact of the ground configuration discussed in the preceding section.

4.3.1 Configuration A to B Effects (Filters Only)

Configurations A and B correspond to the panels off/filters off and panels off/filters on configurations respectively. The common data relates to test point 407 which is the intra-office cable bundle on the line side of the PCLM filters. The transfer function gain is presented in **Figure 4-9**. The effect of the filters appears to be 20 dB reduction in the extrapolated signal in the 30 to 100 MHz band and a 10 dB gain in the .1 to 1 MHz band. Thus the filters reduce the high frequency component while enhancing the low frequency component. This low frequency enhancement may be due to the impulse ring down of the filter reflecting back onto the cable. The norm attributes for the two configurations is presented in **Table 4-3**. It is interesting to note that all norms have decreased by a factor of 2, with the filters installed except for peak impulse, which has increased.
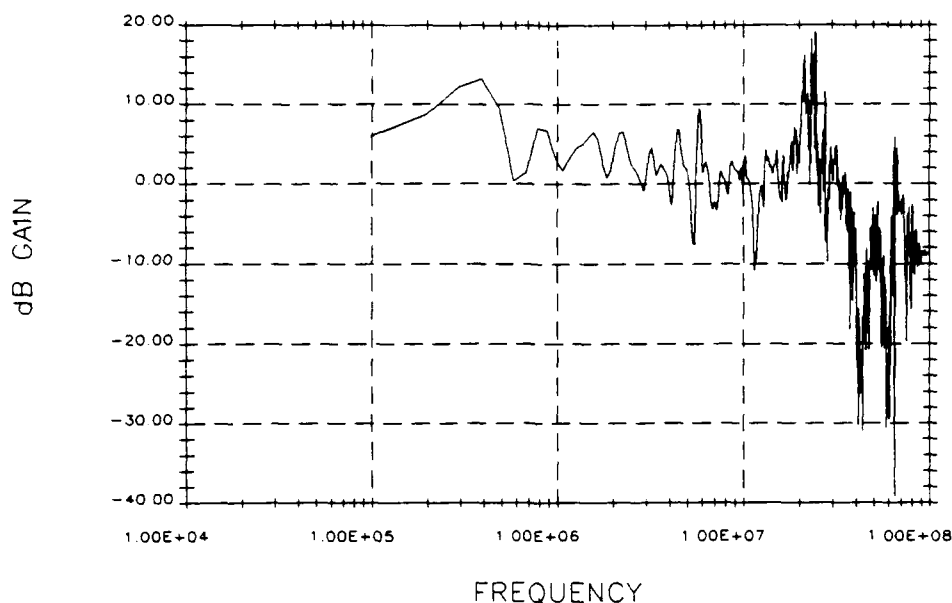
Figure 4-9. Configuration A to B Transfer Function

Table 4-3. Norm Data

	FL OFF B407AA30	FL ON B407BA30
PEAK	208.	109.
PEAK DERV	5.196E+10	1.799E+10
IMPULSE	3.032E-06	5.274E-06
REC IMPULSE	4.594E-05	3.175E-05
RMS ACTION	3.723E-02	2.731E-02

4.3.2 · Configuration A to C Effects (Panels Only)

Configurations A and C correspond to the EMI Filters shorted with the panels off and on respectively. The common data was obtained at test point 404 which is a single wire of the intra-office cable on the line side of the PCLM filters. The gain of the transfer function is presented in **Figure 4-10** and in this case, the lowfrequency enhancement is not present, further indicating that the filter transient response is the likely cause of the low frequency enhancement seen in the A to B data of **Figure 4-9**. There is considerably more structure in the transfer function but a general high frequency roll-off is clearly present, indicating that the panels do provide some high frequency attenuation. The source of the resonances is not understood at this time.

The norm comparison is presented in **Table 4-4.** Again, with the panels installed, all norms have decreased with the exception of the peak impulse. Also, the peak has been reduced by a factor of 2/3, however from the graph of the transfer function, the overall impact is seen to be a strong function of frequency. That norms would be sensitive to configuration is not surprising. However, the strong correlations indicated in the previous section would seem to imply that all norms should behave similarly under configuration changes. That this is not the case implies that the concept of norm correlation is open to interpretation.

Configuration A to D Transfer Function Gain for Testpoint 404
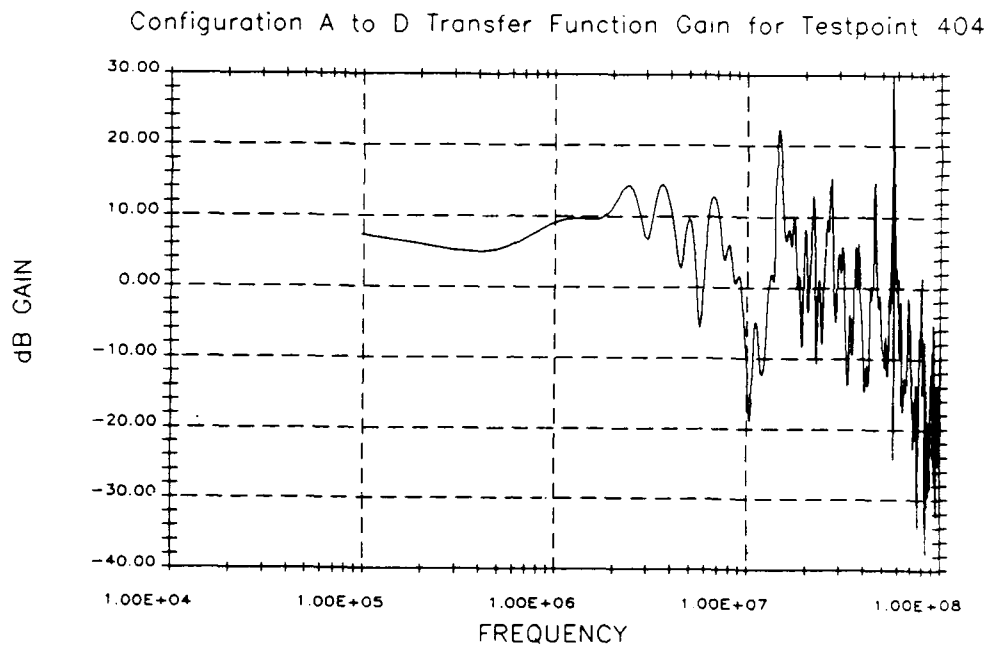
Figure 4-10. Configuration A to C Transfer Function

Table 4-4. Configuration A to C Norm Data

	PANELS OFF C404AA30	PANELS ON C404CA30
PEAK	307.	198.
PEAK DERV	9.774E+10	4.750E+10
IMPULSE	2.117E-06	2.598E-06
REC IMPULSE	6.063E-05	3.179E-05
RMS ACTION	6.160E-02	3.663E-02

4-18

4.3.3 Configuration A to D Effects (Panels and Filters)

Configurations A and D correspond to the EMI package circumvented and in place respectively. Test points 310 and 311 correspond to the outside plant cables on either side of the cable connector ground. Test point 311 is on the switch side of the ground while 310 is on the cable side of the ground. The transfer functions are presented in **Figure 4-11**. In both cases, the internal configuration is seen to have about a 10 dB effect in the 20 to 50 MHz band on the measured response. This is somewhat surprising considering the locations of the test points and may indicate that with the panels in place, the coupling is reduced significantly in this frequency band or that with the filters removed, there is a current reflection enhancing the measurement. Considering the other sources of impedance mismatching, this latter hypothesis seems unlikely and the attenuation is most likely attributable to the EMI shielding of the panels.

Configuration A to D Transfer Function for Testpoint 310

Configuration A to D Transfer Function for Testpoint 311
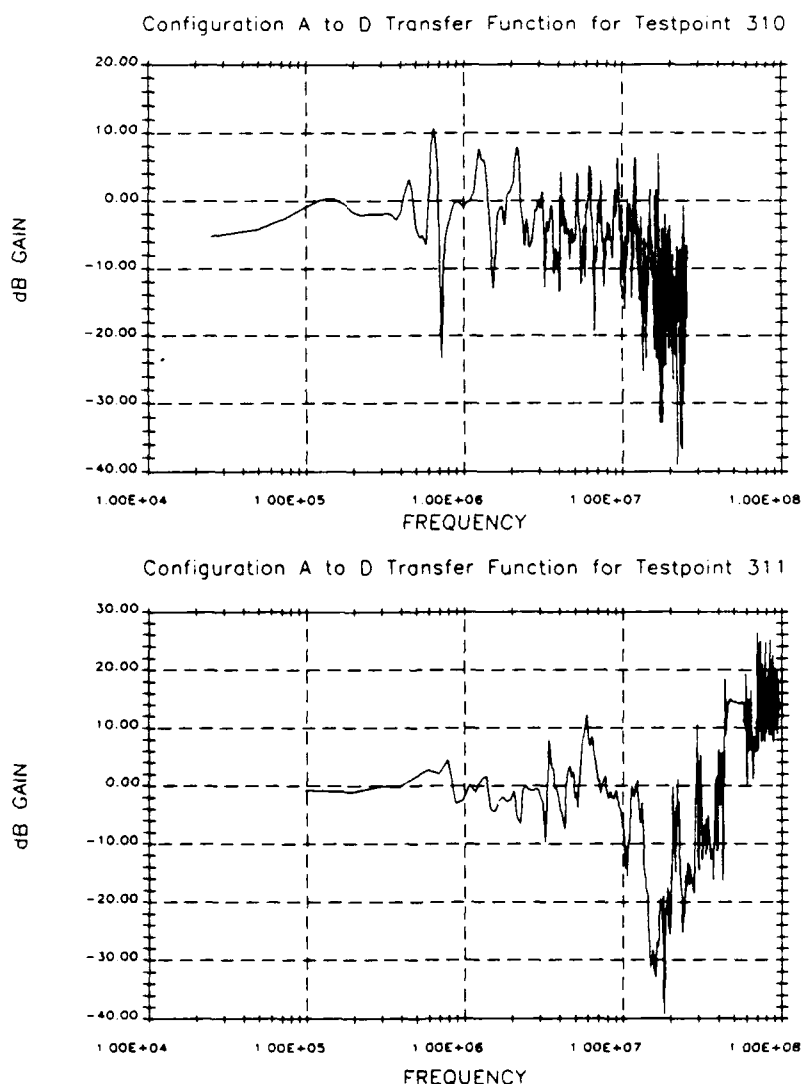
Figure 4-11. Configuration A to D Transfer Functions

The norm attributes are presented in **Table 4-5**. For the two test points considered, there is little difference to be noted. The high frequency effects in the gain of the transfer function are not reflected in the norm attributes in a consistent manner.

Table 4-5. Configuration A to D Norm Data

	w/o EMI C310AA30	w/ EMI C310DA30	w/o EMI C311AA30	w/ EMI C311DA30
PEAK	62.6	40.1	24.9	22.4
PEAK DERV	3.975E+09	1.438E+09	1.206E+09	1.019E+09
IMPULSE	1.330E-05	1.124E-05	5.728E-06	5.327E-06
REC IMPULSE	4.881E-05	5.286E-05	1.488E-05	1.245E-05
RMS ACTION	2.507E-02	2.313E-02	9.861E-03	8.061E-03

4.3.4 Configuration A to E Effects (DNPC Shield & Trunk , Filters On)

Figure 4-12 presents the transfer functions for the A to E measurements for test points 411, 415 and 707. Configuration E differs from A only in that the DNPC (Computer) panels were in place and the trunk filters in the CCC rack were installed. Otherwise, the EMI package was circumvented. Test points 411 and 415 are in the PCLM rack while test point 707 is an open wire hung between the two DNPC racks. From the figures, there is no impact on measurements in the PCLM racks as would be expected. With respect to test point 707, since the cable was open on both ends, this almost represents a noise measurement and has no interpretation related to the DMS-100. These particular data do provide some indication of the variability of the data with configuration changes and indicates that 5 to 10 dB variations in the transfer function gains may be more configuration dependent than real attributes of the data.

Table 4-6 presents the norm comparisons. Ignoring test point 707 for the reasons discussed above, it is seen that the configuration impact is somewhat mixed with testpoint 411 showing an increase while 415 actually decreased. This illustrates the complex nature of the coupling in the DMS-100 system.

Table 4-6. Configuration A to E Norm Data

NORM/TSTPNT	C411AA30	C411EA30	C415AA30	C415EA30	C707AA30	C707EA30
PEAK	8.42	19.1	17.6	11.6	1.40	1.74
PEAK DERIV	2.133E+09	7.196E+09	6.459E+09	4.334E+09	3.978E+08	7.556E+08
IMPULSE	1.053E-07	1.503E-07	2.007E-07	1.290E-07	8.836E-09	6.460E-09
REC IMPULSE	2.767E-06	5.849E-06	5.754E-06	3.285E-06	3.713E-07	5.840E-07
RMS ACTION	2.278E-03	4.415E-03	4.770E-03	2.796E-03	2.972E-04	4.438E-04

Configuration A to E Transfer Function Gain for Testpoint 411
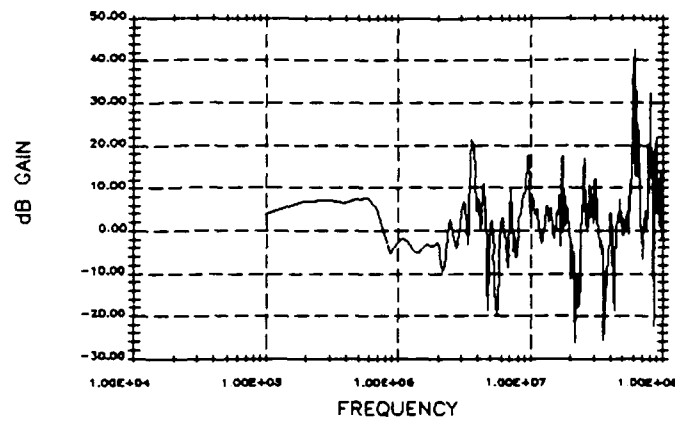
Configuration A to E Transfer Function Gain for Testpoint 415
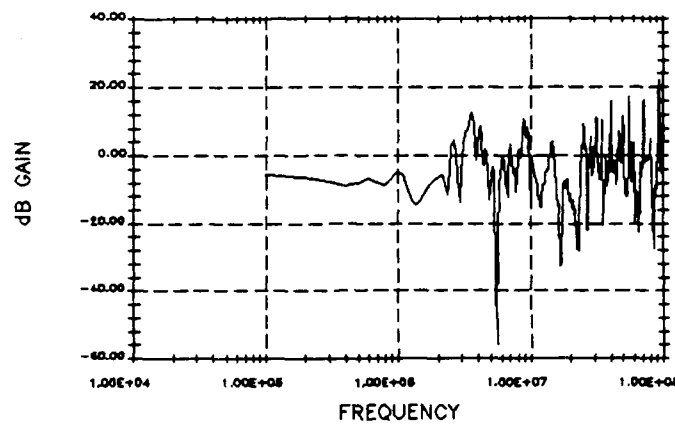
Configuration A to E Transfer Function Gain for Testpoint 707

Figure 4-12. Configuration A to E Transfer Functions

Configuration C to D Transfer Function Gain for Testpoint 105

Configuration C to D Transfer Function Gain for Testpoint 201

Figure 4-13. Configuration C to D Transfer Functions

4.3.5 Configuration C to D Effects (Filter Effect with Panels On)

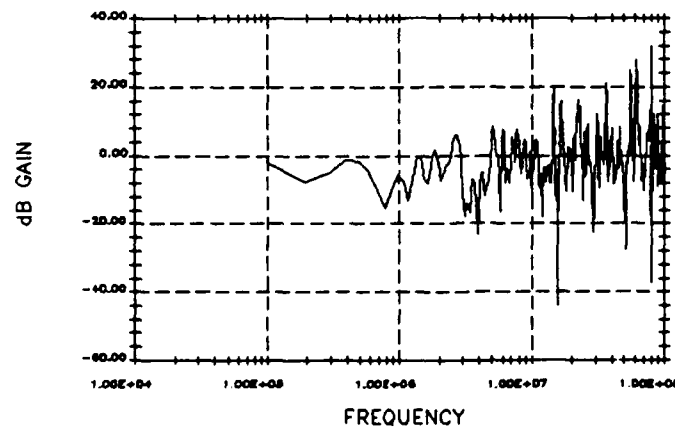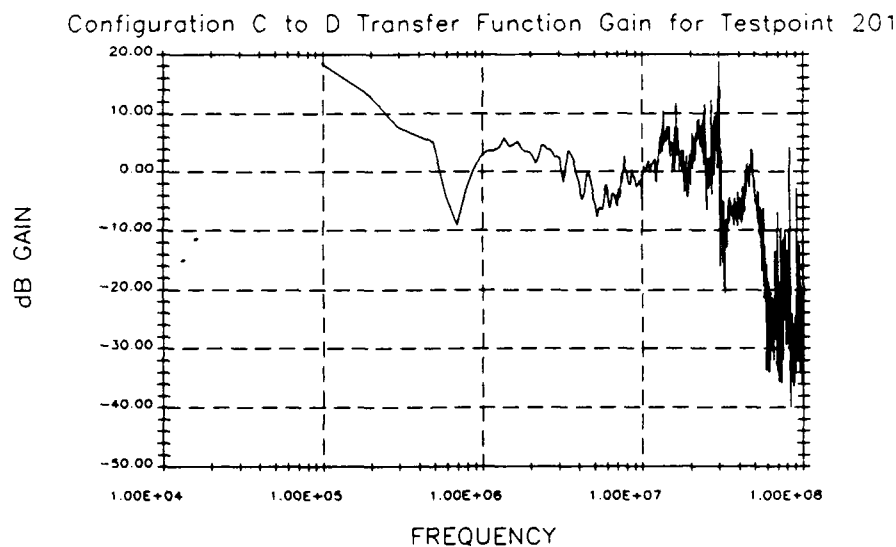This configuration variation illustrates the effect of the filters when the panels are in place. Configuration C has the filters removed while D has them in place. The data for test points 105 and 201 is presented in **Figure 4-13**. Test point 105 is the DC output of the power supply rectifiers while 201 is the power supply ground . These two cases are interesting in that the effects of the filters is opposite for the two measurements. The effect of the filters on the output of the power supply (test point 105) is to enhance the high frequency component of the signal by up to 40 dB, while the signal for the power supply ground is reduced by 10 to 20 dB at the higher frequencies. This may be more indicative of the pervasiveness of the ground circuits than the action of the filters but the data is consistent with other ground measurements.

4-22

The norm data are presented in **Table 4-7** and again appear confusing in that test point 105 shows an increase while 201 shows a decrease similar to the transfer function results. Again the norm behavior is not well correlated. In this case, the impulse norm for 105 is ill behaved. It may well be that the presence of filter devices affects the norm behavior more extensively than previous studies have indicated.

Table 4-7. Configuration C to D Norm Data

	w/o FL C105CA30	w/ FL C105DA30	w/o FL C201CA30	w/ FL C201DA30
PEAK	7.04	29.8	215.	151.
PEAK DERV	1.833E+08	6.708E+09	4.302E+10	1.708E+10
IMPULSE	1.132E-06	1.193E-06	4.357E-06	1.078E-05
REC IMPULSE	5.760E-06	7.631E-06	3.235E-05	2.994E-05
RMS ACTION	3.653E-03	6.261E-03	3.377E-02	2.821E-02

4.3.6 Configuration D to E Effects (LCM Panels and Filters Off)

The EMI package was degraded by removing the LCM rack panels and filters while leaving the computer rack protected. Common measurements were made at test points 300 and 407. Test point 300 is the outside plant cable bundle at the interface to the MDF and test point 407 is the intra-office cable bundle at the PCLM on the line side of the by-passed filters. The data are presented in **Figure 4-14**. There was no effect at the MDF interface, however, some effect at test point 407 can be seen. Test point 407 data are also presented in **Figure 4-14** for the A to B configuration, indicating the effect of the filters. It is reasonable that the D to E effects should be similar and it is at the higher frequencies. However, the low frequency gain is not present when both panels and filters are removed in the LCM rack. This seems to imply that the low frequency shielding provided in the D configuration is attributable to the filters in the LCM rack.

Norm data presented in **Table 4-8** are in agreement with the transfer functions. However, the impulse, rectified impulse and RMS action norms for 407 are very ill behaved. This may again indicate that filters have a deleterious effect on the utility of norms. The norms for testpoint 300 are well behaved, however, as illustrated by the transfer function, this testpoint is unaffected by the configuration change.

Table 4-8. Configuration D to E Norm Data

	C300DA30	C300EA30	C407DA30	C407EA30
PEAK	20.6	24.2	182.	88.9
PEAK DERV	7.446E+08	1.190E+09	3.642E+10	2.046E+10
IMPULSE	1.835E-06	1.577E-06	3.696E-06	4.373E-06
REC IMPULSE	1.422E-05	1.307E-05	3.429E-05	3.936E-05
RMS ACTION	9.603E-03	9.324E-03	3.049E-02	3.281E-02

Configuration D to E Transfer Function Gain for Testpoint 300

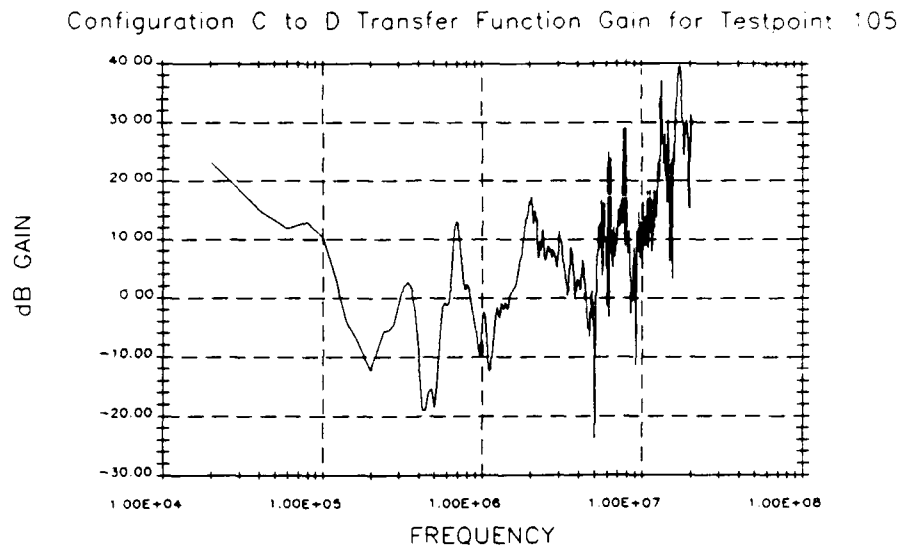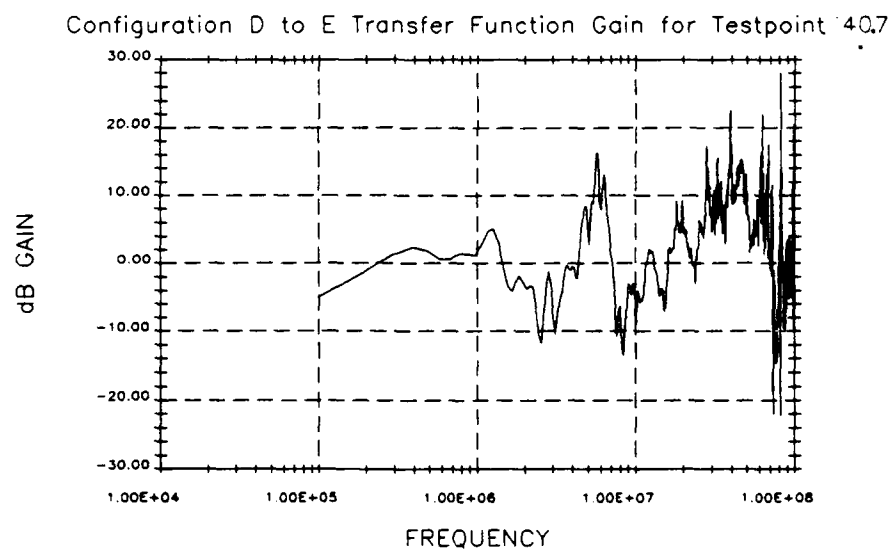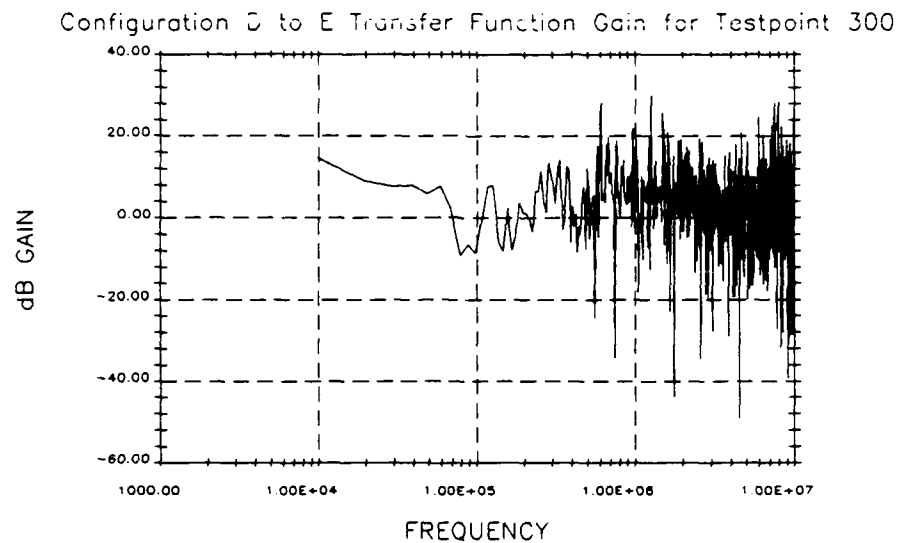Configuration D to E Transfer Function Gain for Testpoint 40.7

Figure 4-14. Configuration D to E Transfer Functions

4.3.7 Configuration E to F Effect (LCM Cable Routing)

In all other configurations, the LCM cable was placed in a cable tray running the length of the trailer. In order to determine the sensitivity of the results to cable routing, the LCM cable was formed into a loop to maximize the H field coupling. The effect for test point 325 is presented in **Figure 4-15**. The dominant effect is a low frequency enhancement of 20 dB which is what would be expected. Inspection of the norm attributes in **Table 4-9** reveals little difference in the two configurations insofar as norms are concerned.

Configuration E to F Transfer Function Gain for Testpoint 325

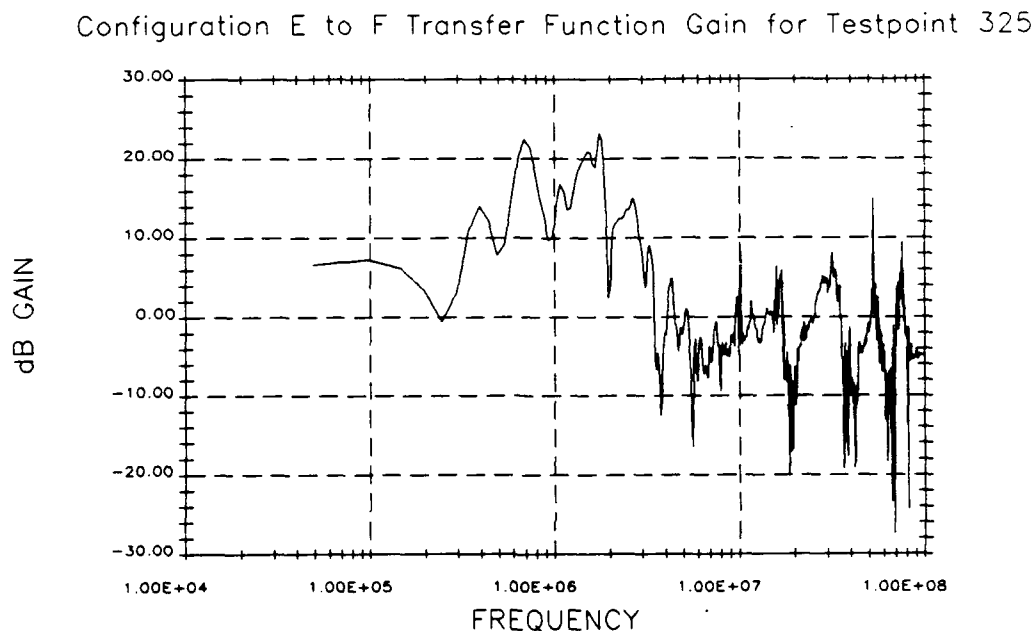**Figure 4-15. Configuration E to F Tranfer Function**

Table 4-9. Configuration E to F Norm Data

NORM/TSTPNT	C325EA30	C325FA30
PEAK	1.336E+03	1.138E+03	
PEAK DERV	3.011E+11	2.715E+11
IMPULSE	3.192E-05	7.191E-05
REC IMPULSE	1.769E-04	2.778E-04
RMS ACTION	0.233	0.250

5.0 NORM ATTRIBUTE DEPENDENCE OF FIELD LEVEL

The utility of norm attributes would be greatly enhanced if they could be used to compare data taken at different simulators. This section has as its objective the quantification of the variability of the norm attributes as a function of the incident field. To meet this objective, data from AESOP will be compared. There are three field level measurements (30 kV/m, 45 kV/m and 60 kV/m) for which data will be compared. In addition, for each measurement, the data are compared for linear scaling to 60 kV/m extrapolation to DoD-STD-2169 early time, and DoD-STD-2169 early time extrapolated data converted to a minimum phase signal. Scaling extrapolation involves simply multiplying the data by the appropriate scale factor to achieve a peak field of 60 kV/m. Extrapolation to DoD-STD-2169 early time involves multiplying the frequency domain representation of the data by the transfer function presented in **Figure 5-1**. Since the environment field was not planer over the test article, phase delays may have been induced in the measurement. The minimum phase transform is used to remove these phase delays and approximate the signal that would be measured in a plane wave environment. This minimum phase representation has the same energy and power spectrum as the DoD-STD-2169 early time extrapolated signal, however, phase wraps have been minimized which results in an increased peak amplitude.

Much of the following discussion is highly statistical in nature. It is not to imply that statistical relationships necessarily imply causal relationships, but rather to develop a graphical method of comparison presenting the results in a concise manner. Also, previous comparisons have employed statistical methods for comparing norm attributes. If norm attributes are to be used in development of an EMP specification, then certain statistical properties would enhance their utility.

The most common statistical measure of norms is the correlation between the peak amplitude norm and the others. The extrapolated AESOP data were aggregated into a common data base and the averages, standard deviation and linear correlation coefficients between the peak amplitude norm and the others were determined. This information is presented in **Table 5-1**.

All norms are relatively highly correlated to the peak amplitude. Furthermore, the effect of the minimum phase transform is apparent in the increase in the average peak amplitude by 35% and the average peak derivative by 75%. However, the impulse norm has actually decreased by 30%. The reason for this occurrence is that the peak value of the datum will occur at an earlier time and thus the value of the integral up to this peak will also occur over a smaller integration period, which results in a smaller value of the norm. The effect of the minimum phase transform on the rectified impulse and the action integral is minimal as it should since these norms are related to the energy in the waveform and the minimum phase representation has the same energy as the original signal with the exception of round off error.

Table 5-1. Linear Statistics and Correlation Coefficients for Scaled, Extrapolated, and Minimum Phase Data

NORM	SCALED DATA			EXTRAPOLATED DATA			MINIMUM PHASE DATA		
	AVG	SIGMA	CC	AVG	SIGMA	CC	AVG	SIGMA	CC
PEAK	71.	1.54E+02		92.	2.10E+02		1.24E+02	3.07E+02	
PEAK DER	9.91E+09	2.42E+10	.73	1.84E+10	5.19E+10	.81	3.21E+10	9.68E+10	.97
IMPULSE	2.39E-05	6.12E-05	.84	4.01E-06	9.41E-06	.63	2.77E-06	5.16E-06	.63
REC IMP	8.22E-05	1.75E-04	.84	3.25E-05	5.41E-05	.93	3.34E-05	5.72E-05	.87
ACTION	3.49E-02	7.48E-02	.91	2.26E-02	4.62E-02	.99	2.14E-02	4.30E-02	.98

The actual linear relationships are developed in log-log space. This is required because the range of values taken on by the norms is very great and attempting to perform a least squares fit in a linear space would result in loss of numerical accuracy. The coefficients are presented in **Table 5-2** for each case. Also, the standard deviation of the coefficients is presented in parenthesis. From **Table 5-2**, the value of the norm in the left column may be expressed as:

$$V = PEAK^A + 10^B$$

where V is the value of the norm derived from the fit.

Table 5-2. Norm Fit Coefficients and Their Standard Deviations to Peak Amplitude
Norm $V = Peak^A + 10^B$

NORM		SCALED DATA	EXTRAPOLATED DATA	MINIMUM PHASE DATA
PEAK DERIVATIVE	A	8.18 (0.106)	8.01 (0.121)	8.02 (0.136)
	B	0.81 (0.007)	1.06 (0.008)	1.10 (0.008)
IMPULSE	A =	-7.27 (0.158)	-7.47 (0.183)	-7.53 (0.197)
	B =	1.30 (0.091)	0.99 (0.105)	0.93 (0.107)
REC IMPULSE	A =	-6.18 (0.121)	-6.05 (0.130)	-6.27 (0.142)
	B =	1.08 (0.070)	0.82 (0.074)	0.88 (0.076)
ACTION INTEGRAL	A =	-3.28 (0.095)	-3.36 (0.112)	-3.50 (0.121)
	B =	1.000(0.039)	0.90(0.051)	0.90(0.052)

It can be seen from **Table 5-2** that the relationship of the norms is relatively independent of the type of data and also that the standard deviation of the coefficients is small relative to the coefficients. This implies a relatively tight fit in log-log space. While there may be some intuitive arguments for the power relationships, there is no physical reason which would justify these relationships. This is especially true for the

correlation between the peak amplitude and peak derivative. However, these relationships have been observed for other test data and indeed, they also hold for the DMS-100 data. **Figure 5-1** presents the norms plotted against the peak value for each of the three sets of data on a log-log scale.
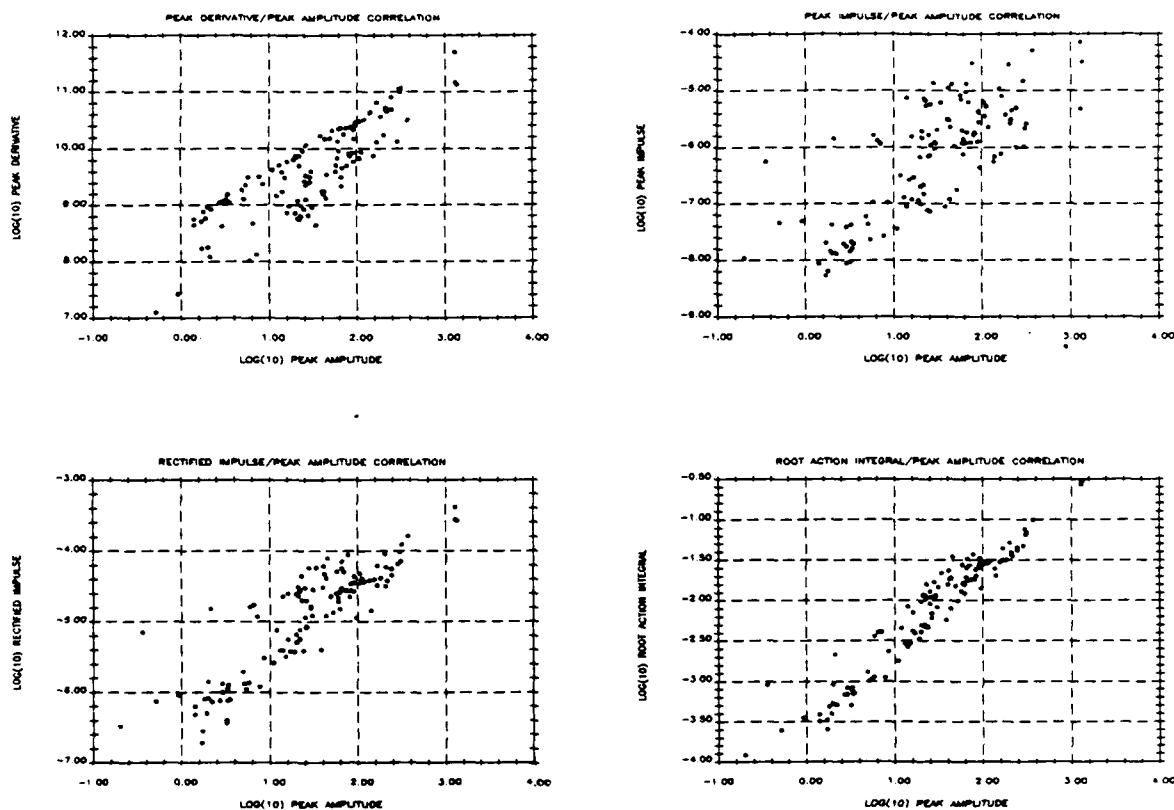

Figure 5-1. Norms vs. Peak Amplitude Norm

While the aggregated data norms have the same type of relationships as observed in previous test, these relationships provide no indication of the differences between simulator environments. To investigate these differences, the data was analyzed to determine if the distributions of the norms are dependent upon the data treatment. The results are presented in **Figures 5-2 - 5-6**. These graphs plot the cumulative probability distribution with the vertical axis interpreted as the probability that the norm will have a value less than the corresponding value on the horizontal axis.

There are two conclusions to be reached from these figures. First, the distribution does depend upon the data treatment which, implies that the extrapolation process is critical to the use of norms for comparing results from different test. Secondly, it is apparent that the norms obey a log-normal distribution from the shapes of the cumulative distribution functions. This would imply that using norms as a system level descriptor is somewhat dangerous since large outrider values will have little effect on the statistical description of the system response.

The next area to be covered specifically addresses the impact of the simulator environment on the extrapolated data. This will be accomplished using two methods. First, the cumulative distribution functions of the norms will be compared for the three field levels used at the AESOP. Secondly, common test points for the same configuration at different field levels will be compared directly.

The cumulative distributions are compared using the Kolmogorov-Smirnoff(KS) statistic. This statistic is a measure of the maximum difference in the cumulative distribution function at any value of the particular norm. Associated with the KS statistic is a probability that the two samples were drawn from the same distribution. The results of this comparison are presented in **Table 5-3**. The maximum value of the KS statistic is unity. As is seen in **Table 5-3**, comparison of extrapolated data for the three field levels results in a very poor KS statistic with the exception of the 45/30 kV/m data. Even for this subset of data, it is only the peak amplitude norm which has a good probability of being invariant across the three field levels. It is difficult to determine what an appropriate level of acceptance should be to support the hypothesis that the norm attributes are insensitive to the simulator environment, however probabilities less than .7 would usually be sufficient cause to reject the hypothesis. Unfortunately, there is not an associated confidence level to make a firmer statement. However it does again appear that the use of norms in a specification requires extreme attention to simulator environment and data processing. It is also not clear that more data would alter these results,however, common test points under common configurations are rare in the available data. On the other hand, one would usually expect the aggregated data to be better behaved than individual data points when changing environments and configurations. Additionally, the argument can be made that operational configurations are seldom adequately sampled during an EMP test of a complicated system.
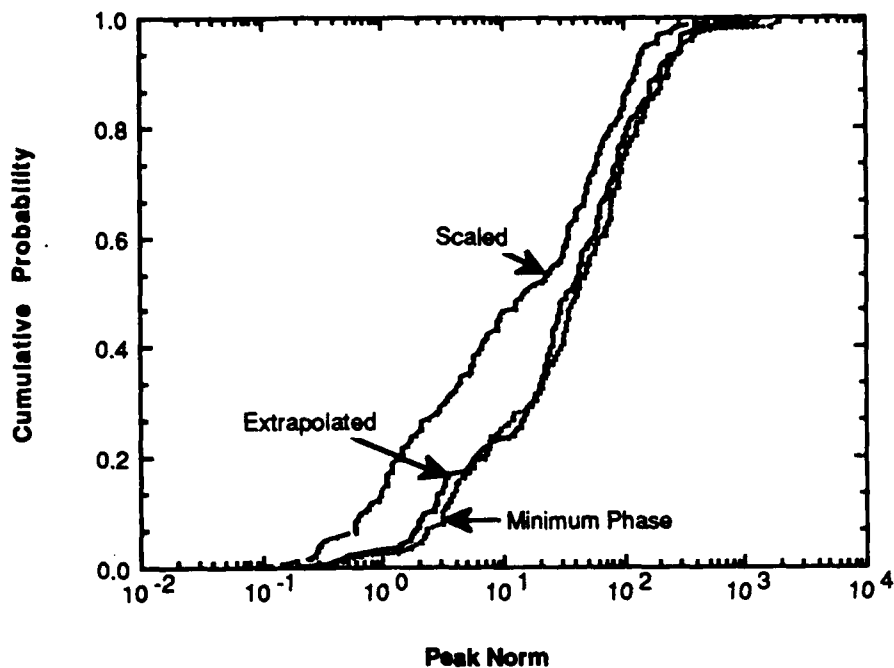
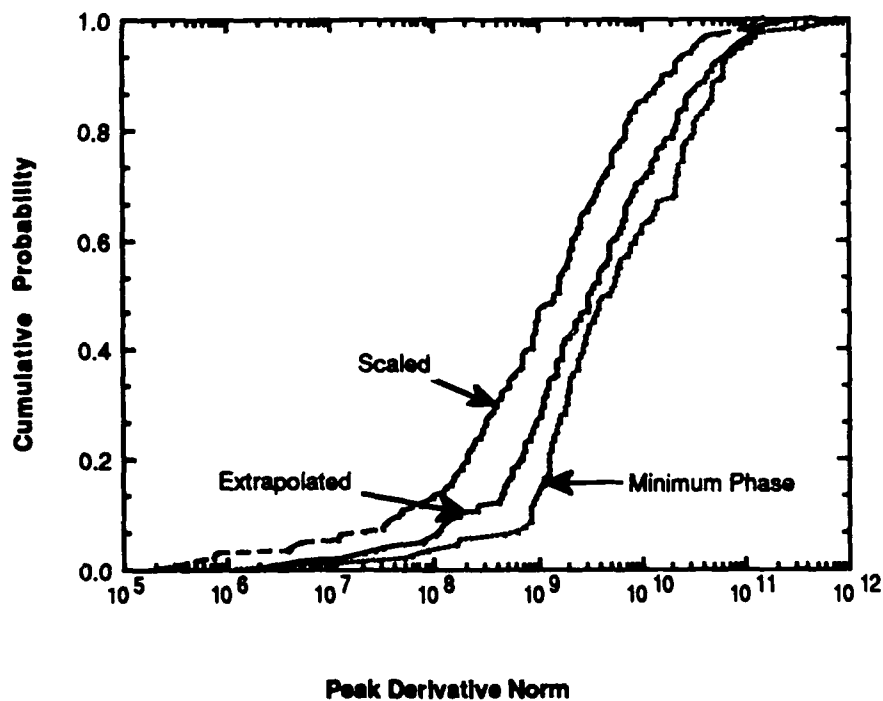**Figure 5-2. Cumulative Probability Versus the Peak Norm**

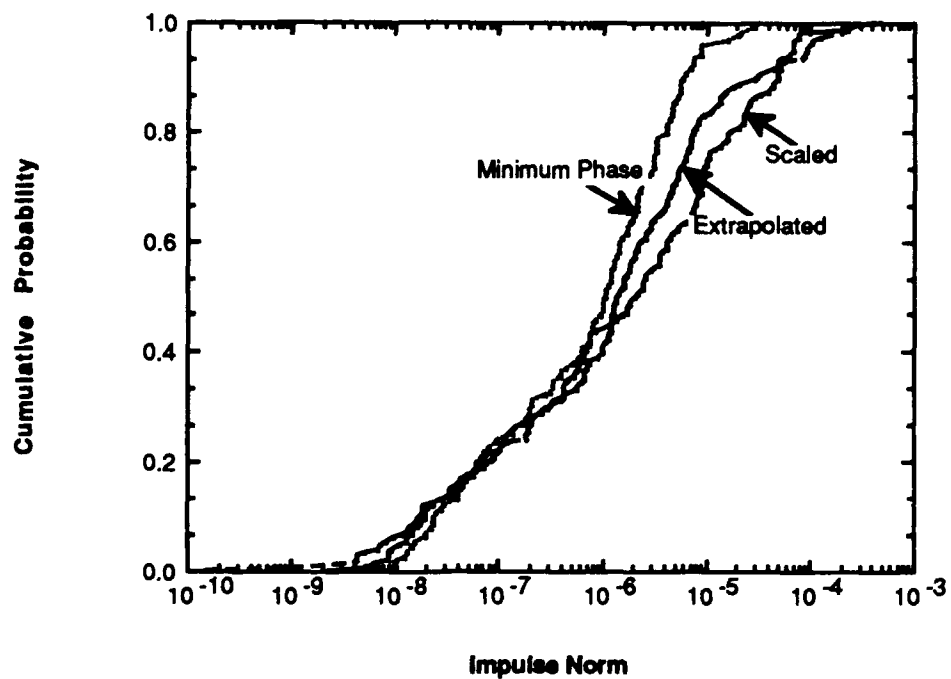**Figure 5-3. Cumulative Probability Versus the Peak Derivative Norm**

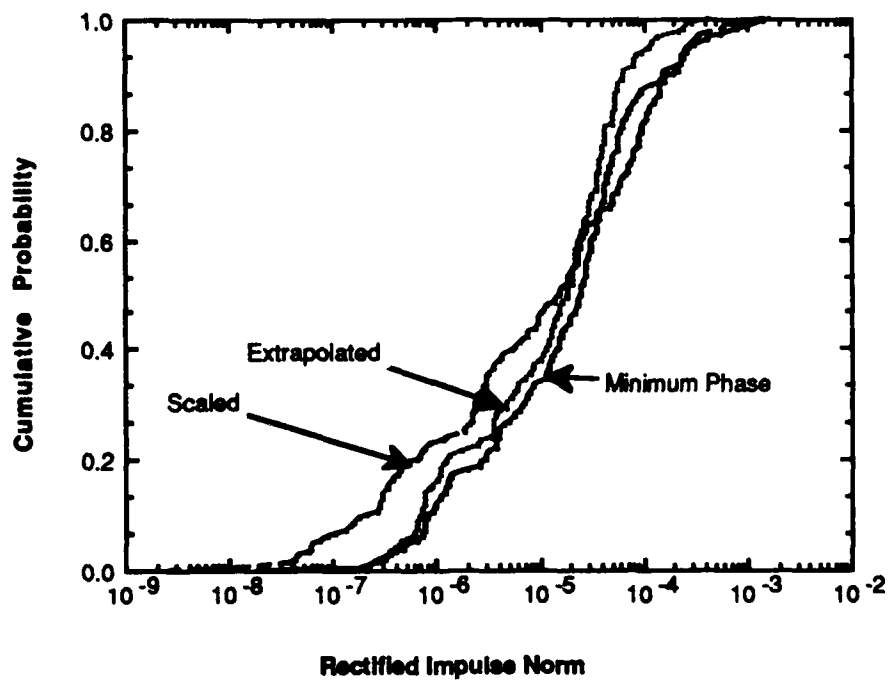**Figure 5-4. Cumulative Probability Versus the Impulse Norm**

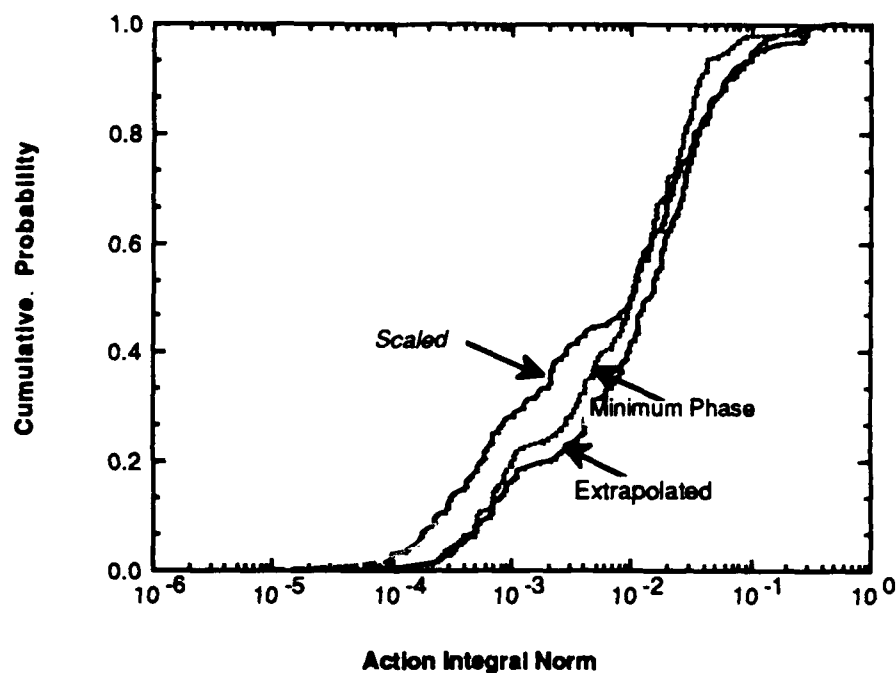**Figure 5-5. Cumulative Probability Versus the Rectified Impulse Norm**

Figure 5-6. Cumulative Probability Versus the Action Integral

Table 5-3. Kolmogorov-Smirnoff (KS) Statistic and Probability of Same Distributions (Ps)
for Scaled (S), Extrapolated (E) and
Minimum Phase (M) AESOP Data at Three Field Levels

NORM/FIELD		60/45		60/30		45/30	
		KS	Ps	KS	Ps	KS	Ps
Peak Amplitude	(S)	.49	.01	.39	.06	.12	.87
	(E)	.30	.29	.31	.22	.12	.83
	(M)	.27	.42	.28	.34	.14	.73
Peak Derivative	(S)	.39	.10	.35	.11	.18	.38
	(E)	.23	.61	.18	.83	.20	.26
	(M)	.22	.71	.23	.57	.23	.14
Max Impulse	(S)	.35	.16	.38	.07	.22	.19
	(E)	.32	.23	.28	.34	.24	.12
	(M)	.38	.11	.29	.28	.23	.14
Rect Impulse	(S)	.35	.17	.36	.09	.21	.21
	(E)	.34	.17	.22	.65	.21	.23
	(M)	.33	.21	.22	.65	.22	.19
Action	(S)	.41	.06	.32	.18	.16	.57
	(E)	.34	.17	.25	.44	.12	.76
	(M)	.33	.20	.25	.46	.12	.87

6.0 SUMMARY AND CONCLUSIONS

The goals of this volume are to determine if the performance of the DMS-100 system would be different in the DoD-STD-2169 early time environment and also the effect of the simulator and configuration on the extrapolated data.

From the results of Section 4, it is very likely that the DMS-100 switch was overdriven in the AESOP environment. However, this may not be the case in all systems. With the exception of the trunk cables, the lack of a DoD-STD-2169 early time simulator should have little effect on the use of data obtained during the test. A more complete statement could be made if the trunk cable were driven using current injection at analytically derived threat levels.

The impact of the grounding scheme overwhelmed all other effects for direct simulator comparison and there are only two test points with the same configuration at different field levels. However, there are some successes which are worthy of note. First, it does appear that the distribution of the norms is dependent upon the simulator environment and, given that all else remains the same, norm values are very sensitive to the field and extrapolation procedure. In aggregate, the DMS-100 norms behave as other systems have behaved in the past. The presentaticn of the configuration effects indicates that norm attributes are also sensitive to configurations and furthermore, that norms for individual test points do not necessarily behave as the group. This is not a surprising result since by their very nature, statistical methods should not be greatly influenced by the deviations of the components. If box or pin level norm based specifications were place on a system, it would be very difficult if not impossible to adequately sample the system configurations to validate the system survivability. The statistical relationships most likely have little if any physical meaning and it does appear that EMI filters can distort the meaning of the norm attributes. One is naturally led to question if the statistical relationships are not simply a manifestation of the central limit theorem and if correlation in log-log space is simply desensitizing the data by the reduction of the variation inherent in replacing the data by the logarithm.

It was shown that the grounding configuration has a large effect on the data. This is also not unexpected but does illustrate the pervasive nature of the " back-door" entry into systems. Specifically, for the DMS-100 system, variations in ground configurations may dominate the overall performance and could possibly lead to burnout of some devices even though no such events occurred during the test.

It has been shown that the simulator environment does affect the norm distributions under the constraint of the extrapolation procedure used for this analysis. It would be beneficial to conduct a thorough field mapping at AESOP as a function of field levels and to incorporate field variations into the analysis to determine if this conclusion holds up. If this proves to be the case, then survivability statements based on norm comparisons would have to be tailored for each test simulator unless the design requirements were over specified to the point where the system were inherently survivable in any simulator environment. In this case, all HEMP tests would simply

be hardness validation tests. However the cost impact of this approach may be prohibitive both for initial design of a system and for HM programs.

No attempt has been made to identify signal attributes related to the upset of the switch. This would require extensive instrumentation and monitoring. It is not even clear that it can be accomplished on such a large system given the configuration dependencies and the inability to isolate signals. Again, a direct drive test would certainly facilitate the development of this type of knowledge.

7.0 RECOMMENDATIONS

It would be remiss to not state that this data analysis was fraught with difficulty. As a minimum, further test should have adequate field mapping to support the extrapolation process. Furthermore, the simulator environment should be monitored on a shot by shot basis and the data utilized in both time tieing and extrapolation. The instrumentation and data acquisition limitations are somewhat severe and are far from the state of the art in such systems.

Perhaps the most important recommendation is conduct a direct drive test on the DMS-100 to eliminate any question concerning the conducted currents on the trunk cables. Such a test could also provide the controlled environment to further assess the utility of the norm attribute.

APPENDIX A.
DMS-100 CONFIGURATION AND TEST POINT LOCATIONS

Test Setup and Test Points

The test setups used in the REPS and AESOP tests had basically the same configuration. These test setups are shown in **Figures A-1** and **A-2**. The two major differences in the configurations were the existence of a HP54111D installed next to the switch trailer and the grounding configuration. The location of the oscilloscope had no bearing on the test results, however as mentioned in the body of the report the differences in grounding configuration had a large effect on the measured signal strength. The grounding configuration of the REPS and AESOP were shown in **Figure 4-1** and **4-2**. In the REPS configuration, a ground loop was formed this caused the peak of the REPS data to be larger than it would have if the system had been properly grounded.

The location of the test points for this program is shown in **Figures A-3** through **A-7**. **Figure A-3** shows a general view of how the cabling is routed through the switch trailer. All of the 100 series test points are power test points, and as can be seen from the drawing test points 300-304 measured signals on the outside plant cables. **Figure A-4** shows the test points on the PCAM and the PCPM. The test points listed in this page provided measurements detailing the effects of the filters. **Figure A-5** shows the location of the test points on the grounding system and the outside plant cables. **Figure A-6** shows the test points going to the PCLM. **Figure A-7** shows the test points on the DS-30 lines and an unterminated wire hung between the two DNPC frames.
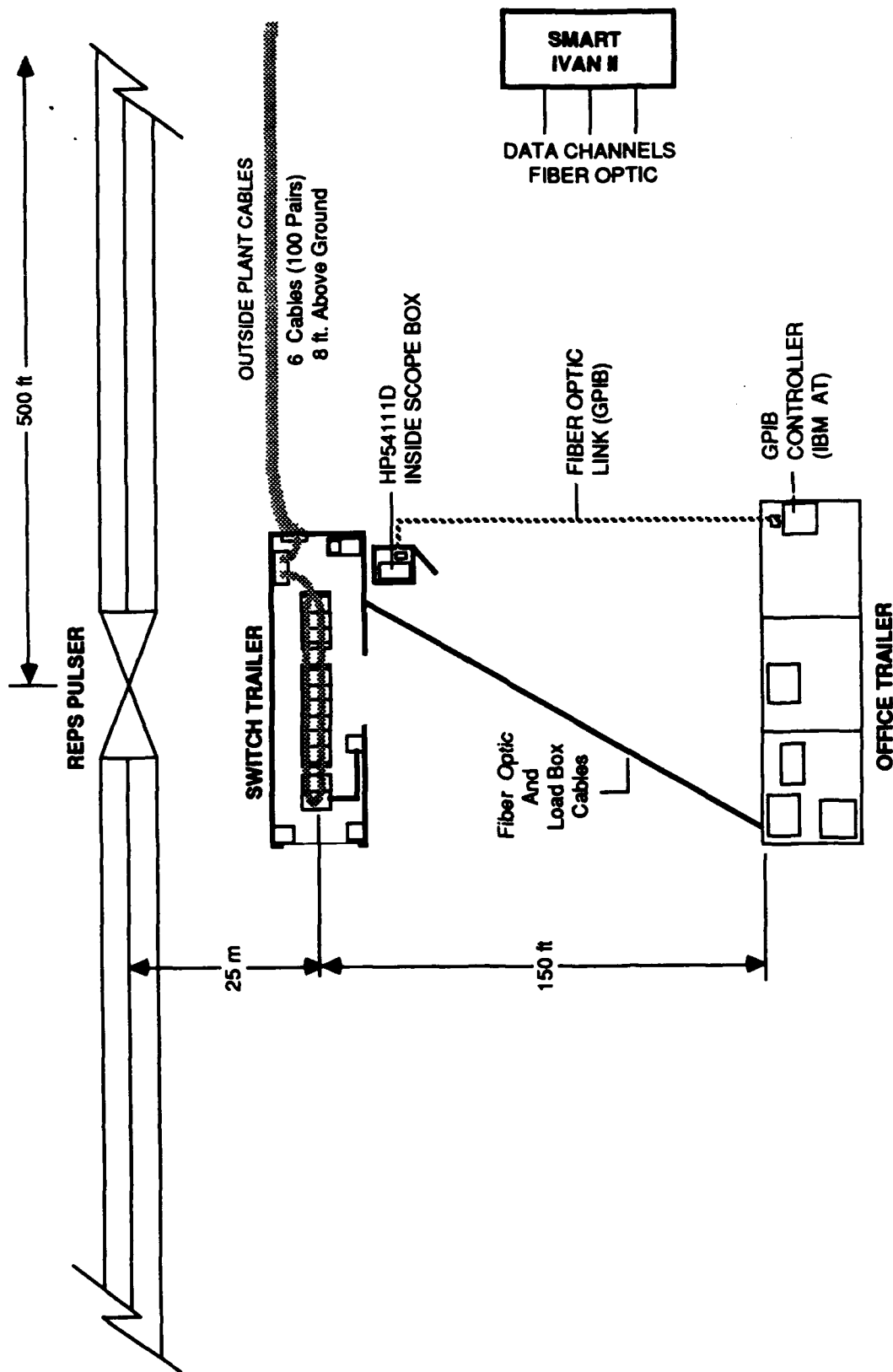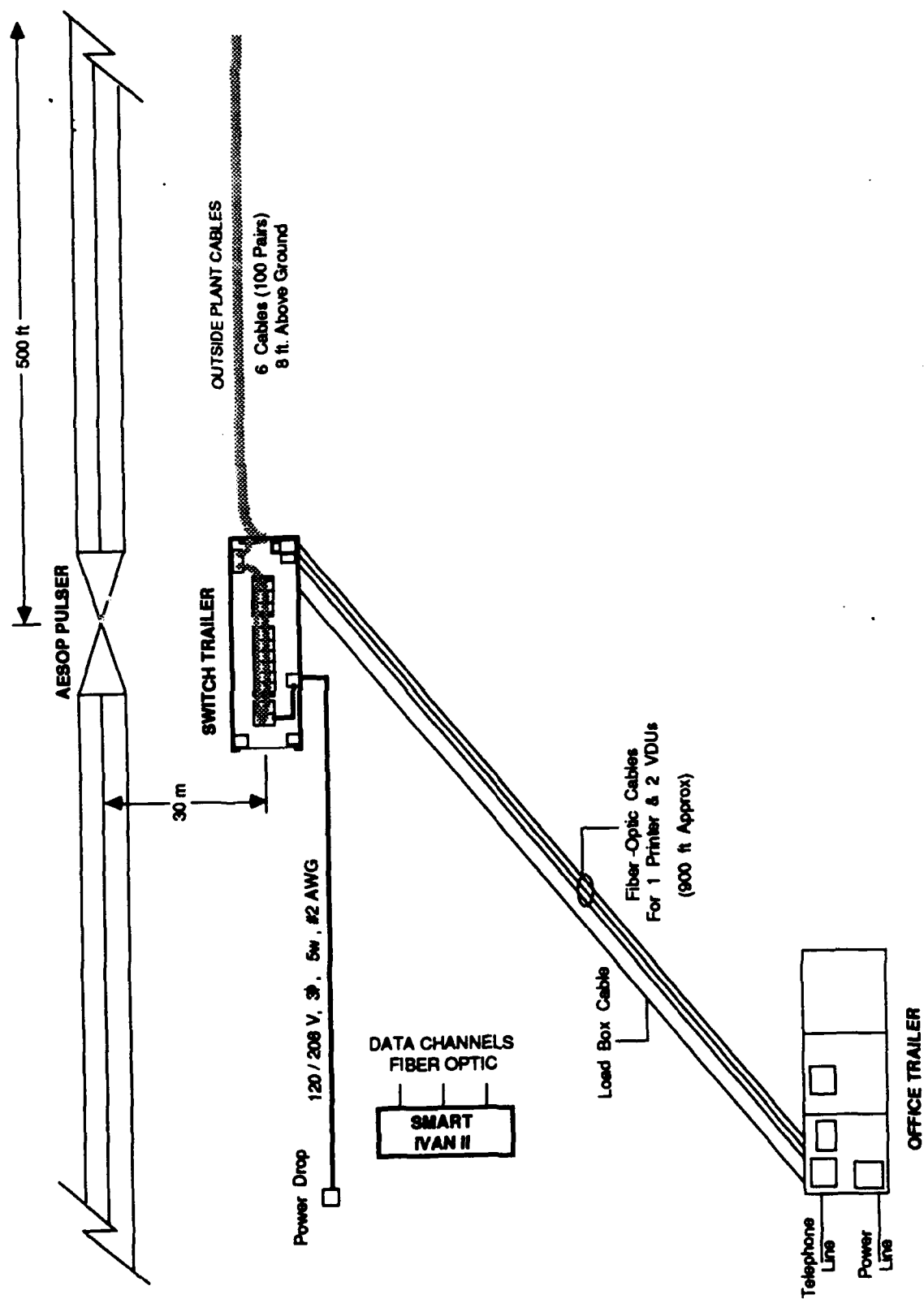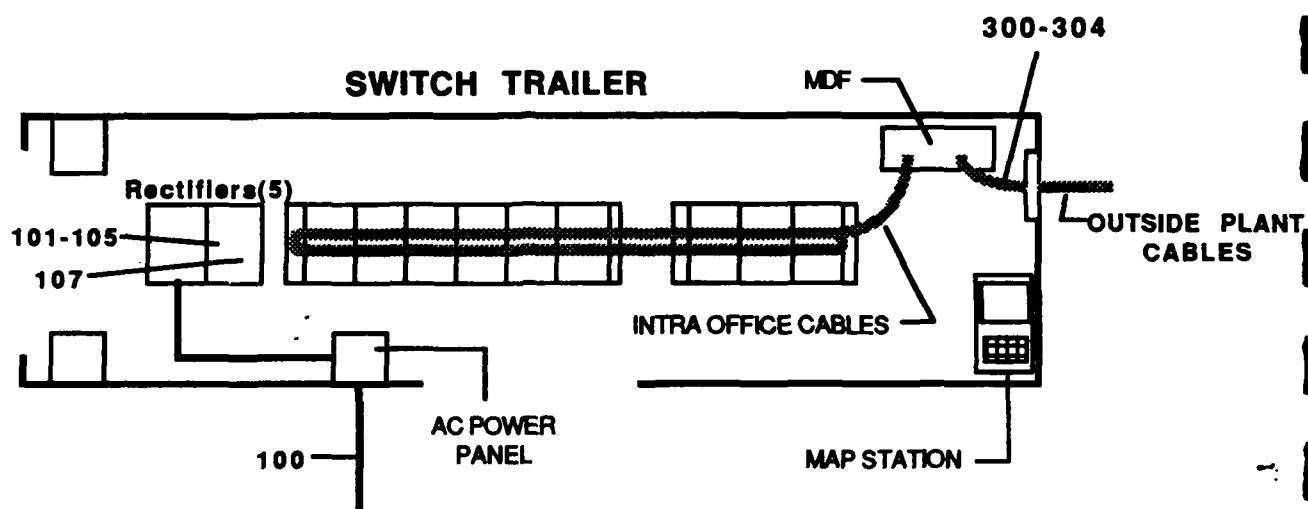
**Figure A-1. Physical Test Configuration (REPS)**

Figure A-2. Physical Test Configuration (AESOP)

SWITCH TRAILER

300-304

MDF

Rectifiers(5)

101-105

107

OUTSIDE PLANT CABLES

INTRA OFFICE CABLES

AC POWER PANEL

100

MAP STATION

Notes:

1. 100 is the 5-wire power cable.
2. 101-105 are the D.C. output cables of the rectifiers.
3. 107 is a bundle 4 wires (-48 VDC).

Figure A-3. Cable Routing Through the Switch Trailer

A-4

Figure A-4. Location of 100 and 200 Series Test Points
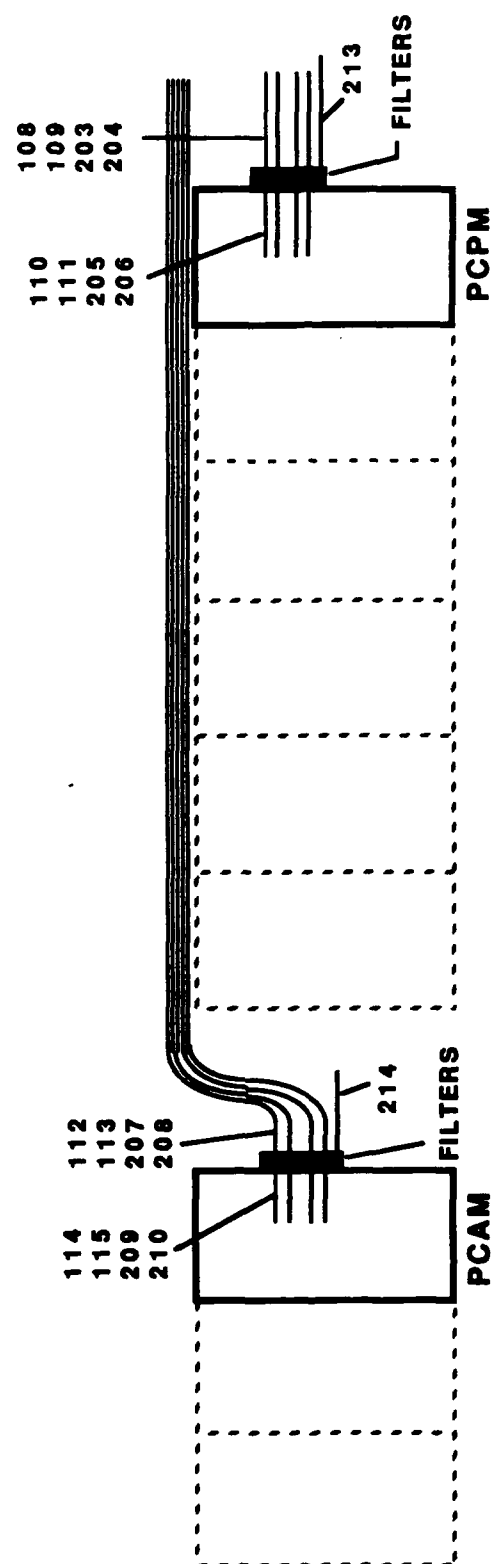
Notes:

1. 100's are cables used for the -48VDC power.
2. 200's are cables used as power return or ground.
3. 213 and 214 are frame grounds which terminate on the C.O. ground.
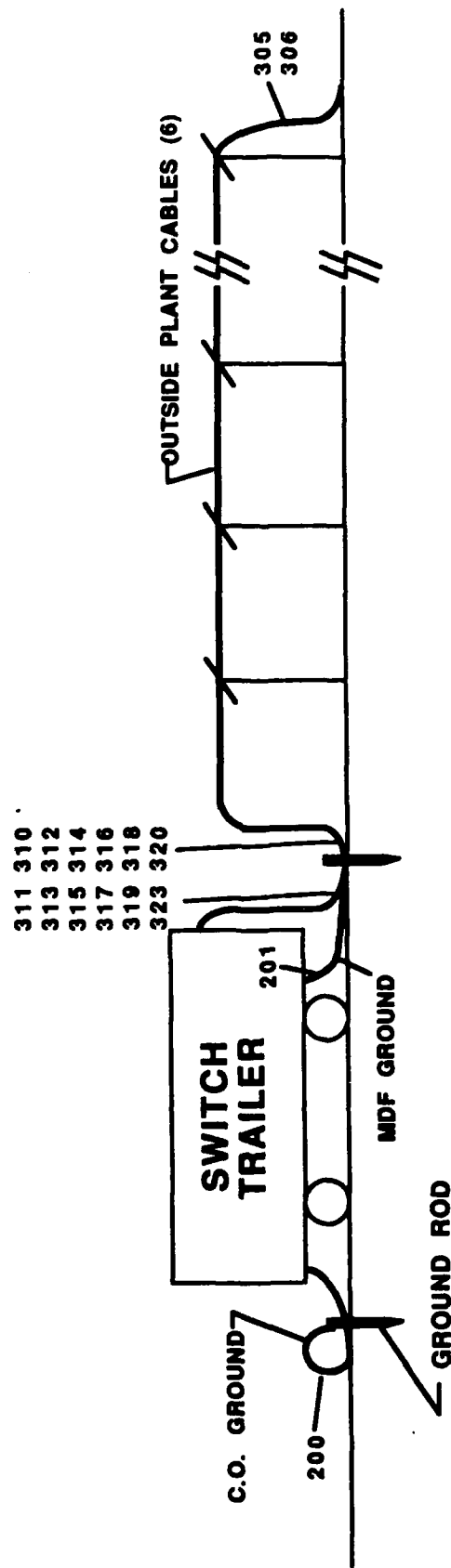
Figure A-5. Location of Outside Plant Cable Test Points

INTRA-OFFICE CABLES

FILTERS

MULTIPLE CABLES

412-415

408-411
416-419
421-423

404

403

PCGM   PCLM   PCAM
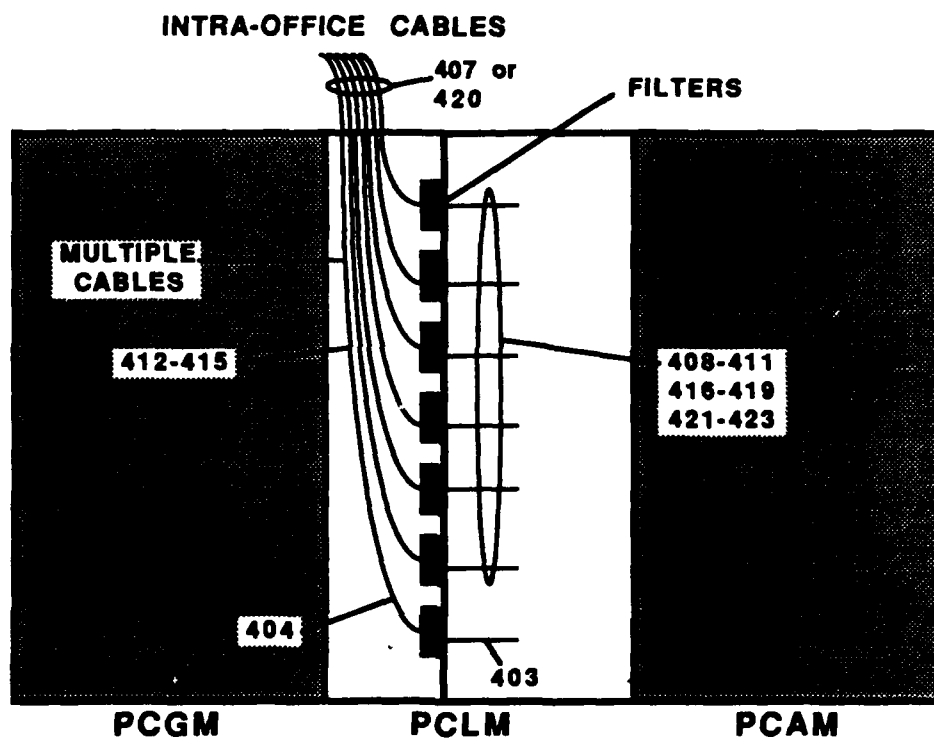
Notes:

1. 407 and 420 are identical test points.
2. 412-415 and 408-411 are 32-pair cables
3. 403 and 404 are multiple (10) cables.
4. 416-419 are 1-pair wires (filtered).
5. 421-423 are 1-pair wires (unfiltered).

Figure A-6.   Location of 400 Series Test Points

A-7

Figure A-7. Location of 500 and 700 Series Test Points
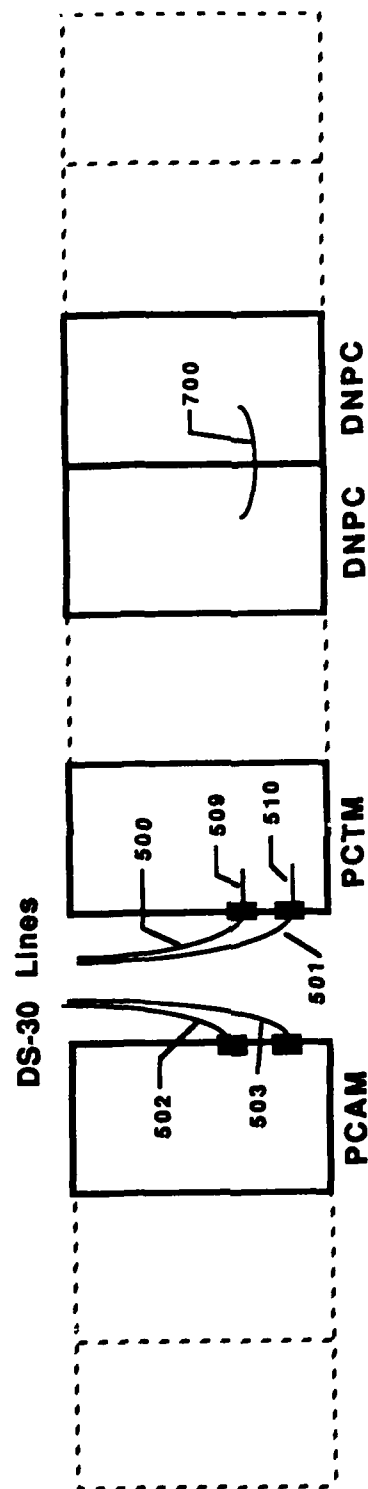
Notes:

1. 700 is a single wire hanged (unterminated) between the 2 DNPC frames.
2. The DS-30 lines are 33-pair cables (100' long) and terminate on the PCAM and PCTM frames.
   The DS-30 lines (500-503) are shielded with copper braids and are unfiltered.

APPENDIX B

The following table presents the values of the norm attributes for all extrapolated DMS-100 data sorted by test point. The facility and configuration keys identify the specifics of the data. All data represents current measurements and has units derived from amperes.

Table B.1 presents the values of the norm attributes for all extrapolated DMS-100 data sorted by test point. The facility and configuration keys identify the specifics of the data. All data represents current measurements. There is little commonality of the norms at any given test point/configuration.

TABLE B.1 - AGGREGATED NORMS FOR ALL DATA

FACILITY KEY
A - AESOP   (30KV/M)
B - AESOP   (45KV/M)
C - AESOP   (60KV/M)
R - REPS   (6KV/M)
O - OTTAWA (2.5KV/M)

CONFIGURATION KEY
A - PANELS OFF, FILTERS OFF
B - PANELS OFF, FILTERS ON
C - PANELS ON, FILTERS OFF
D - PANELS ON, FILTERS ON
E - CCC PANELS ON, TRUNK FILTERS ON, LCM
    PANELS OFF, LCM FILTERS ON
F - CCC PANELS ON, TRUNK FILTERS OFF, LCM
    PANELS OFF, LCM FILTERS ON, LCM CABLE
    LOOPED AROUND

TPT F C A F C G	PEAK AMPLITUDE	PEAK DERIVATIVE	IMPULSE	RECTIFIED IMPULSE	ACTION INTEGRAL
100 B A	92.	5.79E+09	4.06E-06	3.52E-05	2.56E-02
100 C D	1.07E+02	6.52E+09	3.55E-06	3.59E-05	2.88E-02
101 B D	90.	8.29E+09	1.27E-06	2.65E-05	2.69E-02
101 R A	19.	2.60E+08	7.28E-06	9.39E-05	1.92E-02
103 B D	2.99E+02	1.13E+11	1.03E-06	9.66E-05	7.58E-02
104 C D	62.	8.91E+09	1.40E-06	1.51E-05	1.22E-02
104 R A	46.	7.34E+09	7.41E-06	7.47E-05	2.70E-02
105 C D	30.	3.97E+09	1.18E-06	1.23E-05	8.27E-03
105 C C	7.1	1.33E+08	1.14E-06	1.18E-05	4.08E-03
107 C A	83.	7.29E+09	1.81E-06	3.43E-05	2.41E-02
108 B D	29.	3.16E+09	9.38E-07	1.67E-05	1.16E-02
108 C A	26.	3.34E+09	7.17E-07	8.34E-06	6.12E-03
108 R A	45.	7.48E+08	4.62E-06	5.72E-05	1.78E-02
108 O D	1.68E+02	2.58E+11	1.31E-06	6.96E-06	2.12E-02
109 C A	25.	2.68E+09	6.96E-07	1.15E-05	9.11E-03
110 A A	6.5	4.78E+08	1.30E-06	1.74E-05	4.06E-03
110 C D	0.36	2.57E+06	5.59E-07	7.07E-06	9.05E-04
110 R A	46.	2.17E+10	2.04E-06	1.26E-05	9.77E-03
110 O D	26.	3.11E+07	4.31E-05	3.14E-04	6.01E-02
111 A B	2.1	1.22E+08	1.40E-06	1.52E-05	2.15E-03
111 C D	26.	1.14E+10	7.26E-08	8.64E-06	6.96E-03
111 O D	29.	2.15E+07	6.45E-05	7.83E-04	0.11

TABLE B.1 (cont'd)

TPT F C A F C G	PEAK AMPLITUDE	PEAK DERIVATIVE	IMPULSE	RECTIFIED IMPULSE	ACTION INTEGRAL
115 C A	19.	6.34E+09	1.13E-07	3.70E-06	3.38E-03
139 A B	24.	8.99E+09	7.82E-08	3.88E-06	4.67E-03
140 C A	2.44E+02	8.02E+10	1.01E-06	4.55E-05	4.54E-02
200 C D	84.	2.39E+10	1.74E-06	2.75E-05	2.01E-02
200 R A	3.09E+02	9.97E+09	4.95E-05	1.67E-04	0.10
200 O D	3.05E+02	4.81E+09	2.76E-04	1.03E-03	0.32
201 B A	2.87E+02	1.32E+10	1.49E-05	6.53E-05	4.75E-02
201 C C	2.16E+02	4.49E+10	4.38E-06	3.81E-05	3.54E-02
201 C D	1.55E+02	7.39E+09	1.08E-05	4.00E-05	2.97E-02
202 R A	82.	1.75E+09	1.86E-05	2.24E-04	4.58E-02
203 B D	29.	2.56E+09	1.23E-06	1.57E-05	1.12E-02
203 C A	49.	1.49E+10	1.04E-06	2.28E-05	1.52E-02
203 O D	30.	1.14E+08	7.21E-05	2.44E-04	6.16E-02
203 O D	30.	1.12E+08	7.17E-05	2.43E-04	6.13E-02
209 B A	16.	7.30E+08	1.53E-06	2.49E-05	7.10E-03
209 O D	2.7	2.01E+06	5.24E-06	3.99E-05	7.26E-03
209 O D	0.49	1.84E+09	2.22E-09	1.83E-08	5.35E-05
211 B A	1.37E+02	4.23E+10	5.57E-07	3.83E-05	2.47E-02
213 B D	40.	1.78E+09	3.09E-06	3.05E-05	1.57E-02
213 R A	1.02E+02	2.74E+10	6.62E-06	5.03E-05	3.43E-02
213 O D	1.02E+02	7.73E+07	2.11E-04	1.44E-03	0.28
213 O D	1.11E+02	1.14E+10	8.43E-06	3.19E-05	4.26E-02
215 C D	45.	3.45E+09	1.31E-05	7.84E-05	3.51E-02
300 B A	42.	1.74E+09	3.01E-06	4.73E-05	1.83E-02
300 C D	21.	5.74E+08	1.90E-06	2.32E-05	1.17E-02
300 C E	25.	8.55E+08	1.65E-06	3.03E-05	1.29E-02
301 B A	44.	1.32E+09	2.26E-06	4.10E-05	1.91E-02
301 C D	31.	9.21E+08	2.03E-06	2.84E-05	1.46E-02
301 C F	58.	5.01E+09	7.04E-06	5.09E-05	2.77E-02
301 C E	60.	6.69E+09	2.00E-06	2.15E-05	1.60E-02
302 A C	68.	4.48E+09	1.84E-06	2.82E-05	1.77E-02
302 B A	21.	1.18E+09	1.44E-06	3.07E-05	1.15E-02
303 B A	81.	8.01E+09	1.65E-06	2.25E-05	1.82E-02
304 B D	23.	9.64E+08	6.59E-06	4.45E-05	1.59E-02

TABLE B.1 (cont'd)

TPT F C A F C G	PEAK AMPLITUDE	PEAK DERIVATIVE	IMPULSE	RECTIFIED IMPULSE	ACTION INTEGRAL
310 C D	41.	1.57E+09	1.12E-05	6.10E-05	2.33E-02
310 C A	66.	3.10E+09	1.33E-05	5.63E-05	2.54E-02
310 O D	4.33E+02	2.12E+09	4.46E-04	1.67E-03	0.51
311 C D	23.	6.34E+08	5.35E-06	2.01E-05	1.08E-02
311 C A	26.	1.26E+09	5.72E-06	1.99E-05	1.10E-02
311 O D	44.	4.91E+08	7.24E-05	1.97E-04	7.02E-02
311 O D	75.	6.71E+10	4.09E-07	2.68E-06	8.43E-03
313 R A	85.	7.80E+08	1.50E-05	2.20E-04	4.52E-02
314 B A	1.05E+02	2.94E+10	6.36E-06	4.86E-05	2.91E-02
314 O D	1.48E+02	3.52E+09	5.03E-05	2.29E-04	0.13
315 B A	57.	3.88E+09	8.28E-06	2.50E-05	1.30E-02
316 B A	28.	6.61E+08	1.36E-05	5.75E-05	1.69E-02
316 C D	70.	1.76E+10	6.25E-06	5.00E-05	2.70E-02
317 B A	22.	5.45E+08	7.18E-06	2.74E-05	1.16E-02
318 B A	66.	2.14E+09	9.47E-06	7.06E-05	3.28E-02
318 C D	34.	4.42E+08	6.11E-06	5.80E-05	2.17E-02
318 O D	50.	2.73E+10	6.87E-07	3.05E-06	9.41E-03
318 O D	1.66E+02	1.57E+09	7.76E-05	4.11E-04	0.17
319 B A	5.9	1.05E+08	1.61E-06	1.62E-05	3.61E-03
319 C D	26.	2.27E+09	1.09E-06	8.41E-06	6.11E-03
319 O D	63.	8.67E+10	1.20E-06	4.63E-06	1.25E-02
319 O D	1.66E+02	5.00E+09	2.04E-05	6.73E-05	5.42E-02
322 B A	14.	1.74E+09	7.39E-06	2.28E-05	8.39E-03
323 B A	77.	4.96E+09	3.08E-05	8.75E-05	3.74E-02
325 A B	3.73E+02	3.17E+10	5.17E-05	1.61E-04	9.92E-02
325 C E	1.35E+03	1.34E+11	3.24E-05	2.66E-04	0.30
325 C F	1.30E+03	1.44E+11	7.20E-05	4.09E-04	0.30
326 A B	2.01E+02	1.71E+10	2.87E-05	9.12E-05	5.15E-02
400 B A	91.	1.45E+10	2.77E-06	3.54E-05	2.86E-02
401 B A	3.14E+02	1.14E+11	2.60E-06	1.23E-04	6.88E-02
401 C E	62.	2.22E+10	7.59E-07	2.60E-05	1.59E-02
402 C E	75.	2.28E+10	1.22E-06	2.71E-05	1.83E-02
403 C E	65.	2.29E+10	1.20E-06	2.97E-05	1.94E-02

TABLE B.1 (cont'd)

TPT F C A F C G	PEAK AMPLITUDE	PEAK DERIVATIVE	IMPULSE	RECTIFIED IMPULSE	ACTION INTEGRAL
404 C C	2.07E+02	4.91E+10	2.58E-06	3.19E-05	3.67E-02
404 C A	3.07E+02	9.87E+10	2.15E-06	7.13E-05	6.50E-02
407 A B	1.67E+02	1.29E+10	7.92E-06	6.20E-05	4.39E-02
407 B C	2.44E+02	4.86E+10	4.93E-06	5.57E-05	4.20E-02
407 B B	1.12E+02	8.61E+09	5.28E-06	4.13E-05	2.93E-02
407 B A	2.10E+02	5.21E+10	3.03E-06	5.91E-05	3.92E-02
407 C D	1.83E+02	3.64E+10	3.70E-06	4.18E-05	3.15E-02
407 C E	91.	2.09E+10	4.37E-06	4.40E-05	3.33E-02
409 C E	92.	2.38E+10	4.33E-06	4.30E-05	3.33E-02
410 C A	1.66E+02	6.42E+10	7.70E-07	3.27E-05	3.15E-02
411 A B	52.	2.06E+10	1.79E-07	1.34E-05	9.87E-03
411 C A	8.5	2.37E+09	1.05E-07	3.04E-06	2.33E-03
411 C E	22.	7.30E+09	1.51E-07	7.73E-06	4.75E-03
414 C A	16.	5.87E+09	1.18E-07	5.63E-06	4.16E-03
415 C A	20.	7.34E+09	1.98E-07	6.56E-06	5.00E-03
415 C E	13.	5.13E+09	1.30E-07	3.94E-06	2.96E-03
415 R A	1.34E+02	7.02E+10	3.34E-07	1.33E-05	2.20E-02
416 A A	2.9	4.22E+08	3.87E-08	1.00E-06	8.34E-04
416 B A	3.3	1.07E+09	2.15E-08	1.11E-06	7.72E-04
416 C A	5.1	1.30E+09	4.37E-08	1.33E-06	1.01E-03
418 B B	0.20	5.14E+06	1.10E-08	3.28E-07	1.21E-04
418 C A	15.	3.10E+09	2.65E-07	3.19E-06	2.95E-03
421 B A	2.7	1.10E+09	1.96E-08	7.56E-07	6.83E-04
422 A B	2.0	1.80E+08	4.23E-08	1.40E-06	9.11E-04
422 B A	17.	9.67E+08	2.91E-07	3.79E-06	3.90E-03
429 B A	4.9	1.86E+09	5.95E-08	1.96E-06	1.30E-03
429 C C	0.91	2.62E+07	4.91E-08	9.04E-07	3.52E-04
440 B A	12.	1.47E+09	3.19E-07	7.63E-06	4.58E-03
450 B A	5.8	3.15E+09	1.07E-07	1.37E-06	1.13E-03
450 R A	16.	2.62E+08	4.09E-06	4.25E-05	9.29E-03
451 B A	43.	1.47E+10	1.20E-07	1.21E-05	7.96E-03
460 C A	20.	6.84E+09	9.82E-08	5.09E-06	4.10E-03
471 C A	7.7	3.22E+09	2.68E-08	1.20E-06	1.11E-03

TABLE B.1 (concluded)

TPT F C A F C G	PEAK AMPLITUDE	PEAK DERIVATIVE	IMPULSE	RECTIFIED IMPULSE	ACTION INTEGRAL
500 B A	1.29E+03	5.04E+11	4.77E-06	2.76E-04	0.27
500 C D	20.	7.13E+08	6.56E-07	2.47E-05	9.70E-03
500 R A	29.	4.95E+08	7.72E-06	7.15E-05	1.85E-02
500 O D	33.	8.12E+07	8.06E-05	5.51E-04	9.18E-02
501 R A	49.	9.91E+08	8.43E-06	6.98E-05	2.34E-02
600 A B	3.2	1.24E+09	1.45E-08	3.96E-07	5.05E-04
600 B A	5.4	2.27E+09	2.33E-08	1.10E-06	1.04E-03
601 B A	3.2	1.24E+09	9.35E-09	3.60E-07	5.03E-04
601 C B	1.7	5.12E+08	5.32E-09	1.89E-07	2.50E-04
602 A B	3.4	1.57E+09	1.64E-08	1.25E-06	7.01E-04
602 C A	1.7	1.72E+08	2.02E-08	2.79E-07	3.31E-04
700 A B	38.	1.66E+10	8.89E-08	3.99E-06	5.75E-03
700 C A	11.	4.20E+09	3.62E-08	2.62E-06	1.79E-03
700 R A	93.	4.77E+10	1.85E-07	5.95E-06	1.62E-02
701 C A	1.4	5.62E+08	8.61E-09	6.29E-07	3.86E-04
702 C A	2.9	1.15E+09	8.92E-09	1.30E-06	6.96E-04
703 A A	2.0	9.18E+08	1.30E-08	8.18E-07	5.32E-04
703 C E	3.3	1.51E+09	4.28E-08	7.55E-07	8.43E-04
705 B A	3.5	1.11E+09	1.99E-08	7.84E-07	7.17F-04
706 B A	2.9	1.13E+09	1.76E-08	9.70E-07	6.81E-04
706 C A	2.2	8.44E+08	1.32E-08	7.27E-07	5.11E-04
707 C A	1.4	4.45E+08	8.96E-09	4.80E-07	3.18E-04
707 C E	1.8	7.63E+08	6.42E-09	7.98E-07	4.83E-04
707 C F	14.	3.88E+09	8.95E-08	3.95E-06	2.69E-03
770 C E	1.9	5.86E+08	1.45E-03	5.02E-07	3.96E-04
771 C E	0.51	1.25E+07	4.62E-08	7.40E-07	2.46E-04
800 C A	60.	1.31E+10	1.19E-06	1.91E-05	1.66E-02
801 C A	22.	4.90E+09	2.19E-07	5.73E-06	5.01E-03
802 C A	1.19E+02	3.21E+10	2.28E-06	3.67E-05	3.04E-02
803 C A	1.40E+02	4.39E+10	6.84E-07	1.44E-05	2.02E-02
804 C A	95.	2.82E+10	4.37E-07	1.13E-05	1.41E-02

APPENDIX C.
CUMULATIVE PROBABILITIES

The following figures show the graph of the cumulative probability versus each of the five norms for the 100 through 800 series test points.
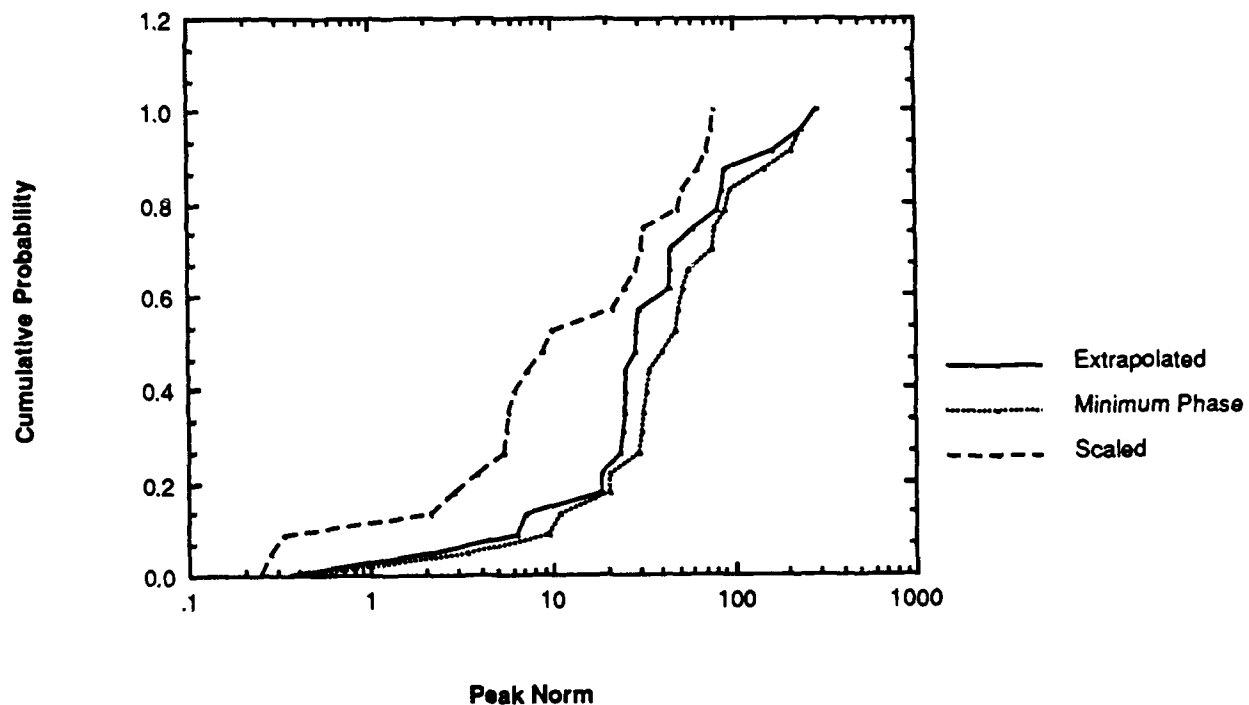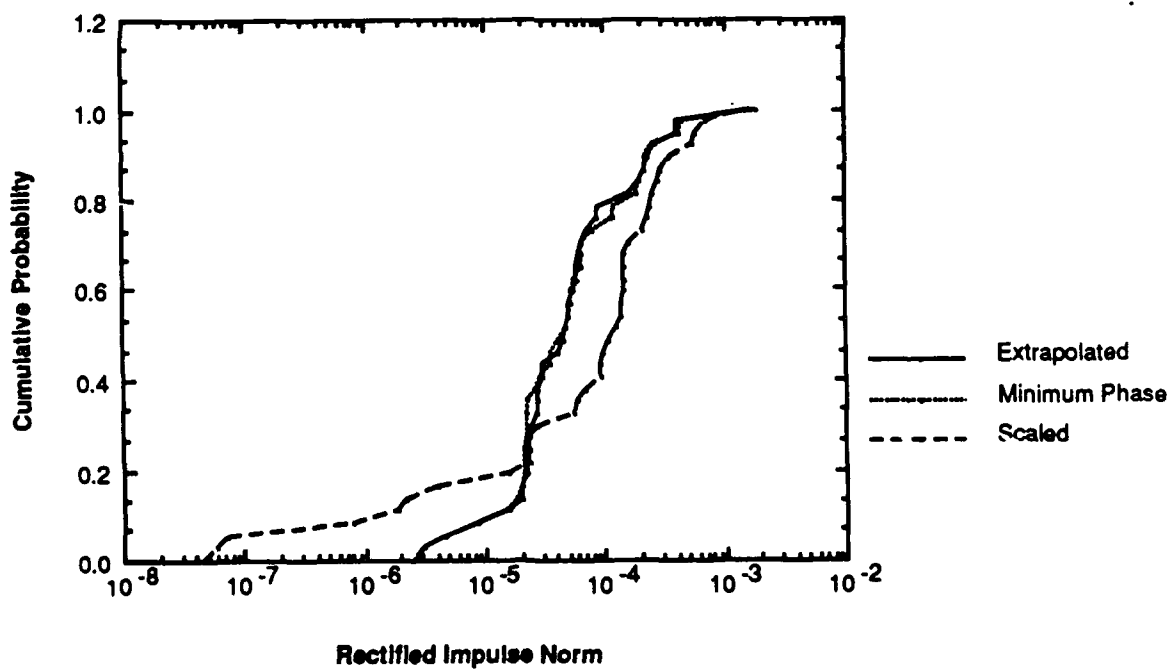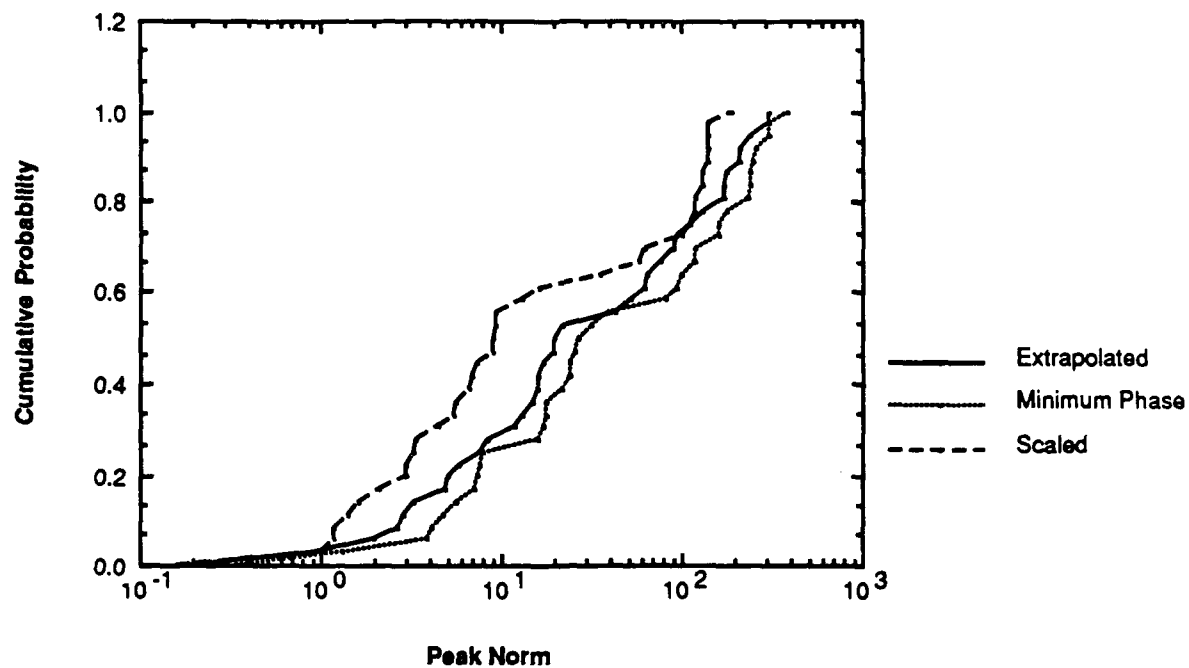
**Figure C-1. Cumulative Probability Versus the Peak Norm for the
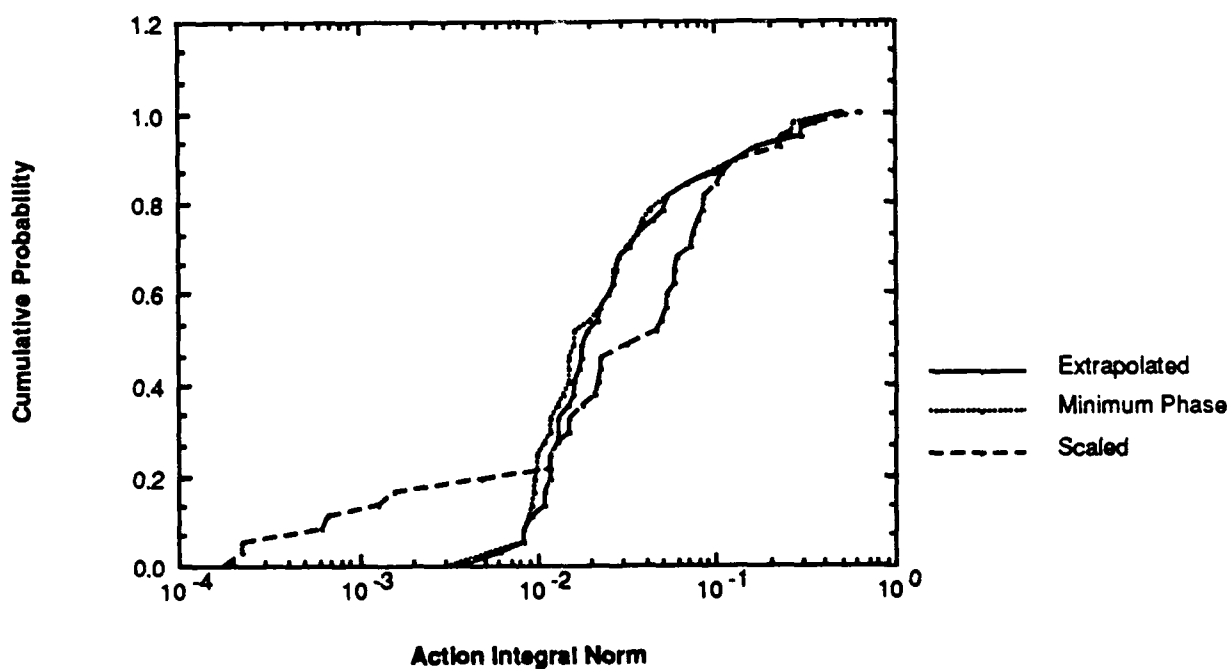100 Series Test Points**
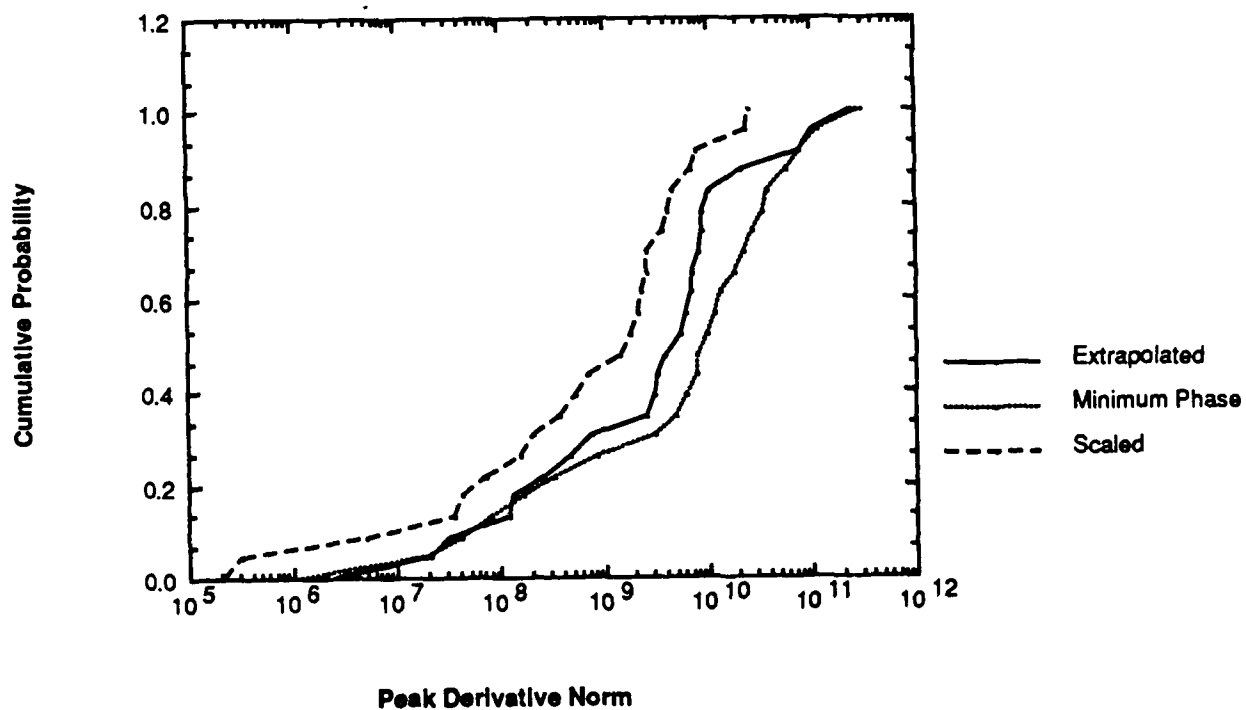
**Figure C-2. Cumulative Probability Versus the Peak Derivative Norm for the
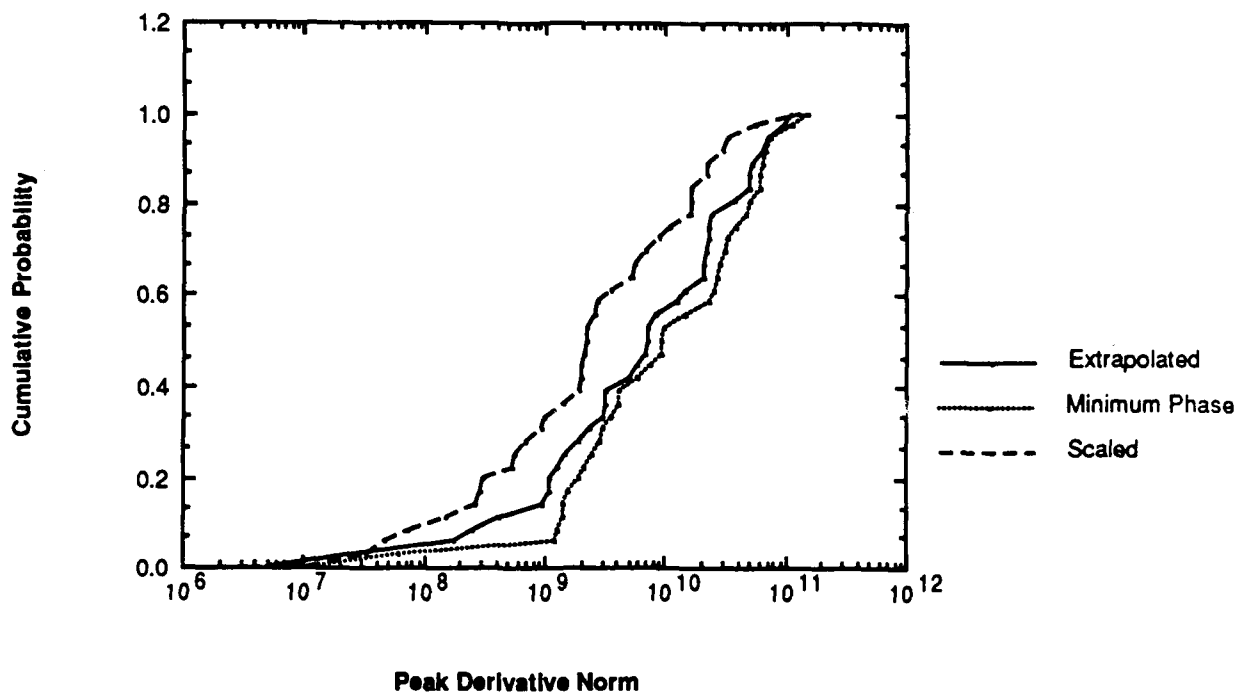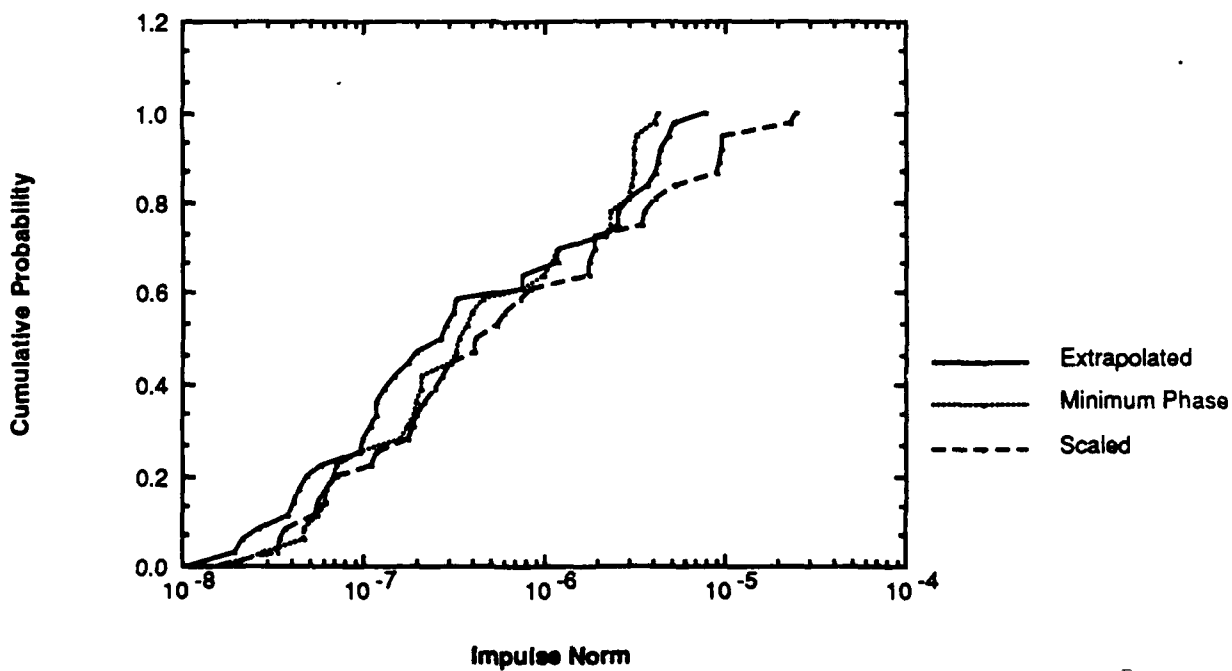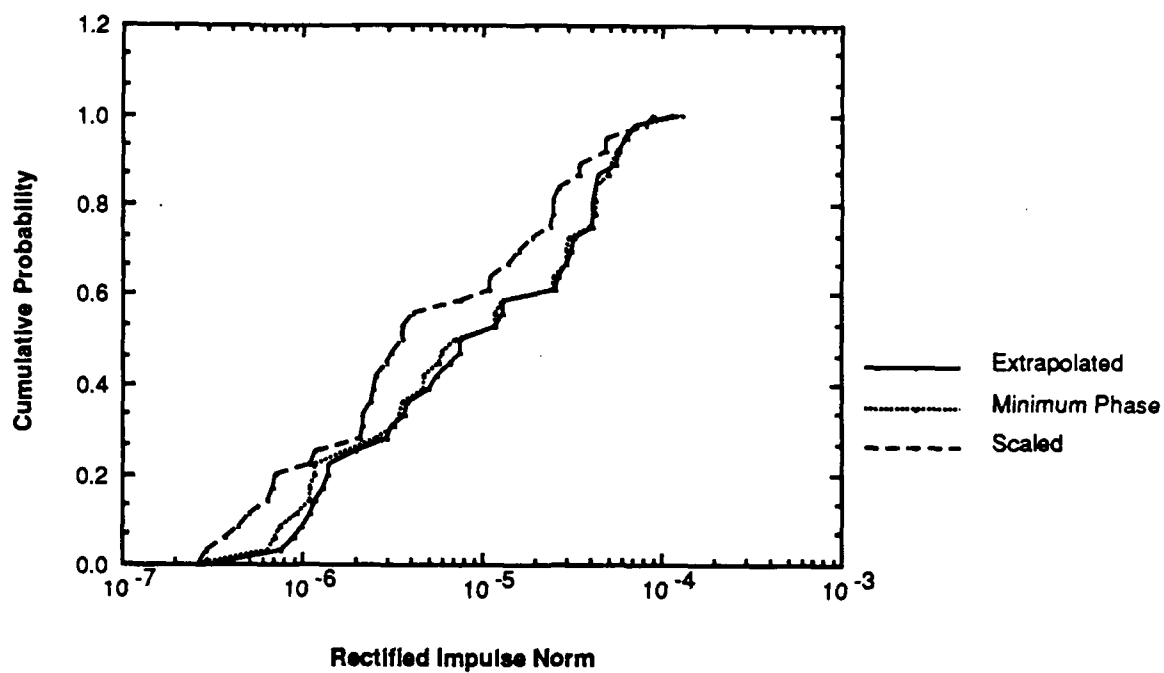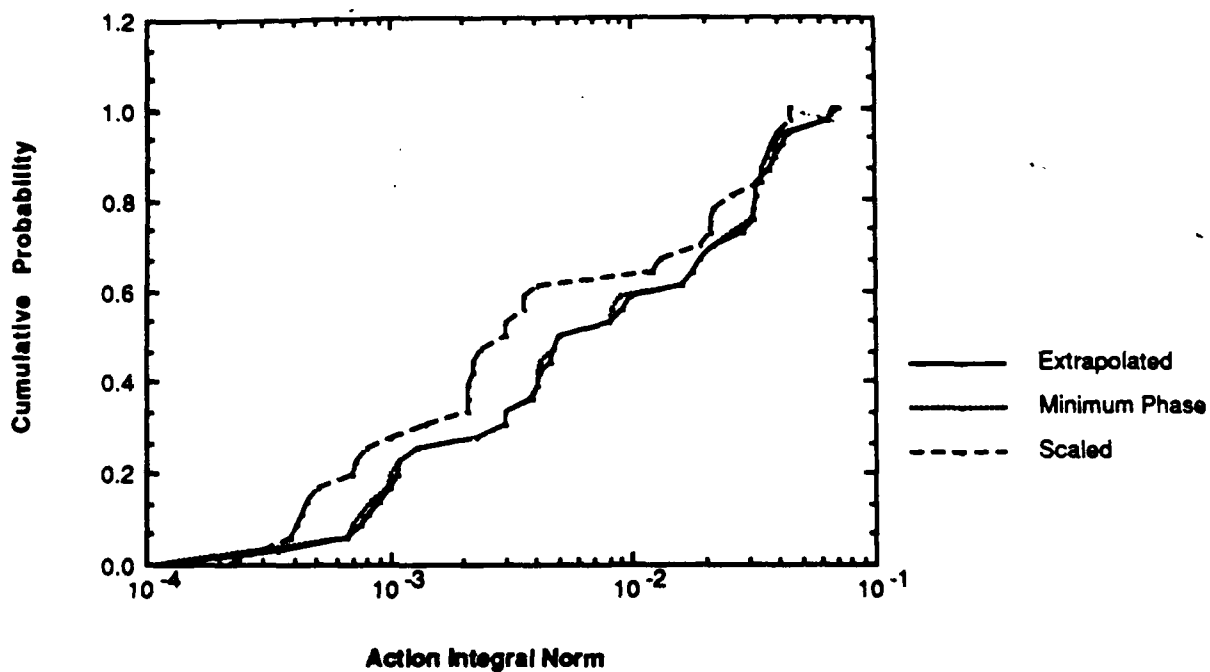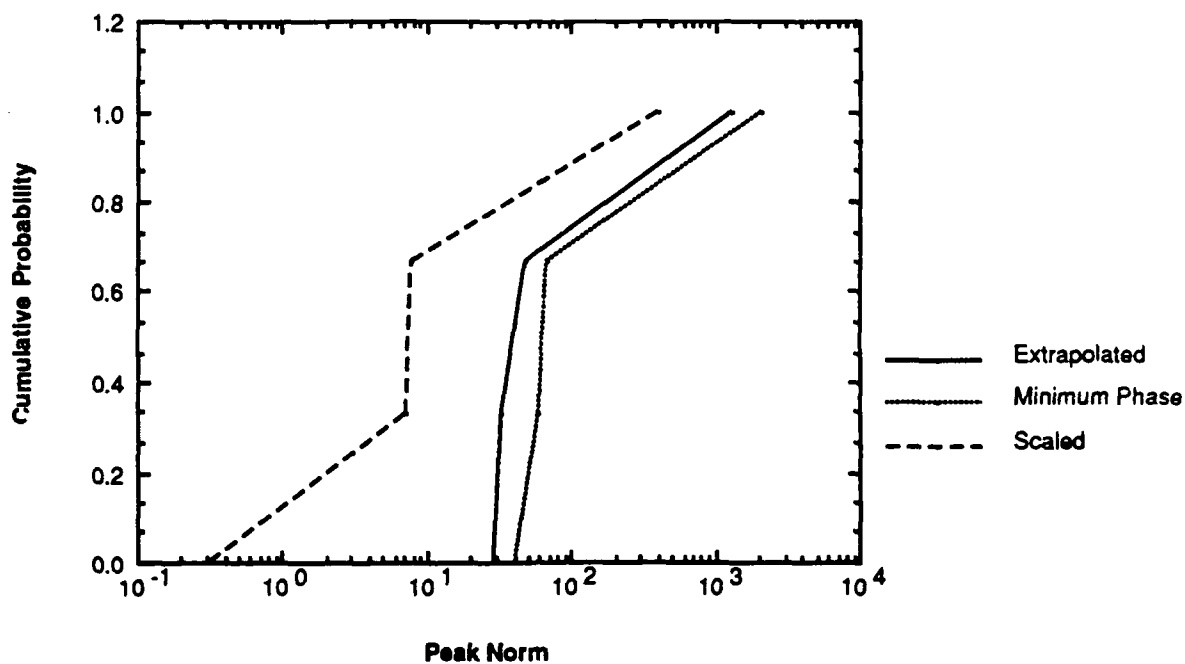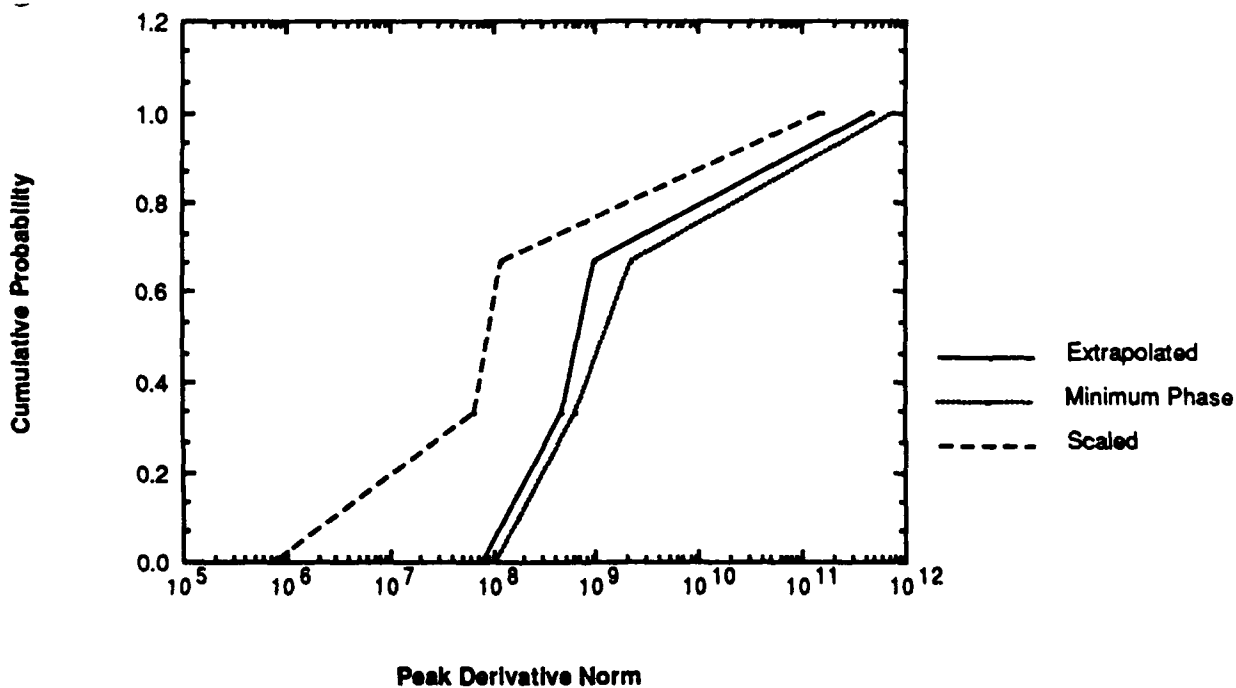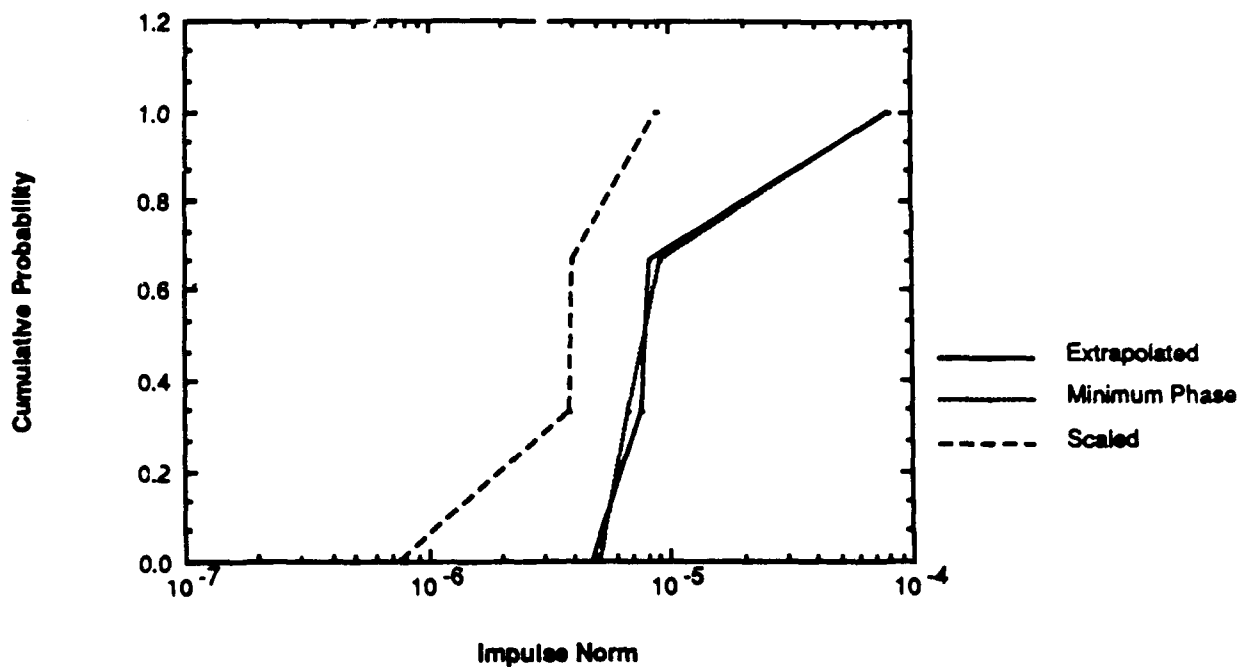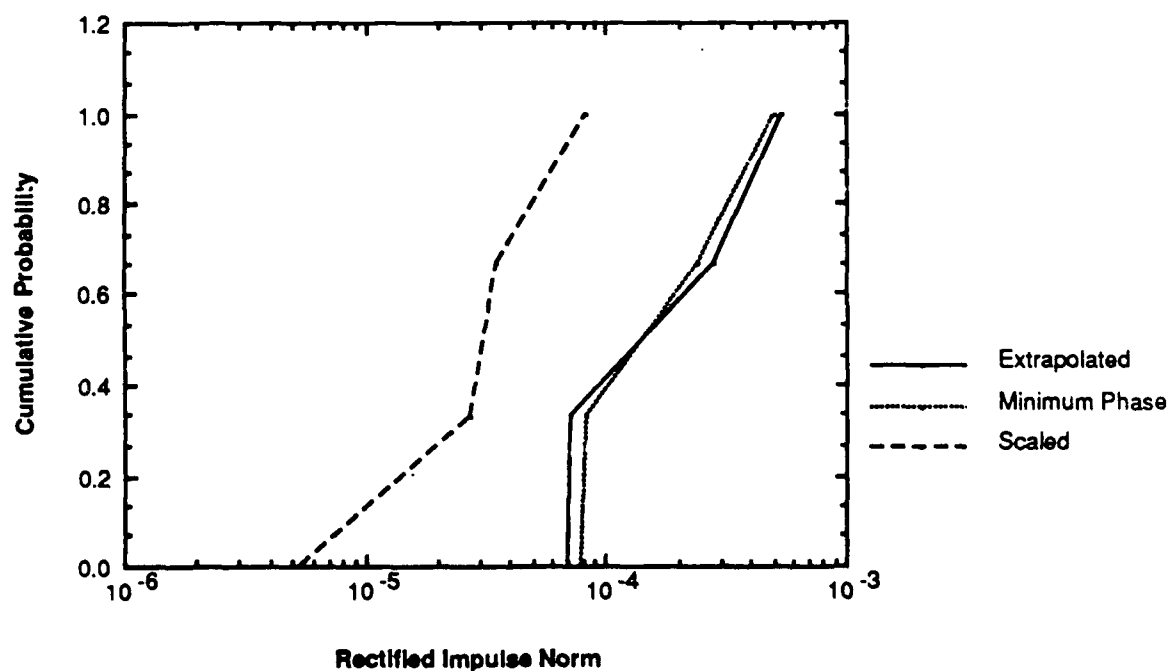100 Series Test Points**

C-2
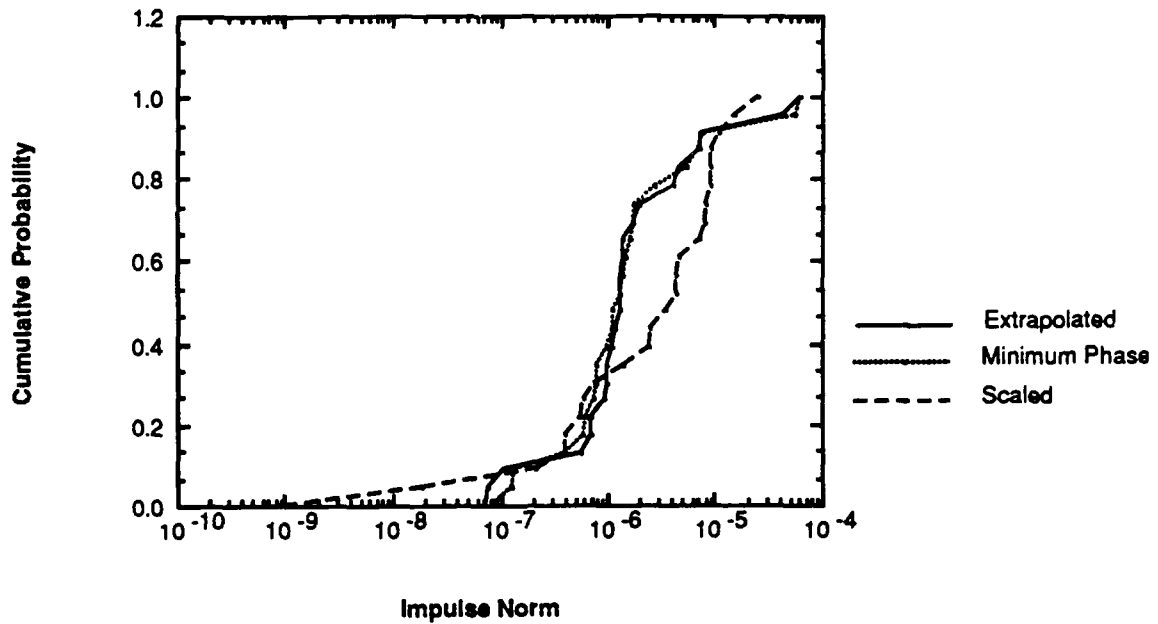
Figure C-3. Cumulative Probability Versus the Impulse Norm for the 100 Series Test Points
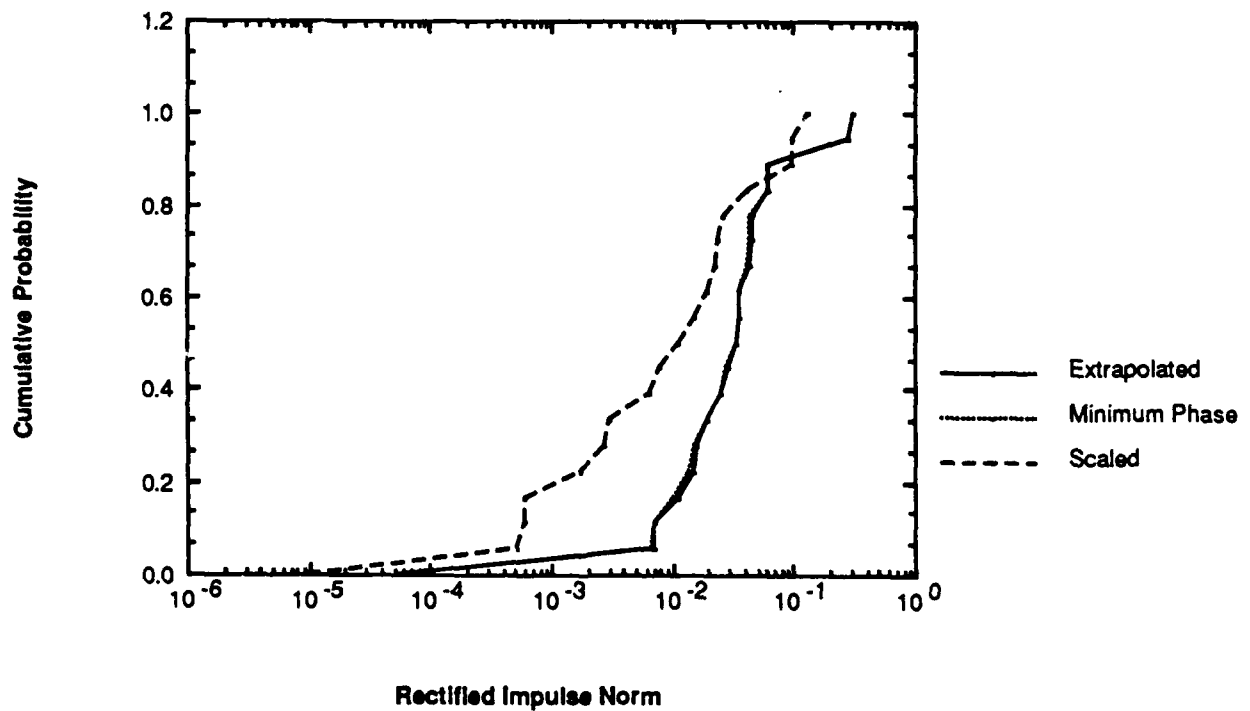
Figure C-4. Cumulative Probability Versus the Rectified Impulse Norm for the 100 Series Test Points

C-3
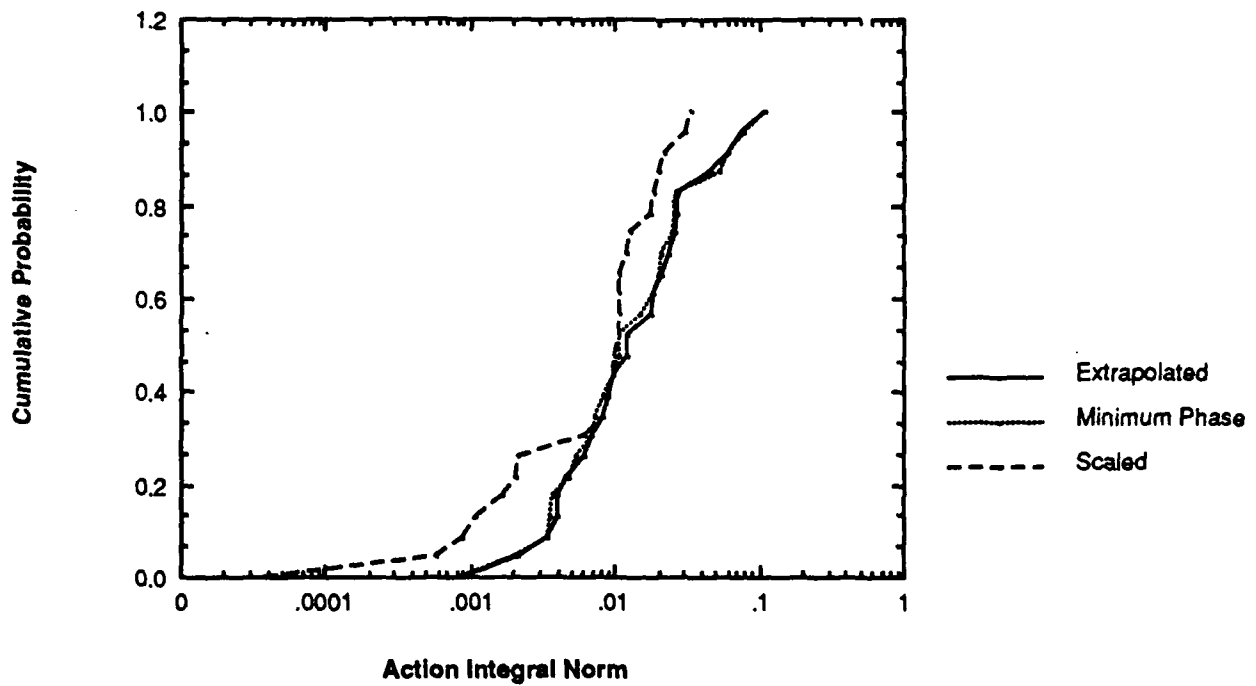
Figure C-5. Cumulative Probability Versus the Action Integral of the 100 Series Test Points
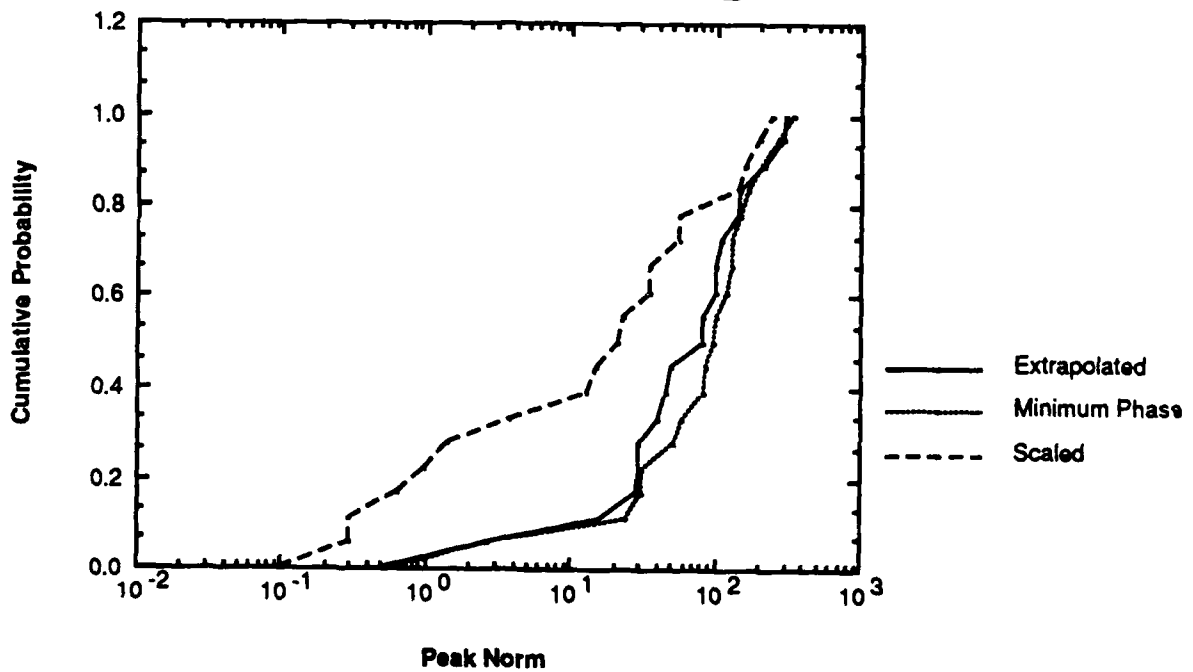
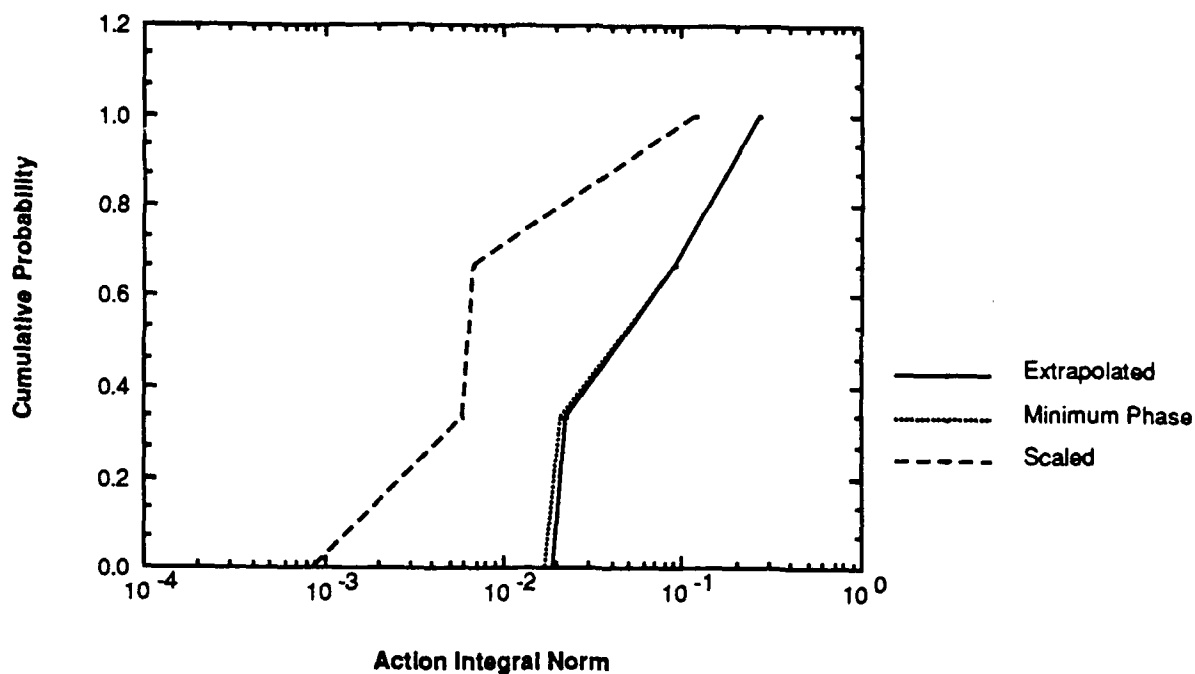**Figure C-6. Cumulative Probability Versus the Peak Norm for the 200 Series Test Points**

C-4
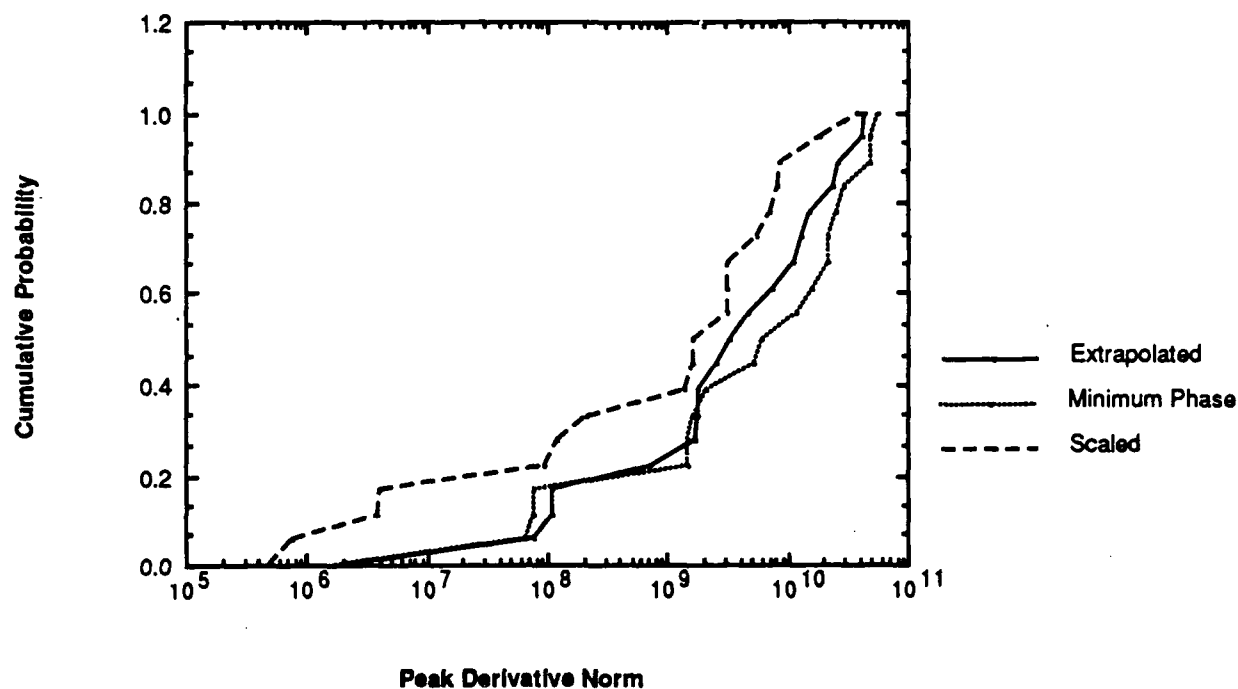
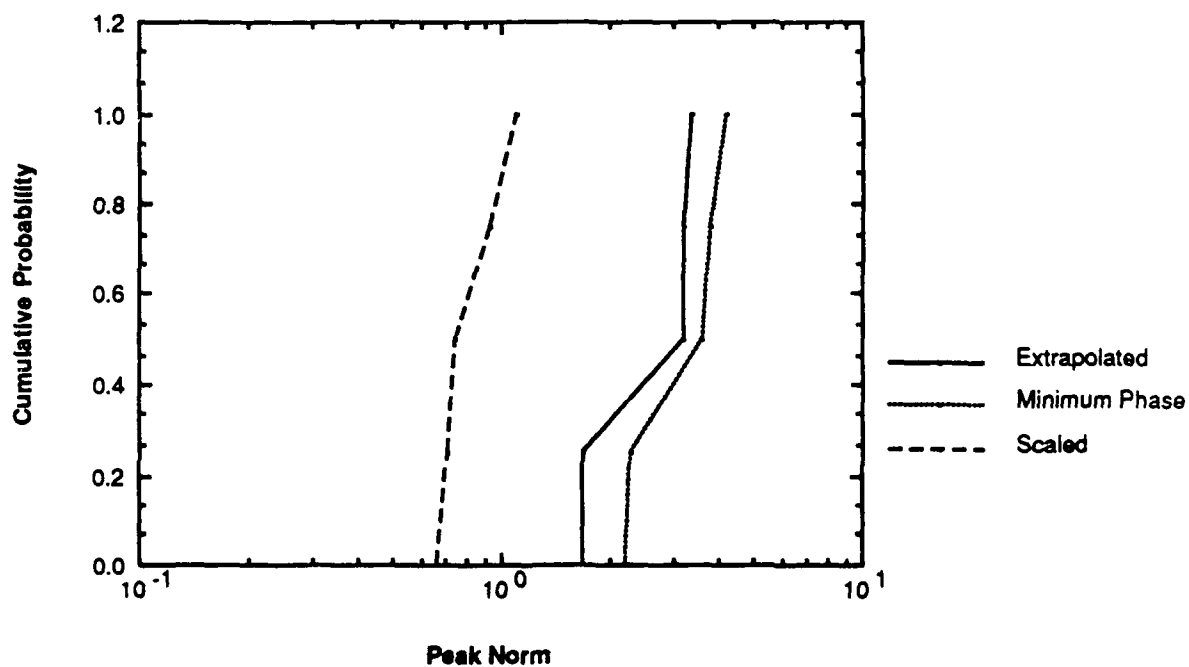**Figure C-7. Cumulative Probability Versus the Peak Derivative Norm for the 200 Series Test Points**
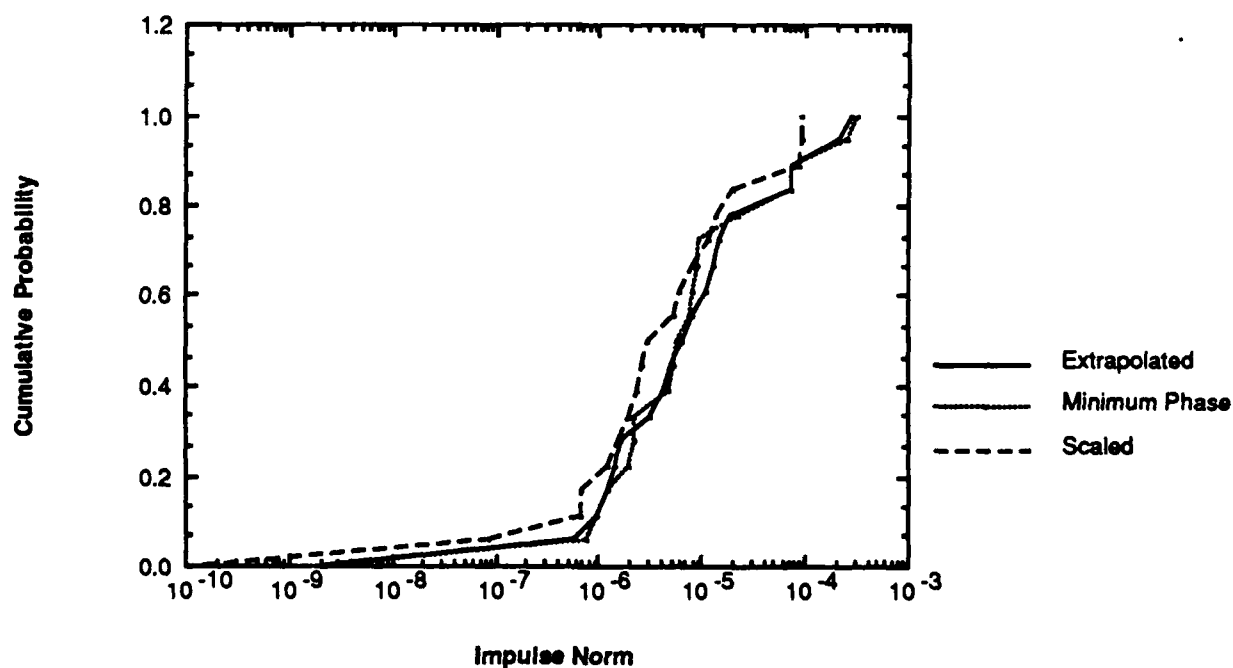
Figure C--8. Cumulative Probability Versus the Impulse Norm for the 200 Series Test Points
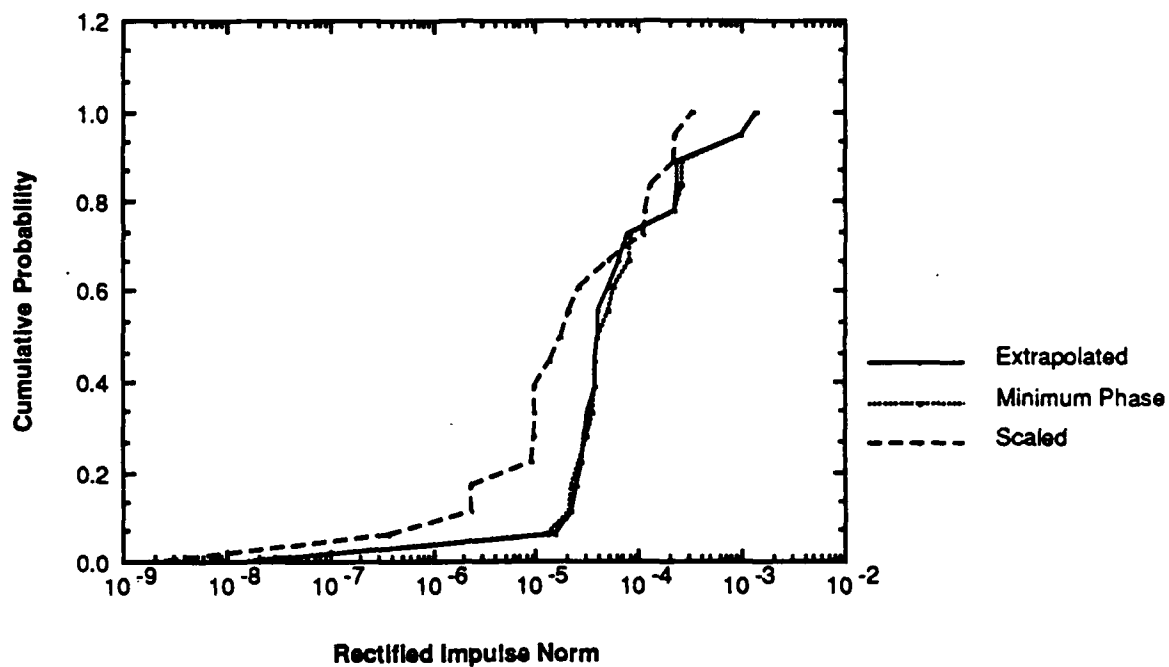
Figure C-9. Cumulative Probability Versus the Rectified Impulse Norm for the 200 Series Test Points
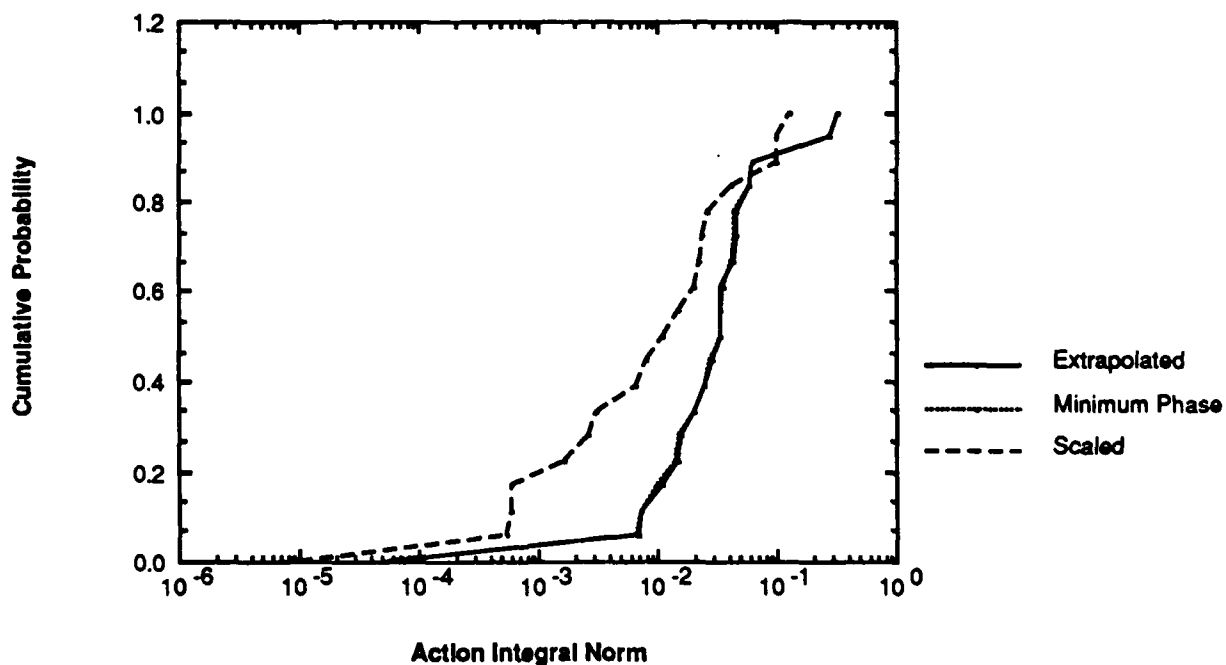
Figure C-10. Cumulative Probability Versus the Action Integral of the 200 Series Test Points
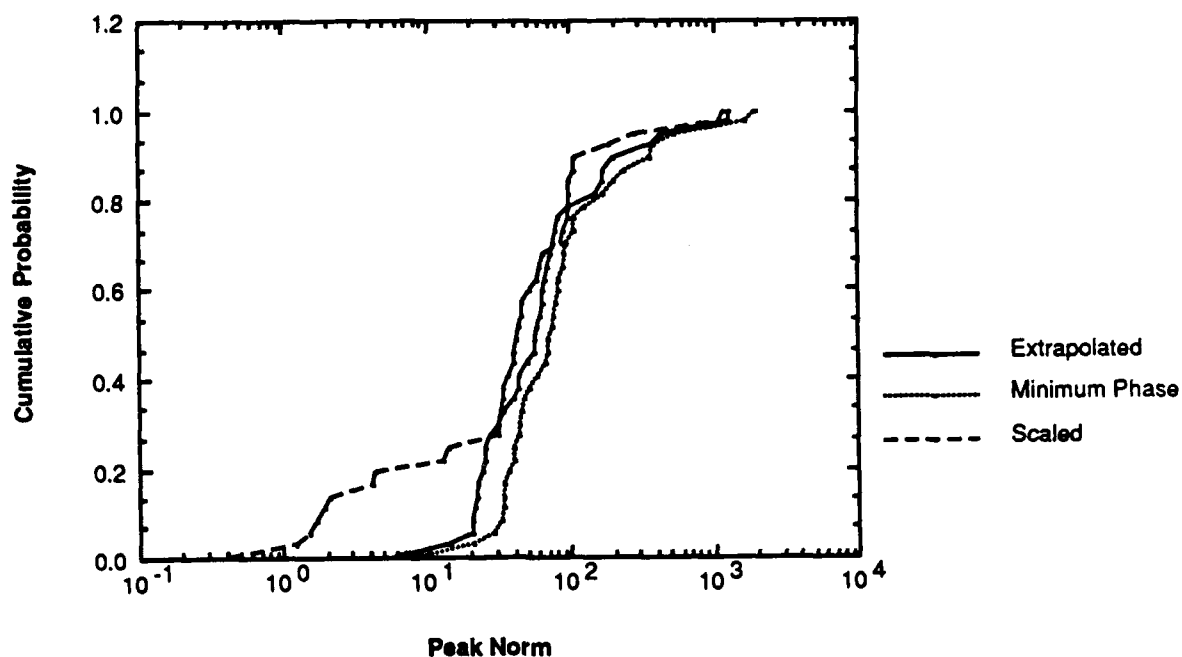
Figure C-11. Cumulative Probability Versus the Peak Norm of the 300 Series Test Points
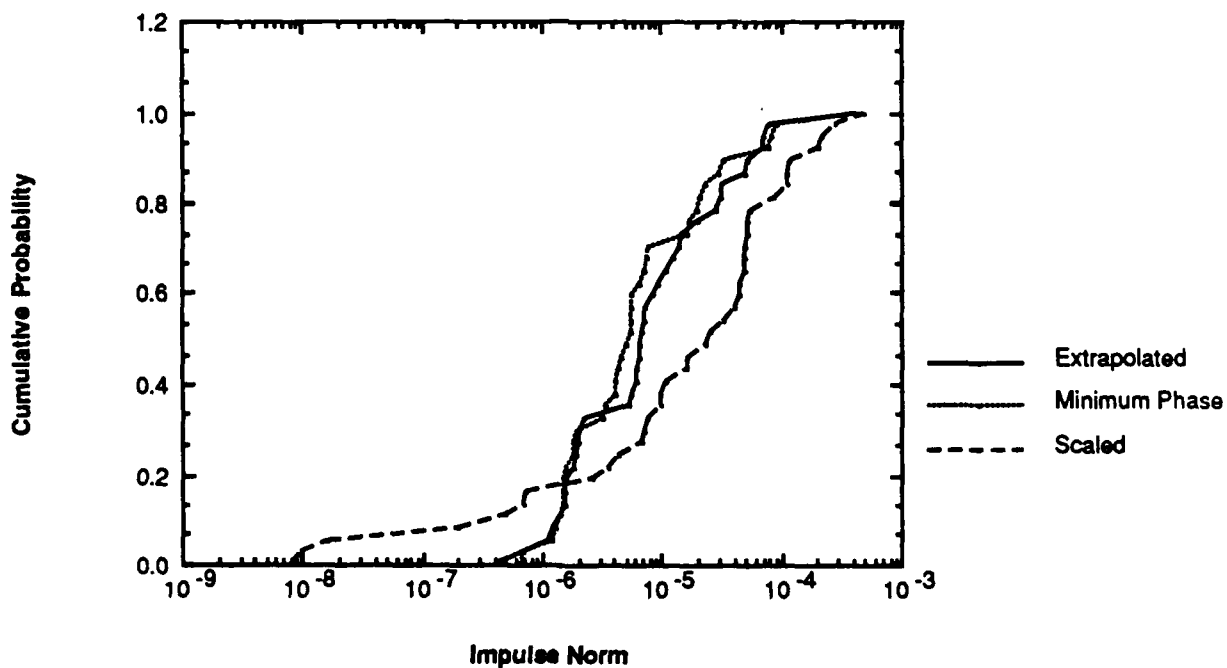
Figure C-12. Cumulative Probability Versus the Impulse Norm for the 300 Series Test Points
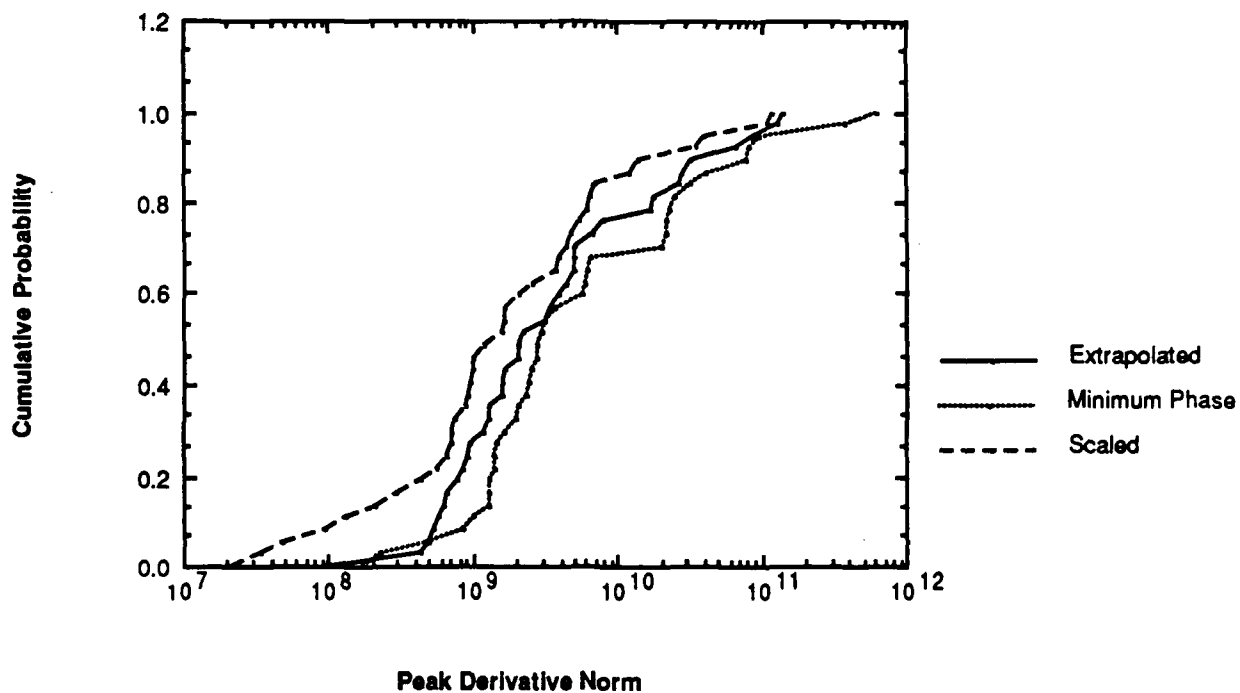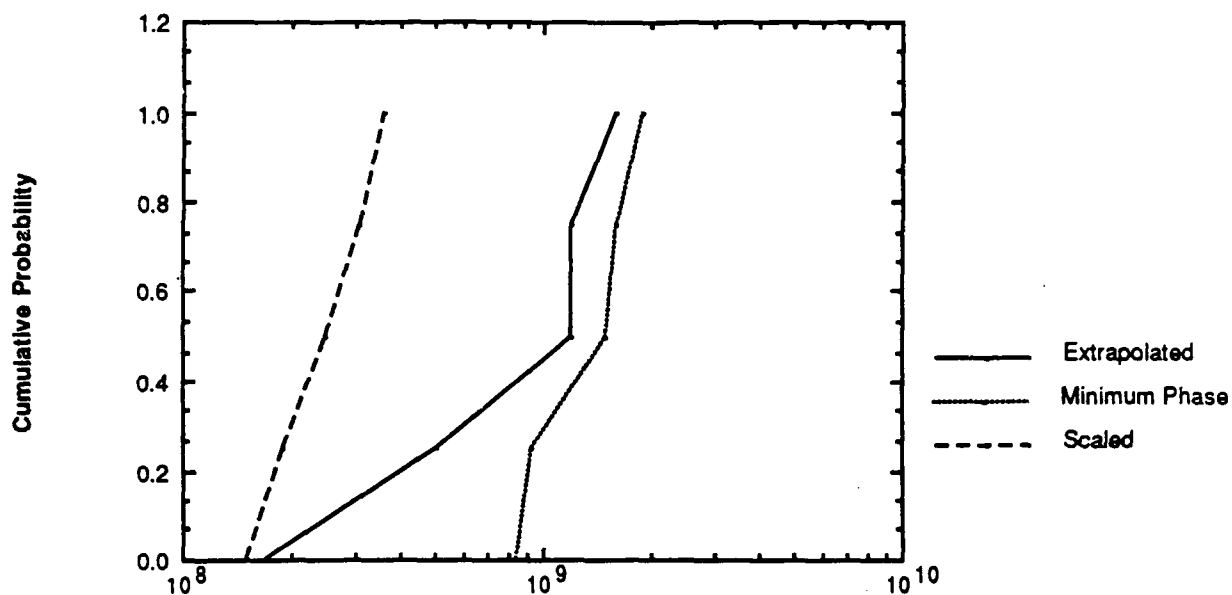
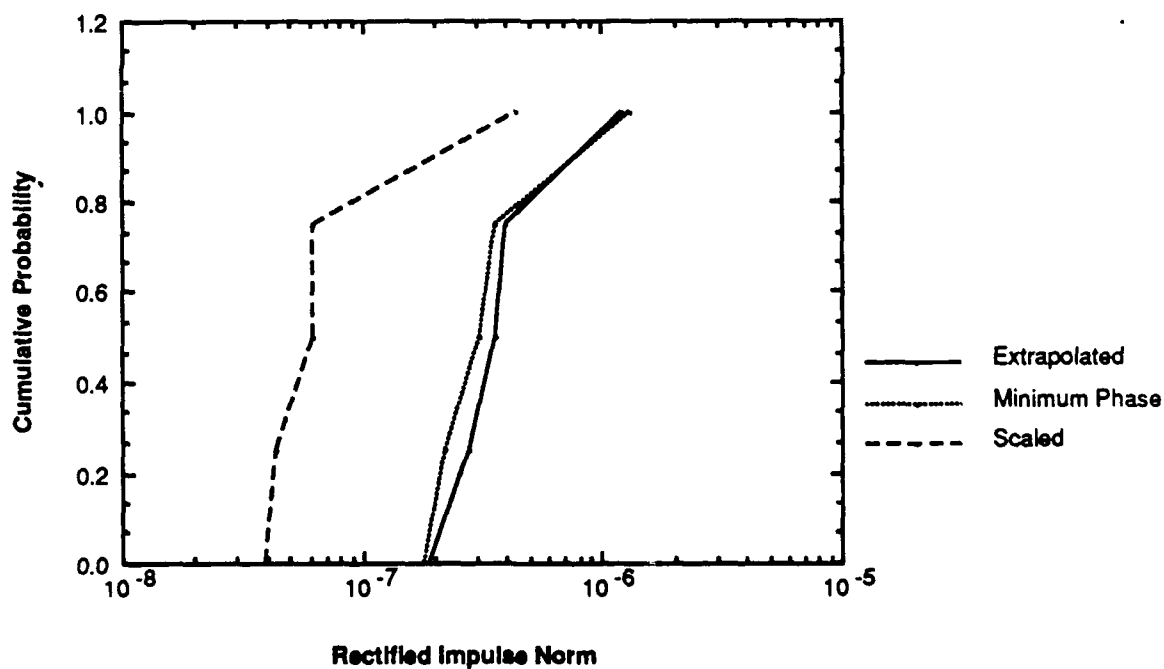**Figure C-13. Cumulative Probability Versus the Peak Derivative Norm for the 300 Series Test Points**

Figure C-14.. Cumulative Probability Versus the Rectified Impulse Norm for the 300 Series Test Points

Figure C-15. Cumulative Probability Versus the Action Integral of the 300 Series Test Points

Figure C-16. Cumulative Probability Versus the Peak Norm for the 400 Series Test Points

C-9

Figure C-17. Cumulative Probability Versus the Peak Derivative Norm for the 400 Series Test Points
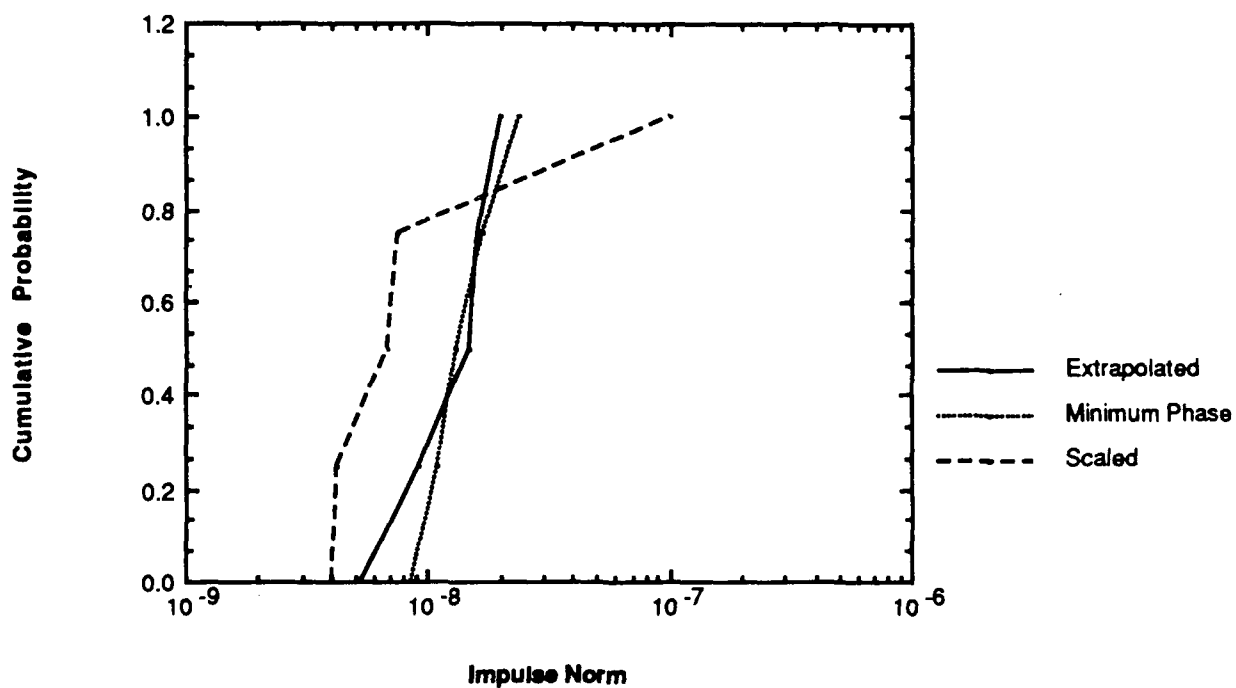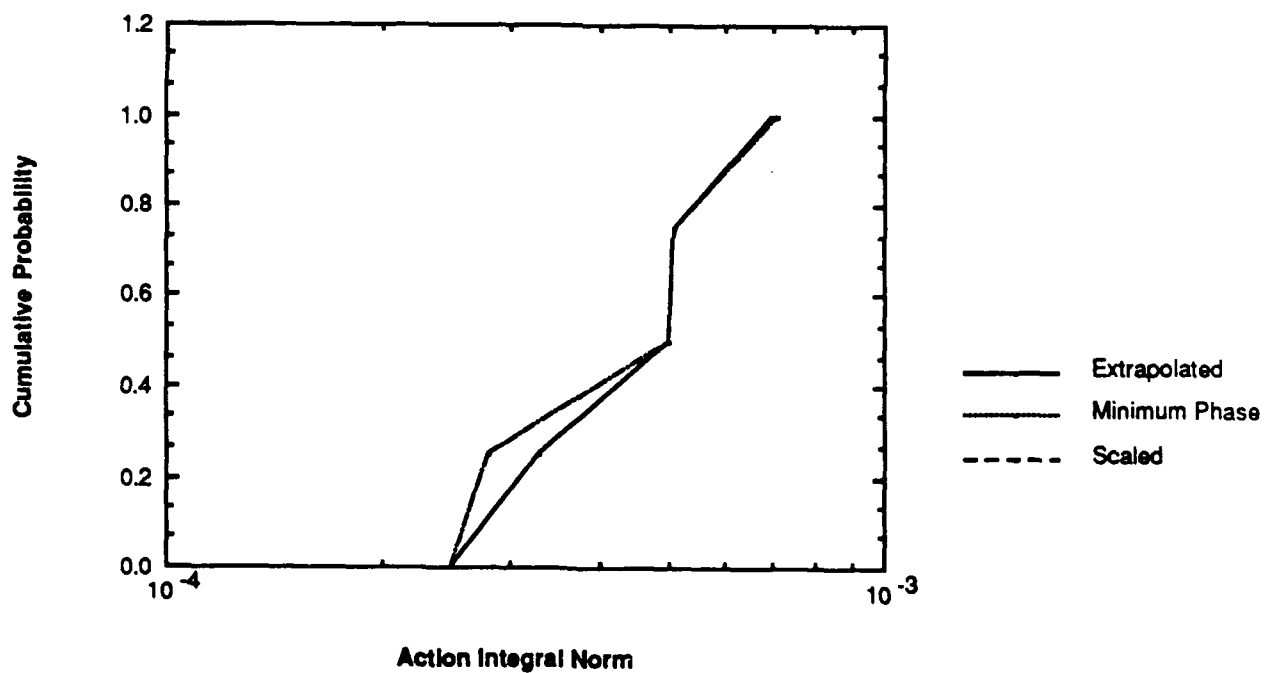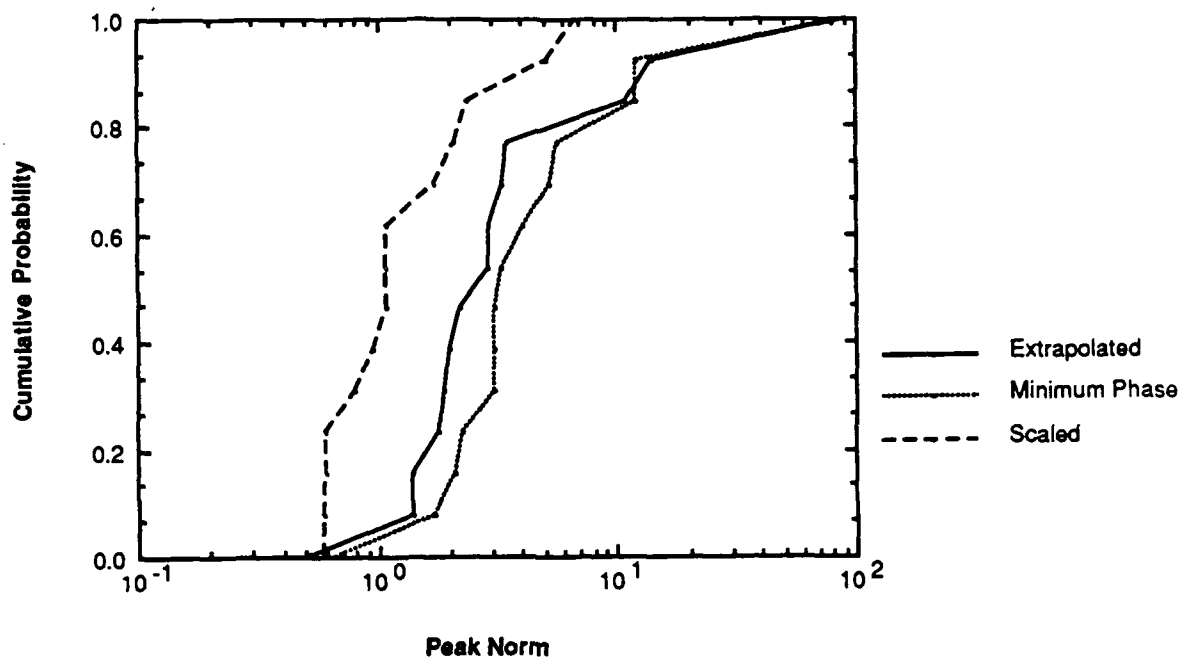

Figure C-18. Cumulative Probability Versus the Impulse Norm for the 400 Series Test Points

Figure C-19. Cumulative Probability Versus the Rectified Impulse Norm for the 400 Series Test Points

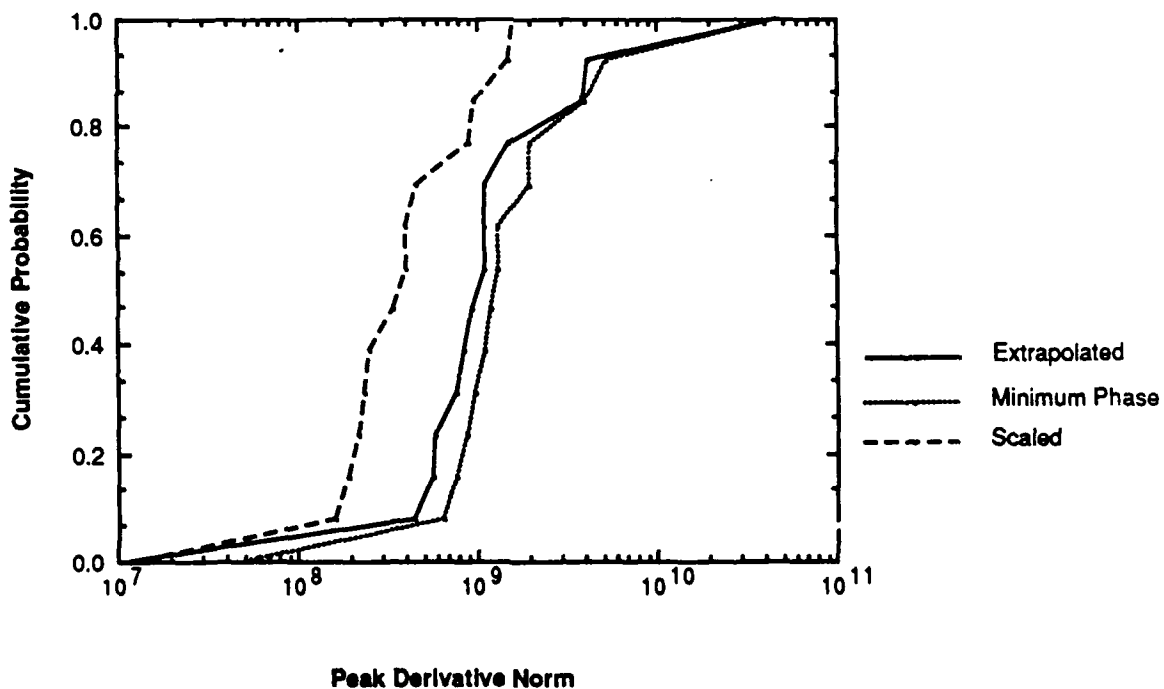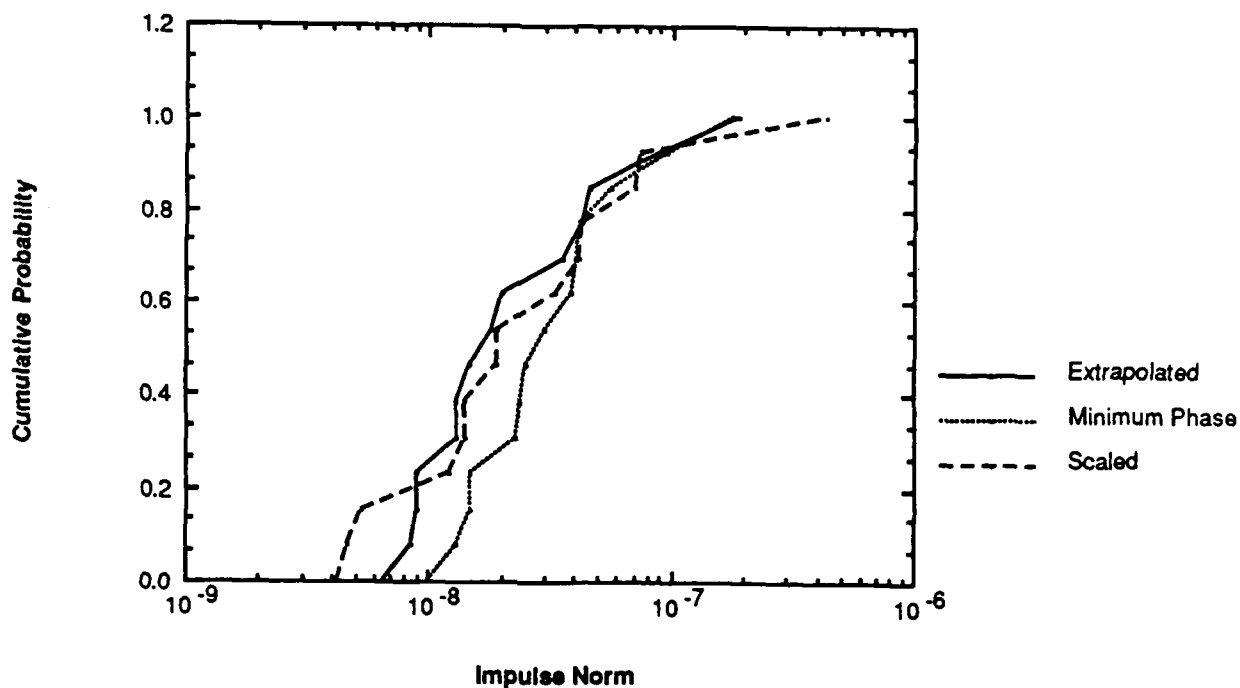**Figure C-20. Cumulative Probability Versus the Action Integral of the 400 Series Test Points**

Figure C-21. Cumulative Probability Versus the Peak Norm for the 500 Series Test Points

Figure C-22. Cumulative Probability Versus the Peak Derivative Norm for the 500 Series Test Points

C-12

Figure C-23. Cumulative Probability Versus the Impulse Norm for the 500 Series Test Points

Figure C-24. Cumulative Probability Versus the Rectified Impulse Norm for the 500 Series Test Points

**Figure C-25. Cumulative Probability Versus the Action Integral of the
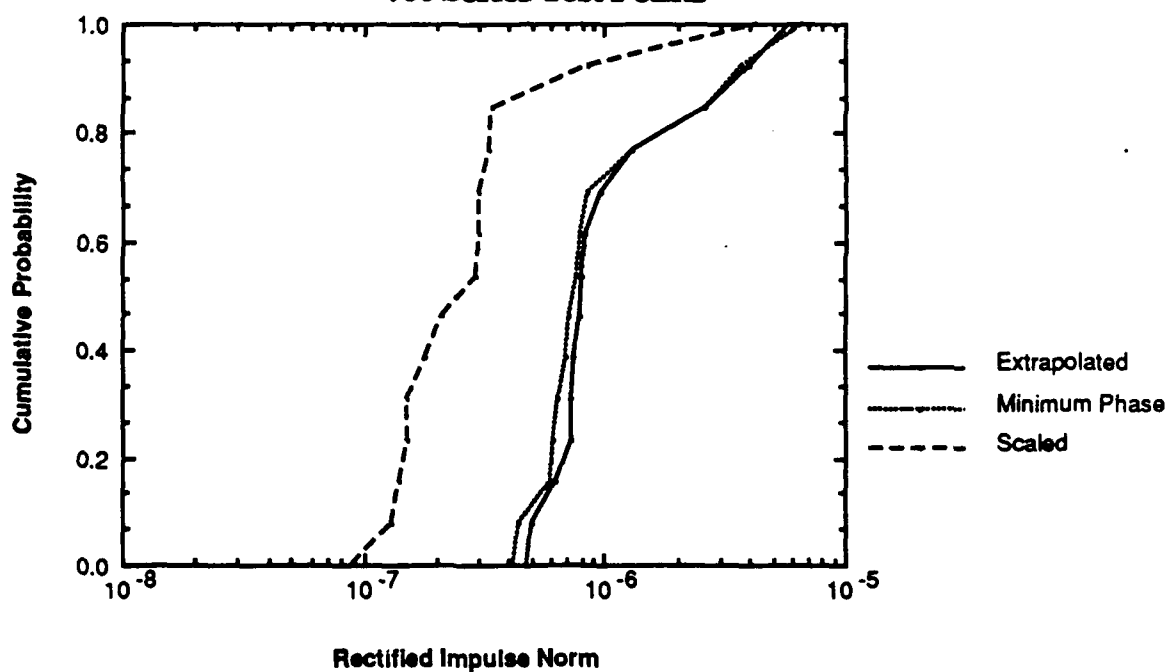500 Series Test Points**

**Figure C-26. Cumulative Probability Versus the Peak Norm for the
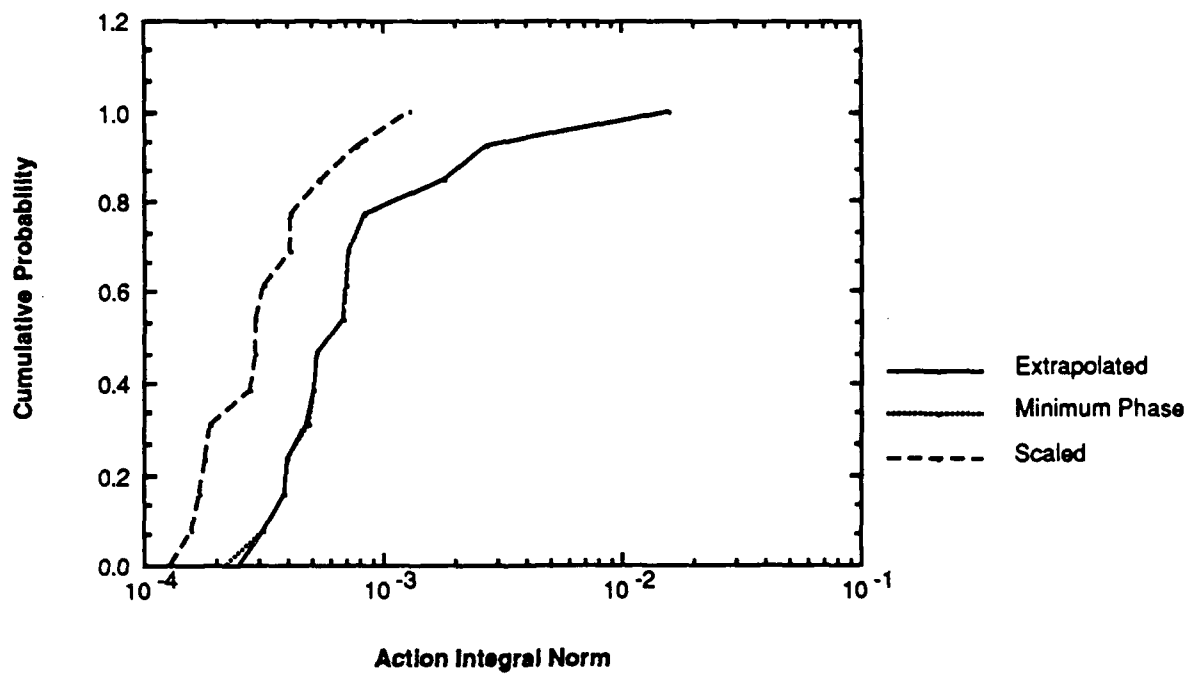600 Series Test Points**

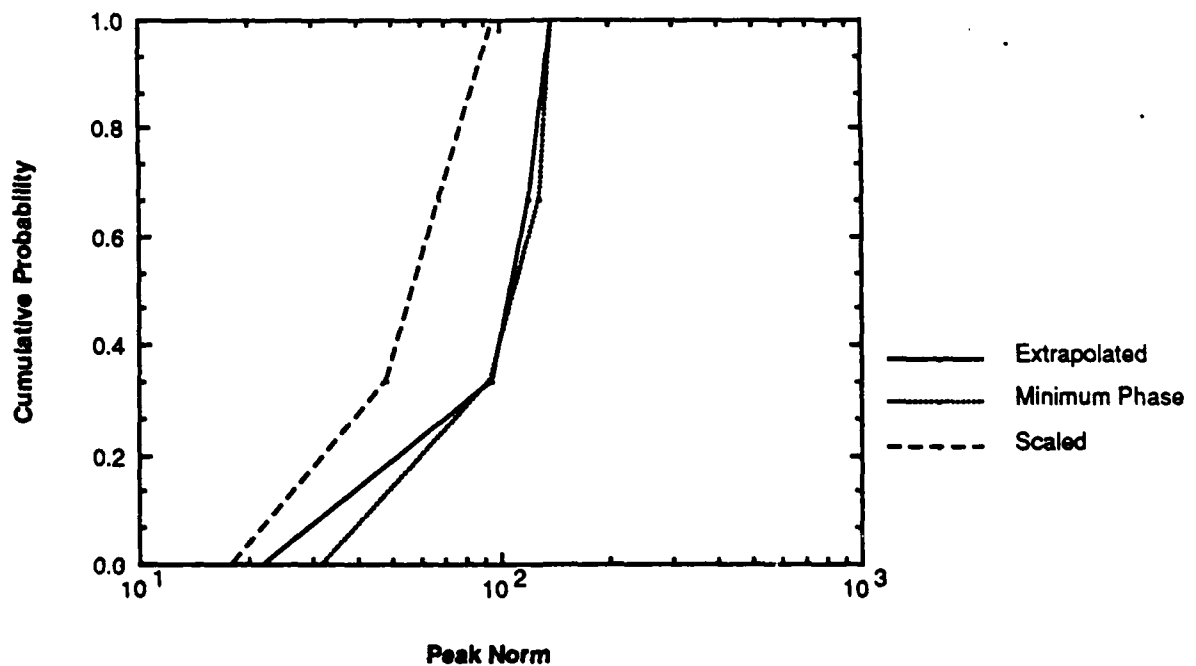**Figure C-27. Cumulative Probability Versus the Peak Derivative Norm for the 600 Series Test Points**

Figure C-28. Cumulative Probability Versus the Rectified Impulse Norm for the 600 Series Test Points

Figure C-29. Cumulative Probability Versus the Impulse Norm for the 600 Series Test Points

Figure C-30. Cumulative Probability Versus the Action Integral of the 600 Series Test Points

Figure C-31. Cumulative Probability Versus the Peak Norm for the 700 Series Test Points

Figure C-32. Cumulative Probability Versus the Peak Derivative Norm for the 700 Series Test Points

Figure C-33. Cumulative Probability Versus the Impulse Norm for the 700 Series Test Points

Figure C-34. Cumulative Probability Versus the Rectified Impulse Norm for the 700 Series Test Points
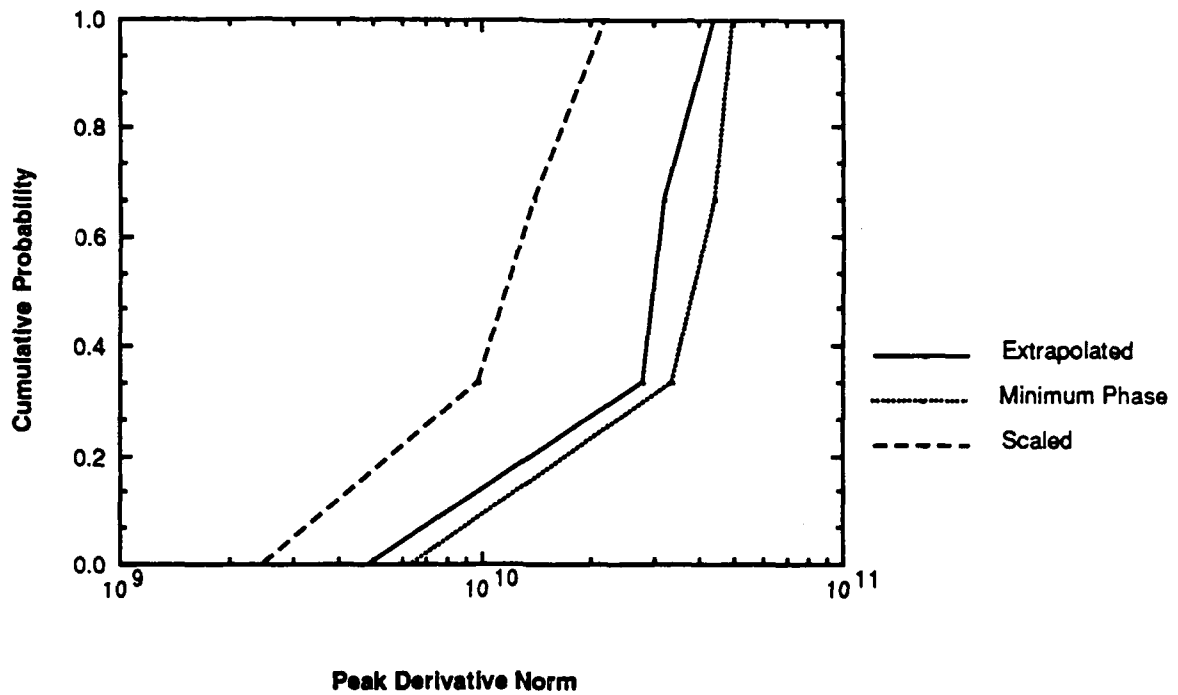
Figure C-35. Cumulative Probability Versus the Action Integral of the 700 Series Test Points
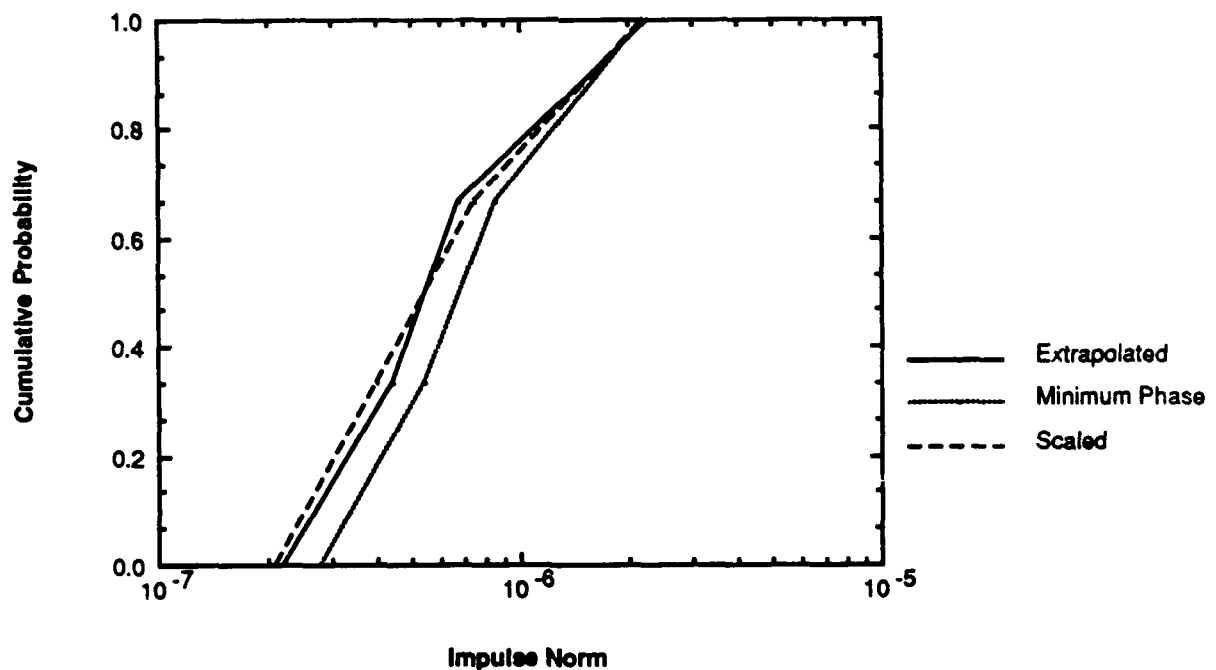

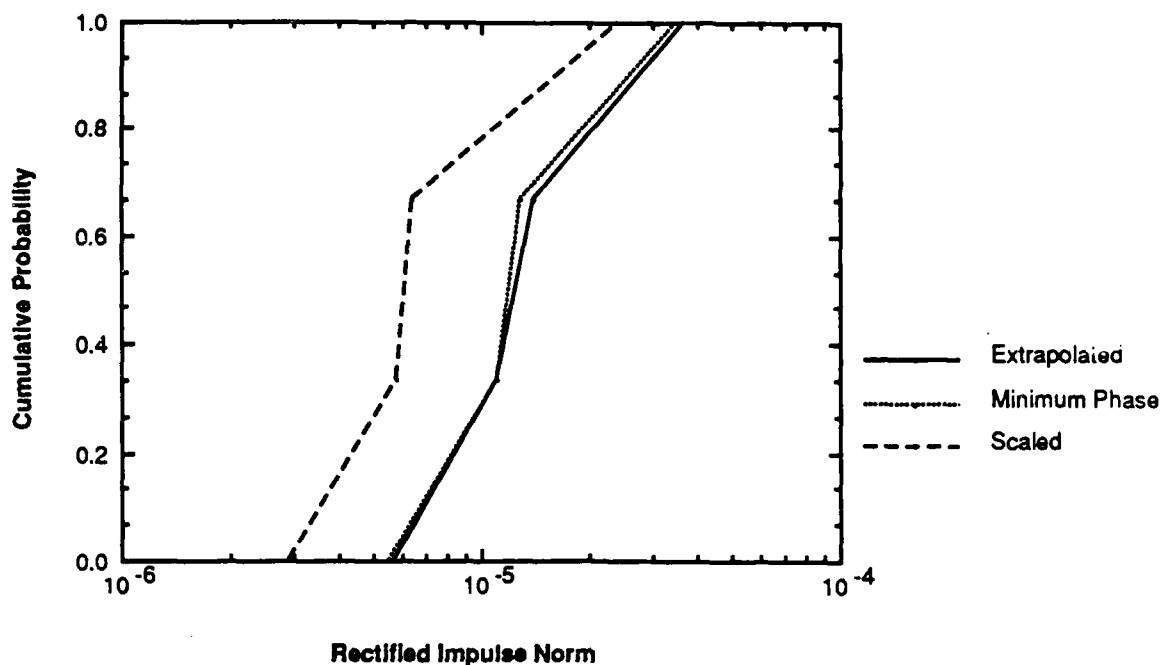**Figure C-36. Cumulative Probability Versus the Peak Norm for the 800 Series Test Points**
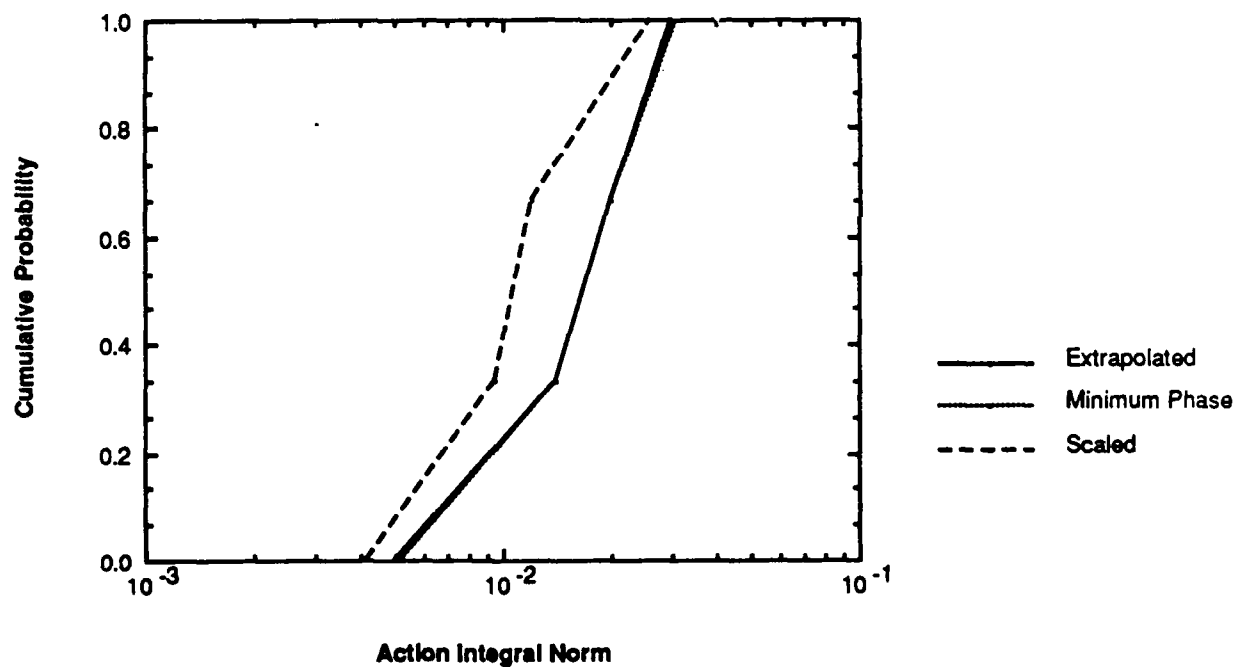
Figure C-37. Cumulative Probability Versus the Peak Derivative Norm for the 800 Series Test Points

Figure C-38. Cumulative Probability Versus the Impulse Norm for the 800 Series Test Points

Figure C-39. Cumulative Probability Versus the Rectified Impulse Norm for the 800 Series Test Points

Figure C-40. Cumulative Probability Versus the Action Integral of the 800 Series Test Points

APPENDIX D.

REFERENCES

1. R. Balestri, "EMP Data Processing, Time Tying, Data Quality, and Data Conditioning," Proceeding on IEEE International Symposium on Electromagnetic Compatibility, 1985.

2. R. Balestri, "Development of Automatic Time Tie Algorithm, Final Report" BDM Report 226-RTA-84-002, 15 Nov 1984, Contract F29601-821-C-0030.

3. R. K. Otnes and L. Enochson, "Applied Time Series Analysis, Vol. 1 Basic Techniques, "John Wiley, New York, 1978.

4. R. Balestri and R. Brown, "Adaptive Time Domain Noise Cancellation for EMP Measurement," Proceeding on IEEE International Symposium on Electromagnetic Compatibility, 1985.

5. C. E. Brown, "Norms of Time-Domain Functions and Convolution Operations," Mathematics Note 86, Air Force Weapons Laboratory, Dec 1985.